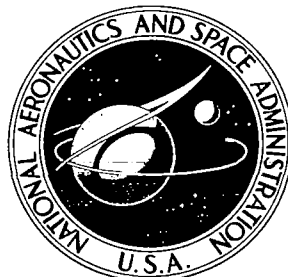


NASA CONTRACTOR REPORT



NASA CR-1503

0060699



TECH LIBRARY KAFB, NM

NASA CR-1503

LOAN COPY: RETURN TO
AFWL (WLOL)
KIRTLAND AFB, N MEX.

AN APPLICATION OF THE "REQUIREMENT VS CAPABILITY" ANALYSIS TO ESTIMATING DESIGN RELIABILITY OF SOLID ROCKET MOTORS

by C. R. Herrmann, G. E. Ingram, and E. L. Welker

Prepared by
GENERAL ELECTRIC COMPANY
Santa Barbara, Calif.

for



**AN APPLICATION OF THE "REQUIREMENT VS CAPABILITY" ANALYSIS
TO ESTIMATING DESIGN RELIABILITY OF SOLID ROCKET MOTORS**

By C. R. Herrmann, G. E. Ingram, and E. L. Welker

Distribution of this report is provided in the interest of information exchange. Responsibility for the contents resides in the author or organization that prepared it.

Issued by Originator as Report No. 68 TMP-78

Prepared under Contract No. NAS 7-556 by
GENERAL ELECTRIC COMPANY
Santa Barbara, Calif.

for

NATIONAL AERONAUTICS AND SPACE ADMINISTRATION

For sale by the Clearinghouse for Federal Scientific and Technical Information
Springfield, Virginia 22151 - Price \$3.00

ACKNOWLEDGMENTS

The authors acknowledge the assistance and constructive criticism provided to them by Messrs. D. K. Lloyd, M. Lipow, and N. R. Garner of TRW Systems, Mr. E. Wyszpolski of the Office of Advanced Research and Technology of NASA Headquarters (NASA)/OART, Mr. J. A. Mattice of Jet Propulsion Laboratories (JPL), and Messrs. J. M. Amaral and D. B. Syrek of Aerojet General Corporation (AGC) in the conduct of this study and in the preparation of this report. Under separate contracts from NASA/OART, AGC was assigned the responsibility for providing input data and equations required in the performance of this study, and TRW Systems was given the responsibility for providing coordination and technical direction of the efforts of AGC and TEMPO.

ABSTRACT

This report describes the results of the research work of G. E. / TEMPO on the continuing studies of the reliability of large solid rocket motors. The basic concepts of the study methodology were presented in G. E. / TEMPO document number 66TMP-90, 1 March 1967 prepared for NASA/OART under contract number NAS 7-383. The present report is devoted primarily to a description of the application of this methodology to an existing solid rocket motor system. A hypothetical example serves to explain the basic concepts and to illustrate both hand and computerized computational procedures. The solid rocket motor example demonstrates the practicality of the methodology in a realistic case, showing that the data and design relationships can be obtained and that the computational work load is not unreasonable.

Briefly, the reliability analysis methodology can be described as follows. For each significant failure mode, transfer functions are derived to express the requirements (or stresses) which will be imposed on the motor and the capability (or strength) of the motor to withstand these requirements. (The words "requirements" and "capabilities" are used in preference to "stresses" and "strength" to avoid the incorrect implication that the method is restricted to structures.) Using the initials, the method is called the R||C analysis technique. All input and output parameters are treated probabilistically to provide proper realism. Simultaneous consideration of analyses for the various modes yields the system reliability estimate. TEMPO elected to use the General Electric time sharing computer system for performing the computations. It provides speed, convenience, and flexibility sufficient to permit design engineers or their analysts to apply R||C analysis themselves, thus allowing the technique to serve as an effective design tool.

The main body of the report contains (1) a brief description of the concepts associated with the R||C approach, (2) an application of the technique using the engineering information and data supplied by the Aerojet General Corporation (AGC), and (3) conclusions and recommendations resulting from the study. The appendices contain (1) data on input parameters supplied by AGC, (2) a discussion of the detailed analysis

which was performed in the course of the study, (3) some computer printouts resulting from an R||C analysis of failure modes for which data was available, (4) a brief description of the computational technique used for combining random variables and the computer procedures used to implement the technique, and (5) a mathematical discussion of a portion of the theory of the R||C analysis technique.

TABLE OF CONTENTS

ACKNOWLEDGEMENT	iii
ABSTRACT	v
SECTION	
1 SUMMARY AND INTRODUCTION	1
2 OBJECTIVES OF THE PHASE III STUDY PROGRAM	4
3 THE FUNDAMENTAL CONCEPTS OF THE METHODOLOGY	7
4 GENERAL COMMENTS ON DATA AND TRANSFER FUNCTIONS USED IN THIS STUDY	10
5 APPLICATION OF THE METHODOLOGY TO A LARGE SOLID ROCKET MOTOR	12
6 CONCLUSIONS	32
7 RECOMMENDATIONS FOR FUTURE WORK	35
APPENDIX	
I. SUMMARY OF INPUT DATA AND TRANSFER FUNCTIONS OBTAINED FROM AEROJET GENERAL CORPORATION	I. 1
II. DETAILS OF APPLICATION TO THE LARGE SOLID ROCKET MOTOR	II. 1
III. COMPUTER PRINTOUTS	III. 1
IV. APPROACH CONCEPTS AND COMPUTATION TECHNIQUE	IV. 1
V. COMPUTER PROCEDURES	V. 1
VI. A MATHEMATICAL DISCUSSION OF A PORTION OF THE THEORY OF THE R C ANALYSIS TECHNIQUE	VI. 1
REFERENCES	R.1

1. SUMMARY AND INTRODUCTION

For some time, the Office of Advanced Research and Technology of NASA Headquarters, NASA/OART, has been concerned about the problems associated with designing highly reliable large solid rocket motor systems. Specifically, they would like to be able to estimate the reliability potential of a candidate system design in advance of production in sufficient detail to identify and quantify the sources of unreliability. Of course such an estimation method could also be used to evaluate the reliability of a rocket motor system after fabrication. The familiar "piece part" approach which has proved to be so useful in the evaluations of the reliability of electronic systems is not suitable for solid rocket motors for two critical reasons. In the first place, a solid rocket motor is largely fabricated as a single integrated system from raw materials rather than piece parts. In the second place, system testing in large samples is not feasible since test firings are destructive and large motors are very expensive. Phases I and II of this study program were devoted primarily to examinations of past experience on completed and continuing solid rocket motor developments. These examinations attempted to discover criteria for extrapolating reliability growth experience from past programs to current ones. As a result of these studies, the need for the analytical approach of Phase III was quite clearly established. The present report summarizes the results of this Phase III research work by G. E. /TEMPO*, all phases being performed under the sponsorship of NASA/OART.

In the initial phases of this research, TEMPO explored the possibility of extrapolating test experience from other solid rocket motor programs. This was partially successful for the purposes of reliability estimation and of clarification of the elements of the overall problem. However, the approach was clearly deficient in identifying and quantifying sources of unreliability to assist the design engineer in his efforts to meet desired reliability goals. It became apparent to the study team that the most promising technique would involve analytical studies of the solid rocket motor system to gain an appropriate insight into the physics of the failure phenomena which could occur. This report presents a brief description of the methodology of this approach, including some of the basic theory involved, a simple hypothetical example, and an application of the

* Contributions to this research by Aerojet General Corporation and TRW Systems are described elsewhere in the report.

technique to a number of the failure modes for a realistic solid propellant rocket motor, the 260 inch motor manufactured by AGC.

The main body of the report, of which this section is a part, introduces the reader to the background leading up to this study, states the objectives of the study in terms of the contract work statement, briefly summarizes the fundamental concepts of the methodology, presents general comments on the transfer functions and parameter data used in the study, summarizes the results obtained from applying the methodology to a large solid rocket motor, discusses the results, and presents conclusions and recommendations for future work.

The appendices contain a complete summary of the input data and transfer functions provided by AGC, the details of the application of R||C analysis to a large solid rocket motor, and the computer printouts resulting from this application. They also include a detailed discussion of the approach concepts, computational techniques, and computer procedures used in the study, and a mathematical discussion of a portion of the theory of the R||C analysis technique.

This study had two prime objectives: (1) development of analytical techniques that will enable the design engineer to estimate the reliability of the system (e. g. a large solid rocket motor), and (2) the application of these techniques to a large solid rocket motor system. The results of the study indicate that the techniques are feasible and tractable and provide the designer an efficient and economical analysis tool. For example, using the unmodified data as it was furnished by AGC for the parameters associated with the burn-through failure mode, the R||C analysis for this failure mode indicated that in one region of the motor the probability of burning through to the case wall could be as high as 0.137 depending upon the data used to define the burn-through parameters. The important point here is that this could not have been realized by the designer without describing these parameters probabilistically.

Another failure mode which helped to illustrate the importance of the R||C analysis was that of case rupture in both the cylindrical and spherical portions of the case. The welds are the most critical elements of the case with respect to rupture and it was necessary to consider them in detail, distinguishing between those that were made by machine and those that required hand techniques. All welding was initially done by

machine. According to AGC inspection experience, approximately 10 percent of the total weld length was defective and was reworked by hand welding techniques. Test data derived from representative weld specimens showed that on the average, the hand welds were weaker and their strengths had a larger variability than did the machine welds. Results of the R||C analysis indicated that the failure probabilities associated with this failure mode were relatively small when based only on the machine weld strengths (90% of all welds) but increased many orders of magnitude when the hand weld strengths (10% of all welds) were included. This quantitative result is not immediately obvious to the designer until he considers the probabilistic description of the design parameters in an R||C analysis.

Relatively low probabilities of failure were also obtained from the R||C analysis for the other failure modes when using the standard set of unadjusted AGC data. In many cases, however, further R||C analysis indicated that the probability of failure associated with a particular failure mode could be increased many orders of magnitude by simply changing the mean value and/or the variance of certain of the parameters. On the other hand there was little effect upon the probability of failure resulting from changes in the mean values and/or variances of certain other parameters. Studies based on such changes of the means and/or variances of input parameters are referred to as sensitivity analyses in the text.

The recommendations evolving from this study address themselves primarily to four areas--(1) further analysis of the large solid rocket motor to include those subsystems that have not yet been analyzed by the R||C approach (e. g. ignitor system, nozzle, etc.), (2) a more detailed study in certain areas where the sensitivity analysis indicated a criticality of certain parameters (e. g. maraged steel versus HY series steel), (3) a consideration of system interdependence and engineering trade-offs (e. g. developing criteria for prorating unreliability of total system to individual failure modes), and (4) extending the R||C analysis to other types of motor systems (e. g. smaller solid propellant rocket motors, liquid propellant rocket engines, hybrid motors, etc.).

2. OBJECTIVES OF THE PHASE III STUDY PROGRAM

The TEMPO Phase III study effort was directed toward the accomplishment of two basic tasks. The first task consisted of the development of a methodology for using a physics of failure approach in evaluating the reliability of a large solid propellant rocket motor system. The second task was actually composed of two subtasks. One of these was to apply this methodology to an actual system—the 260 inch motor system was selected for this purpose. The other subtask consisted of the development of computational procedures which were sufficiently simple to constitute a demonstration of the practicality of the analysis methodology. The TEMPO tasks were detailed in the most recent contract work statement as follows.

"Statement of Work

TEMPO shall work toward development of a technique for the assessment of reliability of large solid propellant motors, which relies on an engineering analysis and a description of the motor. Work to include:

Task I

In cooperation of Aerojet General Corporation (AGC), identify and list available failure modes of the Propellant Grain Subsystem and establish priorities for the application of the R||C analysis of these failure modes.

Task II

Define in coordination with AGC the ballistic and hardware performance and reliability requirements of the Propellant Grain Subsystem.

Task III

Identify in coordination with AGC measurable characteristics which characterize the Propellant Grain Subsystem's capability.

Task IV

Define, in coordination with AGC, relationships between requirements and capabilities.

Task V

Identify data format and needs to be submitted by AGC to G. E. for R||C analysis.

Task VI

Apply R||C analysis technique. This will involve setting up a computer program to handle the typical comparisons to be made.

Task VII

Preliminary ground work will be defined as it is associated with the other motor subsystems, such as the case, to insure proper lead time to application of the complete R||C analysis in the next period of this study.

Task VIII

In cooperation with Aerojet-General Corporation (AGC), identify and list failure modes associated with the Case-Liner-Insulation-Propellant Subsystems and establish priorities for the application of the R||C analysis to these failure modes. In consultation with AGC and TRW, and with the approval of NASA, the following failure modes have been tentatively selected for analysis:

1. Case Rupture due to Overpressurization and Flight Loads - parent metal.
2. Case Rupture due to Overpressurization and Flight Loads - welds.
3. Skirt Failure due to Flight Loads - forgings and plate.
4. Forward Cap Failure - bolt failure.
5. Forward Cap Failure - joint flexure.
6. Insulation/Case Bond Failure.

Task IX

Define, in coordination with AGC, a set of the more significant "Requirements" (i. e., to be used in the R||C analysis) that will be placed on the Case-Liner-Insulation-Propellant Subsystems.

Task X

Identify, in coordination with AGC, measurable properties which characterize the Case-Liner-Insulation-Propellant Subsystems' "Capabilities" (i. e., to be used in the R||C analysis) to satisfy the "Requirements" defined in Task IX.

Task XI

Define, in coordination with AGC, relationships between the "Requirements" and "Capabilities" identified in Task IX and Task X.

Task XII

Identify data format and needs to be submitted by AGC to G. E. for the R||C analysis.

Task XIII

Apply R||C analysis technique in line with Tasks VIII thru XII. (This will include any necessary computer programming.)"

Only the first seven of these tasks were listed in the original contract. Tasks eight through thirteen were added later by contract modification as an appropriate follow on or extension of the initial phases of this research.

The basic methodology was developed in the TEMPO Phase IIIA study effort, the results of which are described in the report "The Analytical Approach and Physics-of-Failure Technique for Large Solid Rocket Reliability", C. R. Herrmann and G. E. Ingram, TEMPO Report 66TMP-90, 1 March 1967, (Reference 1). The Phase IIIB study program had as its objective the development of computer methods for performing this analysis, using the propellant subsystem of the 260 inch solid rocket motor, thus initiating the work on the application of the methodology to an actual system. An interim report was prepared on this Phase IIIB work. It was given only limited distribution since it was viewed essentially as a progress report.

The objective of the present report is to describe the results of the entire Phase III effort. Since the Phase IIIA report explained the concepts of the methodology in some detail, we are including only a summary of the methodology herein.

3. THE FUNDAMENTAL CONCEPTS OF THE METHODOLOGY

System failure occurs when the capability or strength of the system is insufficient to withstand the requirements or stresses which are imposed upon it. The reliability of the system is of course the probability that the requirements do not exceed the capabilities for each and every failure mode.* We immediately recognize this as the traditional stress vs strength approach so commonly associated with analysis of structures. TEMPO has chosen to replace the terms "stress and strength" by "requirements and capability" respectively to avoid the incorrect implication that the method is restricted to structures—it applies equally to any system type. Using the initials, we identify the method as the R||C analysis technique. The significant aspect of the TEMPO research is the development of the ways and means for performing R||C analysis—the derivations of formulas, the collection of the necessary data from design group such as AGC, and the actual performance of the required computations.

The details of the R||C analysis methodology are briefly as follows. A list of failure modes must be prepared. For each mode, a pair of transfer functions are derived from the basic design equations. One transfer function expresses the requirement, R, placed on the system by the stresses it will see and the other expresses the capability, C, of the system to withstand these stresses. Each transfer function involves design variables or parameters which must be treated probabilistically if we are to obtain realistic and thus meaningful results from the analysis, meaning that R and C are also treated probabilistically. It will be helpful to describe this process in the symbolism and language of mathematics.

Consider a single failure mode and denote its two transfer functions as follows.

$$\text{Requirement: } R = f_R(x_1, x_2, \dots, x_m)$$

$$\text{Capability: } C = f_C(y_1, y_2, \dots, y_n) .$$

* For brevity, we will usually not make reference to the modifiers in the more precise definition of reliability which cover the system mission, the time span, the definition of satisfactory performance and the conditions of operation. However, these elements are included in the analysis.

When we say that the x 's, y 's, R , and C are treated probabilistically, we mean each of them is described in terms of its probability density function. In the language of probability, the terms random variable and stochastic variable are used to refer to a variable which has an associated density function and we shall use these terms in this sense herein. Thus, we can say that the probabilistic treatment of input variables, x 's and y 's, and output variables, R and C , contrasts with less realistic design approaches in which only single values are used for inputs and hence for outputs and the detail of the arithmetic reflects this distinction. The combination of the density functions of the input variables to generate the densities of the outputs for R and for C according to their respective transfer functions is a significantly larger task than the substitution of single (such as an average or worst case) values as will be illustrated. However, we will show how currently available computer systems perform such computations easily, quickly, and cheaply for most functions and hence make this $R||C$ analysis methodology quite tractable. The probability of system failure by this mode is obtained by computing the probability that C is less than R . This is obtained by deriving the density of the difference, $(C - R)$, and then computing the probability that $(C - R)$ is negative.*

The derivation of the probability density of $(C - R)$ must be completed for each failure mode. The system failure probability is then determined by computing the probability of the occurrence of at least one mode of failure. Obviously there can and perhaps commonly will be dependencies between input random variables in C and R functions for the various failure modes. Therefore it is necessary to treat dependent functions simultaneously to provide proper consideration of the conditional probabilities involved.

Discrete vs Continuous Densities for Input Data and $R||C$ Analysis Output Functions

The density functions of the input random variables—the input data of the $R||C$ analysis—can be presented in one of two forms: (1) discrete variable relative frequency distributions, usually a summarization of test results, sometimes called "batch" data, and (2) a closed form representation—a formula form of the density function. Of course we must be able to carry out an $R||C$ analysis when input densities are in either of these forms or when they are in a combination of them. If

* The parenthesis in the symbol $(C - R)$ is used to denote that we are treating the difference as a single random variable.

one or more input densities are in the discrete form, then the output density is necessarily discrete. Curve fitting procedures could then be used to obtain a continuous approximation and a formula representation. It is always possible to use discrete densities as approximations for continuous ones, and the computer programs which TEMPO has used in its R||C analyses require that this approach be used.

We are especially interested in the case in which all input densities are defined in closed form—a functional representation. In this case, the output densities can be expressed as integrals involving the input densities, but it is not always possible to perform the integration to derive a closed form functional representation for the output, R, C, or (C - R). Of course numerical integration techniques are available to handle such complex integrals. It should be noted that the functional form of an output density is often quite different from those of the inputs. The importance of this point lies in the fact that significant inaccuracy arises when one erroneously assumes an incorrect form of an output density. The most commonly encountered error in this connection is the false belief that Gaussian inputs generate Gaussian outputs. Appendix VI of this report contains a number of examples of closed form solutions to illustrate the integration procedures and to show this transformation of functional forms. Fortunately, the R||C analysis method does not require us to know in advance what form the output will take—the technique is able to generate the appropriate form automatically.

Data Sources

Since the input parameters in the transfer functions are often material properties, it is important to note that data sources need not be restricted to the project's own test programs. For example, data on properties of maraged steel can be obtained from manufacturer's tests or from tests in any program in which maraged steel is used. The application of such data to the system being analyzed is determined by the transfer function from the designer's equations and not from a requirement that the data be generated in tests of the actual system hardware. Thus, one of the great strengths of the R||C technique is its ability to expand the data base through the use of data from other programs which share in materials being used even though the system hardware is entirely different. In fact, the data base is not only extended in this fashion, but it is an appropriate information source which is in existence in advance of the production of any hardware of the system being analyzed by the R||C methodology.

4. GENERAL COMMENTS ON DATA AND TRANSFER FUNCTIONS USED IN THIS STUDY

At the outset of this research program, it was recognized that the derivation of R and C transfer functions and the collection of necessary input data were major tasks. Aerojet General was charged with the responsibility for performing these tasks in their contract with NASA/OART. AGC not only supplied TEMPO with the data and the transfer functions, but they also provided information on data adjustment procedures and on special interpretations of the information which they felt to be appropriate and useful in the subsequent R||C analysis. Comments about specific data and transfer function characteristics are included in the application section of this report. In the present section, we will confine our attention to the general nature of the information supplied by AGC.

Since information unavailability is often alleged, it is extremely important to note that AGC was able to obtain transfer functions and data in spite of the problems involved. Of course, they found it necessary to use some approximations and thus to introduce a degree of uncertainty in the analyses of some failure modes—this is essentially the ever present problem of data shortage coupled with uncertainty about such things as physics of failure and environmental stress profiles. A slight degree of uncertainty was also introduced when AGC was forced to use a design criterion instead of a true physics of failure relationship for one transfer function. It was expected that this would probably lead to an underestimate of reliability since design criteria frequently contain an unquantified degree of conservatism.

On a number of occasions, AGC expressed concern about the small sample sizes which they were sometimes forced to use to generate input densities. They indicated their belief that such data problems should be handled by assuming that input densities should be Gaussian, that sample data tended to give reasonably good estimates of mean values, and that from other information, AGC could obtain good estimates of coefficients of variation. Accepting these assumptions by AGC, TEMPO was required to use Gaussian inputs in all of the R||C analyses reported on herein.

It must be pointed out that TEMPO has some reservations about this widespread use of the Gaussian curve, and AGC recognizes that it is open to question in some cases. For example, a parameter which can never be negative can certainly not have a Gaussian density. One can visualize many parameters which have finite bounds on both sides—web thickness is greater than zero and it surely will never be infinite! In the next phases of this research, it is hoped that data can be obtained in a form which does not force the use of the Gaussian assumption, especially where it is clearly quite inappropriate.

The limited data base which could be developed within the restrictions of time and funding was responsible for one disappointment in this study. It had been hoped that for a few cases, comparative R||C analyses could be performed, one using raw or batch data and the other using the fitted Gaussian functions. Unfortunately, there was no case in which suitable batch data was available, so this comparative analysis was not possible.

5. APPLICATION OF THE METHODOLOGY TO A LARGE SOLID ROCKET MOTOR

A complete reliability study of a system would require the application of the R||C analysis technique for each failure mode by itself, that is, independently of all others, and then an application of the methodology to all failure modes simultaneously, bringing into the analysis all of the interdependencies which exist. Independent analysis of a particular failure mode would tend to focus attention on specific reliability problems in terms of design characteristics as related to that individual mode. However, the study of all failure modes together is essential to arrive at suitable estimates of system reliability. Of course, the combined failure mode treatment can be derived from the separate analyses of individual failure modes if the associated transfer functions are independent. The analysis can often be simplified by neglecting some failure modes, the criterion for the selection of these modes being that their individual and collective contributions to unreliability must be insignificant, assuming an appropriate determination of what we should mean by insignificant in the light of the seriousness of failure. The limited research effort provided by the present contract precluded the simultaneous consideration of failure modes so this report covers only the analysis of individual modes by themselves.

In conference with representatives of NASA, AGC, TRW Systems and TEMPO, the following 14 failure modes were selected for study of the 260/SIV-B Motor System:

1. Hoop Stress Case Rupture
2. Insulation Burn Through
3. Failure of the Forward Motor Skirt Forging in Combined Compression, Shear, and Bending
4. Meridional Stress Case Rupture
5. Rupture of the Nozzle Joint Bolts
6. Separation of the Motor Chamber and Nozzle Flange
7. Propellant Maximum Inner Bore Hoop Strain Storage Condition
8. Propellant/Liner Interface Maximum Radial Bond Stress Failure Mode, Storage Condition
9. Propellant Maximum Combined Stress (Principal Stress), Shear and Tension Storage Condition

10. Propellant/Liner Interface Maximum Shear Stress Flight Condition
11. Propellant Maximum Inner Bore Hoop Strain Flight Condition
12. Insulation/Motor Case Interface Bond Maximum Shear Stress Flight Condition
13. Propellant Auto Ignition Due to Static Discharge
14. Propellant Auto Ignition Due to Self Heating

These failure modes are those selected consistent with contract statements of Tasks I through XIII listed under Study Objectives. The first six failure modes are in general those itemized under Task VIII. However, some trade-offs were made by AGC to cover the aft closure and bolt failure modes instead of the forward areas because better design data was available. In order to gain further insight into the rocket motor failure problems, special analyses were made for a few significant subdivisions of some of the 14 listed failure modes.

Details of the analysis for each of the above listed 14 failure modes is given in Appendix II of this report. In this section, we have included a brief description of the basic nature of each of the failure modes, a table summarizing the transfer function equations for each, a table listing all of the parameters and giving values of means and standard deviations, a table which summarizes the reliabilities associated with each mode, and finally, a table summarizing the sensitivity analyses for failure mode 1. These tabular summaries are followed by a few comments on these study results. The discussion of computational procedure is included in the appendices. Again it should be noted that AGC asked TEMPO to base their analysis on the assumption that all input parameters are Gaussian, recognizing that this is not entirely realistic.

Failure Mode 1. - Hoop Stress Case Rupture

This failure mode is identified as a failure of the longitudinal weld. Past experience by AGC shows that about 10 percent of the machine welds have flaws detectable in inspection. For these, the welds are reworked by hand techniques and experience indicates that hand welds are weaker on the average and they have greater variability in strength than do machine welds. Hence, the failure probability for this mode is computed on the assumption that 90 percent of the welds are by machine and 10 percent are by hand. It is believed by AGC that 40' aft of

motor station 2 (Fig. 1) is the critical station for this mode, so this failure mode probability for the motor is based on an analysis for this station.

Failure Mode 2. - Insulation Burn Through

For this mode, AGC defined failure as burning all of the propellant and burning through the insulation, meaning burning to but not necessarily through the case. Obviously, the burn through probability varies by motor station. AGC suggested that TEMPO consider stations 1, 2, 4, 5, 6, 7 and 12 as identified in Figure 1. At stations 1 and 12, there is no propellant so the transfer function relationship had to be appropriately modified.

Failure Mode 3. - The Failure of the Forward Motor Skirt Forging in Combined Compression, Shear, and Bending

For this mode, failure consists of inelastic deformation and buckling resulting from the joint action of axial compression, transverse shear and bending forces acting on the forward motor skirt forging. The AGC engineers felt that it would be better to use a modification of the usual transfer function approach when considering this mode of failure. Rather than attempting to express requirements in terms of the compressive, shear, and bending forces and the capability in terms of the design and materials parameters, AGC chose to use a design criteria relationship. This empirical relationship combines the ratio of the requirement of each type of load to the corresponding allowable in an interaction formula such that if the sum of the ratios is greater than unity, failure is assumed to occur.

Failure Mode 4. - Meridional Stress Case Rupture Failure Mode

The major failure risk for this mode is the rupture of forward head circumferential welds due to meridional stress. All welds are initially made by machine but inspection shows that about 10 percent are defective. These must be reworked by hand techniques. It will be noted that hand welds on the average have less strength than machine welds and their strength is more variable. The failure probability for this mode is computed as a weighted average using 90 percent machine welds and 10 percent hand welds.

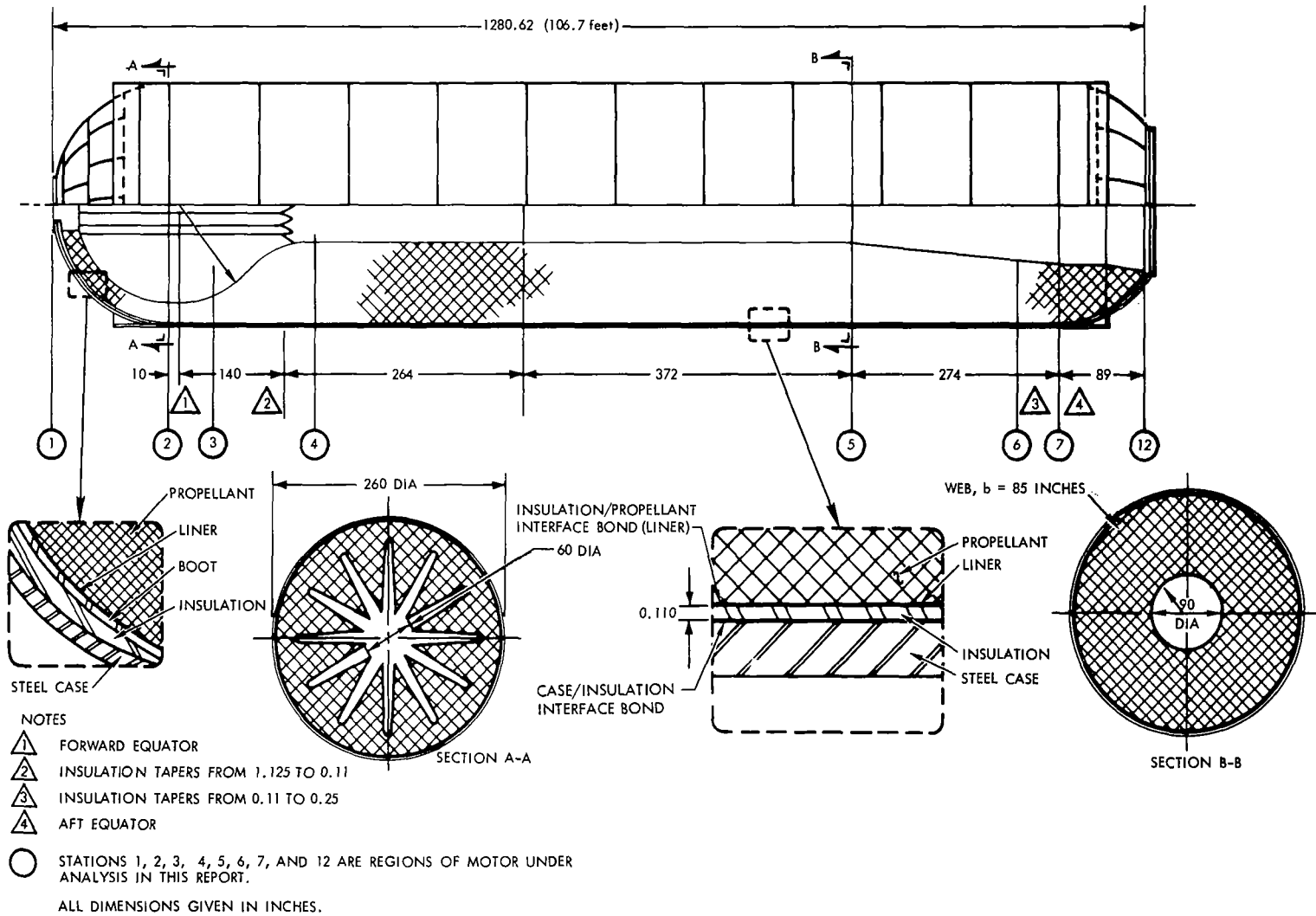


Figure 1. 260/SIVB motor-propellant grain, insulation and case design.

Failure Mode 5. - Rupture of the Nozzle Joint Bolts

For this mode, failure is the rupture of the nozzle joint bolts due to combined loads of pressure ejection and TVC bending moments. The requirement function involves the tension due to pretorquing, a portion of the ejection load due to internal and external pressure and inertia, and the added tension effect due to the thrust vector control moment.

Failure Mode 6. - Separation of the Motor Chamber and Nozzle Flange

This mode involves the same forces as failure mode 5. However, in the case of failure mode 6, we are concerned with the occurrence of leakage due to separation which is a consequence of deformation of the bolts short of rupture.

Failure Modes 7 through 12

Five failure modes, 7 thru 12 inclusive, are related to propellant stress problems. These will be discussed collectively because of their close relationship. The failure modes are as follows.

Failure Mode 7. - Propellant Maximum Inner Bore Hoop Strain Failure Mode, Storage Condition

Inner bore grain Failure in hoop stress due to cool down and storage (undetected), critical station - center region of motor.

Failure Mode 8. - Propellant/Liner Interface Maximum Radial Bond Stress Failure Mode, Storage Condition

Propellant/Liner interface bond fails radially during cool down and storage (undetected), critical station-aft end of motor.

Failure Mode 9. - Propellant Maximum Combined Stress (Principal Stress), Shear and Tension Failure Mode, Storage Condition

Failure of propellant due to combined shear and tension stress during cool down and storage (undetected), critical station - aft end of motor.

Failure Mode 10. - Propellant/Liner Interface Maximum Shear Stress Failure Mode, Flight Condition

Propellant/Liner interface bond fails due to shear stress during cool down and storage (undetected), critical station forward end of motor.

Failure Mode 11. - Propellant Maximum Inner Bore Hoop Strain Failure Mode, Flight Condition

Inner bore grain failure in hoop stress due to pressurization and flight acceleration, critical station - aft end of motor.

Failure Mode 12. - Insulation/Motor Case Interface Bond Maximum Shear Stress Failure Mode, Flight Condition

Insulation/Motor Case Interface bond fails in shear for 2g maximum launch acceleration.

Failure modes 7, 9, and 11 relate to propellant cracking while modes 8, 10 and 12 are concerned with separation between the propellant and the case. The names identify the stresses. These various propellant stress relationships are perhaps the most complex and least understood of all solid rocket motor failure modes. AGC ran a rather complex computer program to obtain some feel for the severity of these failure modes using a set of randomly selected inputs for each run of the computer program. Within the constraints of their analysis and relatively few runs made (because of the cost aspect), the outputs they generated were in the form of R and C functions. AGC also said that these output R and C density functions were Gaussian. Hence we were able to use a closed form solution, Gaussian in this case.

Failure Modes 13. - Propellant Auto Ignition Due to Static Discharge

Failure of motor due to propellant self ignition from static electrical discharges.

Failure Mode 14. - Propellant Auto Ignition Due to Self Heating

Failure of motor due to propellant self ignition from endothermal self heating within the propellant, caused by internal reactions.

These two failure modes, 13 and 14, are similar in that they both involve ignition of the propellant. The causes of ignition do of course differentiate them and the brief descriptions adequately identify these causes.

Discussion and Results - R||C Analysis of Failure Mode 1 - 14

Table 1 shows the Requirement (R) function and the associated Capability (C) function for each of the first six of these failure modes. The parameters involved in these functions are defined in Table 2, "Summary of Parameters". A detailed discussion of this information is given in Appendix II.

It should be noted that the units are not necessarily the same for each of the R functions (Obviously, the units must be the same for an R function and its associated C function.). The units depend upon the type of failure modes being considered and very frequently the preference of the engineer who derives the associated transfer functions. For example, one engineer may prefer to express the requirement on a structural member in terms of a load per unit of area (e. g. pounds per square inch) while another engineer may prefer to express the requirement as the total load (e. g. pounds).

As noted above, Table 1 contains the R and C functions for the first six failure modes. For failure modes 1, 4, 5, and 6 and the R and C functions are engineering relationships which describe an imposed stress or load on the system (R) and the ability of the system to withstand that particular stress or load (C). For failure mode 3, however, the R function is a somewhat different type of relationship. It is a design criterion used to decide on the adequacy of the design of the forward motor skirt under combined compression shear and bending when considering inelastic deformation and/or buckling of the skirt. If the value (which is dimensionless) resulting from this calculation is less than 1.0 then the forward motor skirt is judged to be adequate. For failure mode 2 the R and C functions are gross time relationships. However, in the absence of a more refined description of the time that burning takes place in the motor and the time it will take to burn through to the case wall in terms of the physics and chemistry of the propellant and the insulation, these relationships are very useful for estimating the probability of failure for this failure mode. A few of the parameters in the R and C functions for the first six failure modes are treated as constants rather than as random variables because they have essentially zero variances. A discussion and description of how the random variable are combined, via the appropriate R or C function, to determine the probability of failure is given in Appendix IV.

Table 1. Summary of R||C functions.

Failure Mode #	Requirement (R) Transfer Function	Capability (C) Transfer Function
FM1*	$\frac{P_{cmax} \cdot R_o}{t_c}$	$K_{be} \cdot K_{bx} \cdot S_{umw}$
FM2	$\frac{b'}{r_b}$	$\frac{b}{r_b} + \frac{t_i}{e_r}$
FM3**	$\frac{L_c}{2 \cdot \pi \cdot R_i \cdot t_s \cdot K_c \cdot E_s} + \left[\left(\frac{L_b}{\pi \cdot R_i^2 \cdot t_s \cdot K_b \cdot E_s} \right)^3 + \left(\frac{L_s}{\pi \cdot R_i \cdot t_s \cdot K_s \cdot E_s} \right)^3 \right]^{1/3}$	1
FM4*	$\frac{P_{cmax} \cdot R_o}{2 \cdot t_c}$	$K_{be} \cdot S_{umw}$
FM5*	$K_p \cdot F_{by} + \left[\frac{\tan \alpha \cdot d \cdot 0.8538 \cdot P_{cmax} \cdot A_{ti} \left(1.66642 - \frac{11 \cdot P_a}{0.8538 \cdot P_{cmax}} \right)}{\left(\frac{n}{2} \right) \cdot \left(\frac{D_j}{2} \right)} \right]$	P_y
FM6*	$0.9981 \cdot P_{cmax} \cdot A_{180} \cdot (1 + \gamma \cdot M_{180}^2) - 0.014092 \cdot P_{cmax} \cdot A_{ei} \cdot (1 + \gamma \cdot M_e^2) + P_a \cdot (A_{ei} - A_{180})$ $+ \frac{W_{ni} \cdot (W_p + W_{vi})}{0.8538 \cdot P_{cmax} \cdot A_{ti} \cdot \left(1.66642 - \frac{11 \cdot P_a}{0.8538 \cdot P_{cmax}} \right)}$	$K_p \cdot F_{by}$

$$* P_{cmax} = \frac{W \cdot r_b \cdot K_m / a \cdot e^{\pi k \cdot \Delta t}}{C_w \cdot A_t \cdot b}$$

** See discussion of FM3 on page 14 regarding special characteristics of R and C for this failure mode.

Table 2. Summary of Parameters.

Description, mean values, standard deviations, applicable failure modes

Parameter symbol	Description of Parameter	Location, Motor Station	Average \bar{x}	Std. Dev. σ	Applicable Failure Modes
A _{ti}	Initial Throat Area in ²	Nozzle Throat	6,235	0	5,6
A _{ei}	Initial Exit Area, in ²	Nozzle Exit	56,116	0	6
A _t	Average Throat Area, in ²	Nozzle Throat	6,355	20.9	1,4,5,6
A ₁₈₀	Area at Nozzle Joint, in ²		25,477	0	6
b	Propellant Web, in.	sta 4	87.5	.175	2
b	"	" 5	85.0	.17	1,2,4,5,6
b	"	" 6	71.85	.1437	2
b	"	" 7	70.57	.1411	2
C ₇	Propellant inner bore hoop strain storage in/in	Center Motor	.242	.0392	7
C ₈	Propellant/liner radial bond stress, storage, psi	Aft end Motor	18.3	2.84	8
C ₉	Propellant principle stress, storage, psi	Aft end Motor	18.3	2.84	9
C ₁₀	Propellant/Liner shear stress, flight, psi	Fwd end Motor	418	39.2	10
C ₁₁	Propellant inner bore hoop strain, flight, in/in	Aft end Motor	.441	.0674	11
C ₁₂	Insul. /case bond shear strength, psi		375	64.13	12
C ₁₃	Propellant Ignition threshold jowles	Total Propellant	12.8	.188	13

Table 2 Continued

Parameter symbol	Description of Parameter	Location, Motor Station	Average \bar{x}	Std. Dev. σ	Applicable Failure Modes
C_{14}	Propellant auto-ignition temp, °F	Total Propellant	586	5.5	14
C_w	Mass flow coefficient, sec^{-1}		.0062477	.000019	1, 4, 5, 6
d	dist. TVC port & joint, in.	TVC port	178.84	0	5
D_j	dia. of Nozzle joint, in.	TVC joint	180	0	5
E_o	Propellant	Total Propellant			7-14
E_s	Motor Case Modulus of Elasticity, psi		27,500,000	54,725	3
e_r	Insulation erosion rate, in/sec	1, 2	.003	.000489	2
e_r	"	5, 6	.005	.002586	2
e_r	"	7	.006	.000979	2
e_r	"	12	.0168	.00274	2
F_{by}	Min. Tensile Load per bolt, lb	Nozzle flange	213,310	0	5
K_{be}	Bending/discontinuity factor (ND) (3)	cylinder	.95845	.00693	1, 4

Table 2 Continued

Parameter symbol	Description of Parameter	Location, Motor Station	Average \bar{x}	Std. Dev. σ	Applicable Failure Modes
K_{bx}	Biaxial gain factor, (ND)	spheric al ends	1.106	.0312	1
$K_{m/a}$	Ratio of Avg to Peak chamber press. (ND)	chamber	1.18	.008968	1, 4, 5, 6
K_c	Ratio of Axial Compressive strength to E. (ND)	Fwd Skirt	.0036	.000685	3
K_b	Ratio of pure bending strength to E. (ND)	"	.005	.000968	3
K_s	Ratio of transverse shear to E. (ND)	"	.00288	.00334	3
K_p	Fraction of bolt min. yield, to which bolt is pretorqued (ND)	Nozzle flange	.60	.077	5, 6
L_c	Axial compressive load, lb.	Fwd Skirt	2, 200, 000	0	3
L_b	Pure bending load, lb.	"	94, 000, 000	0	3
L_s	Transverse Shear load, lb.	"	60, 000	0	3
M_{180}	Mach Number of gas stream at joint dia. (ND)	Aft chamber	.0576	0	6
M_e	Mach Number of gas stream at exit plane (ND)	Nozzle Exit	3.205	0	6
n	Nozzle flange bolts, number.	Nozzle flange	220	—	5, 6

Table 2 Continued

Parameter symbol	Description of Parameter	Location, Motor Station	Average \bar{x}	Std. Dev. σ	Applicable Failure Modes
P_{cmax}	Max Chamber Pressure, psi.	Fow'd End	(1) _____	—	1, 4, 5, 6
P_a	Ambient Atmospheric pressure, psi	Nozzle Flange	14, 696	.0735	5, 6
P_y	Nozzle attach bolt Load capability, lb/bolt	Nozzle	245, 307	1987	5
R_7	Propellant Rqm't. corresponding to C_7 through C_{14} .	Center, motor	.037	.0374	7
R_8	"	Aft end, motor	2.47	.282	8
R_9	"	"	5.51	.604	9
R_{10}	"	Fwd. Equator of motor	30.62	9.52	10
R_{11}	"	Aft end, motor	.0749	.0489	11
R_{12}	"		30.62	9.52	12
R_{13}	"	Total Propellant	.015 (max)	0	13
R_{14}	"	Total Propellant	100.1 (max)	0	14
R_o	Outside radius, motor in.	Cyl. portion of case.	130.631	.0261	1
R_o	"	Spherical portion of case.	130.428	.0456	4

Table 2 Continued

Parameter symbol	Description of Parameter	Location, Motor Station	Average \bar{x}	Std. Dev. σ	Applicable Failure Modes
r_b	Propellant burn rate in/sec.	2, 5, 6, 7,	.606	.00361 ⁽²⁾	1, 2, 4,
r_b	"	aft	.606	.00818 ⁽²⁾	5, 6
r_b	"	4	.590	.00351 ⁽²⁾	1, 2, 4,
R_i	Radius to inner surface of nozzle skirt, in.	Nozzle skirt	129.903	.0203	3
R_c	Ratio of axial compressive load reqm't. to material capability (ND)	Fwd skirt	— ⁽¹⁾	—	3
R_b	Ratio of transverse shear load reqm't to material capability (ND)	"	— ⁽¹⁾	—	3
R_s	Ratio of pure bending load requirement to material capability (ND)	"	— ⁽¹⁾	—	3
S_{umw}	Ultimate machine weld strength, psi	case welds	232,000	2,516.6	1, 4
S_{uhw}	Ultimate hand weld strength, psi	case welds	199,333	8,641	1, 4
t_i	Insulation thickness, in.	1, 2	1.125	.01667	2
t_i	"	5	.110	.0033	2
t_i	"	6	.250	.01667	2
t_i	"	7	.43	.01667	2
t_i	"	12	3.6	.01667	2

Table 2 Continued

Parameter symbol	Description of Parameter	Location, Motor Station	Average \bar{x}	Std. Dev. σ	Applicable Failure Modes
t_c	Motor case thickness, in	Cyl.	.6392	.0095	1
t_c	" " " "	Spherical	.428	.0108	4
t_s	Motor skirt thickness, in.	Fwd Skirt	.728	.0093	3
W_p	Propellant Weight, lb.	Motor	3,400,000	6,120	1,4,5,6
W_{ni}	Initial Nozzle Weight, lb.	Nozzle	58,428	0	6
W_{vi}	Initial Launch Weight of vehicle less first stage propellant, lb.	--	726,466	0	6
π_k	Temperature sensitivity coef. %/°F.	Propellant	.16	.00676	1,4,5,6
α	T. V. C. angle, degree	Nozzle	3.6	0	5
γ	Ratio of specific heats (ND)	Propellant	1.2	0	6

- Notes:
- (1) These terms are functions of many parameters, and density functions can be generated for these for a given set of input data.
 - (2) AGC selected these input parameter values. Their selection criteria are briefly discussed in Appendix I.
 - (3) (ND), Non Dimensional

For failure modes 7 through 14, AGC did not submit transfer functions and input parameter densities. Rather, they gave us means and standard deviations for capability and requirement densities which they said were all Gaussian. Hence for all of these modes, we could write a closed form solution since the difference of two Gaussian variables is also Gaussian. The notation is as follows.

	Variable	Mean	Standard Deviation
Capability	C	\bar{C}	σ_C
Requirement	R	\bar{R}	σ_R
Capability minus Requirement	(C-R)	$\bar{C} - \bar{R}$	$\sigma_{(C-R)} = \sqrt{\sigma_C^2 + \sigma_R^2}$

The probability of failure is obtained from tables of the normal function as the area in one tail of the normal curve with zero mean and unit variance beyond the point

$$\frac{\bar{C} - \bar{R}}{\sqrt{\sigma_C^2 + \sigma_R^2}}$$

The basic data supplied by AGC is shown in Table 2. As noted earlier, this data was treated in two ways. First, an R||C analysis was made for each failure mode using the input data with no modification —these were called standard analyses. This was followed by analyses which used a series of data modifications, usually increases or decreases in the input standard deviation and less often by shifts in the value of the mean. These so-called sensitivity analyses were made to establish the criticality of the parameters with respect to the failure probabilities. A listing of the results of all of the standard analyses is shown in the body of Table 3. The footnotes illustrate the kinds of answers obtained in the sensitivity analyses for failure mode 2, these being quite completely described in Appendix II. Table 4 illustrates a more complete sensitivity analysis which was made for failure mode 1.

The case insulation burn through failure mode (FM 2) provides a very good illustration of the value of R||C analysis in terms of the

Table 3. Summary of failure modes R||C analysis.

Failure Mode	Description	Motor Station	P[S] for Standard Run
FM 1	Hoop stress, case rupture	Forward	>.999999
FM 2	Case insulation burn through	1, 2	>.999999
"	" " " "	5	.983907 (1)
"	" " " "	6	.862888 (2)
"	" " " "	7	.988810 (3)
"	" " " "	12	.953370 (4)
FM 3	Failure of forward motor, skirt forging in combined compression; shear and bending	Forward Skirt	>.999999
FM 4	Meridional stress, case rupture forward head	Forward Head	>.999999
FM 5	Rupture of nozzle joint bolts	Nozzle Flange	>.999999
FM 6	Separation of Motor Chamber and nozzle flange	Nozzle Flange	.999998
FM 7	Propellant max. inner bore hoop strain-storage	Center of Motor	.999999
FM 8	Propellant liner interface max. radial bond stress-storage	Aft end, Motor	>.999999
FM 9	Propellant maximum combined stress in shear and tension-storage	Aft end, Motor	.999989
FM 10	Propellant/Liner interface max. shear stress-flight	Forward end Motor	>.999999
FM 11	Propellant max Inner bore hoop strain-flight	Aft end Motor	>.999999
FM 12	Insulation/Motor interface bond. Max shear-flight	Bond Surface	>.999999
FM 13	Propellant autoignition due to static discharge	Total Propellant	>.999999
FM 14	Propellant autoignition due to self heating.	Total Propellant	>.999999

NOTES: (1) For double insulation, P[S] = .999988
 (2) For double insulation, P[S] = >.999999
 (3) 50% increase in insulation, P[S] = .999999
 (4) 50% increase in insulation, P[S] = >.999999

Table 4. Summary of sensitivity analyses for failure mode 1.

Run	Parameter	Variability Factor V_f	σ	$V_f \sigma$	P[S]
Standard	*	1	*	*	> .999999
1	Sumw	4	2516.6	10066.4	.999772
	Suhw	2	8641.	17282.	
2	Sumw	8	2516.6	20132.8	.994983
	Suhw	4	8641.	34564.	
3	r_b	4	.00361	.01444	.999781
4	K_{be}	5	.00693	.03465	.999995
5	K_{be}	10	.00693	.0693	.999832
6	$K_{m/a}$	5	.00897	.04485	.999999
7	$K_{m/a}$	10	.00897	.0897	.999885

NOTE:

*The standard run used the unadjusted data supplied by AGC for all parameters and, consequently, the variability factor is unity. For other runs, unadjusted data was used for all parameters except for those noted in the column labeled "Parameter."

standard data and also of the sensitivity analysis. The reliability of .862888 at station 6, standard data, is entirely too low to be acceptable, a fact which would not have been easily recognized and quantified without R||C analysis. The significance of insulation thickness is shown in the sensitivity analysis, footnote 2, in which a doubling of the insulation thickness at this station raises the reliability above .999999. At stations 7 and 12, an increase of 50% in insulation thickness is ample to provide a reliability increase to the level of .999999 at each of these stations.

The hoop stress failure mode, FM 1, also provides an interesting illustration of the value of R||C analysis, especially with respect to a study of the sensitivity of the failure probabilities to changes in the data inputs. The numerical results of eight runs are summarized in Table 4. The unadjusted AGC data is used in the standard run which yielded an estimated reliability in excess of .999999. The other runs, identified as runs 1 through 7 in Table 4, were based on modifications of the unadjusted standard deviation. The modification consisted merely of multiplying the unadjusted standard deviation, σ , by a variability factor, V_f , as shown in the table. The variability factors should be selected to cover some realistic range for the particular parameter under consideration. Runs 1 and 2 involved modifications in weld strength standard deviations for both machine and hand welds. Each of the other runs involved only one variability factor associated with the indicated parameter. As expected, increases in input standard deviations lowered the reliability estimates, the lowest value being .994983 for run 2. The details of this analysis are given in Appendix II.

In summary, Table 3 indicates that there are a few problem areas in the case insulation burn through, but that for most failure modes, reliabilities are close to the range of .999999 and above. Furthermore, the sensitivity analyses identify those parameters which are most critical in causing the unreliabilities and indeed it measures the extent of the influence of each on the related failure probabilities. Thus, the sensitivity analyses demonstrate the way in which the R||C technique serves as a valuable design tool, quantifying the effect of a proposed modification on reliability in advance of its implementation. In other words, it permits the designer to make more nearly optimum trade-offs in solving his design problems as they arise.

Consideration of System Interactions In Determining the Probability of One or More Failure Modes

To determine the probability of the occurrence of one or more failure modes (i. e. the probability of system failure) or, if one wishes, the probability of no failure mode occurrences (i. e. the probability of system success-or reliability) the correlation between parameters which interact to define the various failure modes must be properly considered. If, for example, no correlation exists (i. e. all failure modes, and consequently all parameters, are statistically independent of one another) then the probability that no failure mode will occur in the system is simply the product of the probability of the non-occurrence of each single failure mode. When correlation exists between failure modes, however, the correlated failure modes must be treated simultaneously to determine the probability of the occurrence of one or more of the modes (It should be noted that this probability will be greater than the probability of the occurrence of any single failure mode.). A detailed discussion of this process is given in Appendix IV, entitled "Computations When There Is Dependence Between Two or More Transfer Functions."

General Comments on the Motor Example

Up to this point the report has provided a brief survey of the background upon which the current work is based, a summary of the current state of development of the R||C methodology, and a description of the application of the method to the reliability analysis of the 260 inch solid rocket motor which has been performed to date. In this discussion of the motor example, we would like to synthesize all of this information into a logical presentation of the current status of this research program and an interpretation of this status in terms of the objectives which we believe we have accomplished and the objectives which should serve to guide future efforts.

Throughout the sequence of studies on the reliability of solid rocket motors, it has been clear that the purpose has been two-fold: (1) provide information which can be used to enhance the reliability assessment of the large solid rocket, or any system, and (2) develop techniques which will help us assess the level of reliability throughout the development of these systems. We have been concerned primarily with the use of the 260 inch

motor system as an example with all the problems attendant an expensive item which will have only limited production and naturally very limited development test firing. These characteristics have necessarily lead us to emphasis on analytical techniques. We feel very strongly that this emphasis on analytical methods has not in any way sidetracked this work from the two practical objectives listed above—we are certainly attempting to provide the design engineer with information which will assist him in his design effort and methods whereby he can assess his progress toward assigned reliability goals.

The application of R||C methodology to the motor example led to several observations. It is felt that the feasibility of performing R||C analyses on real systems has been definitely established. Even though we may not be able to analyze every failure mode, we can cover a large number of them, perhaps the most critical, thus reducing the area of uncertainty. In establishing this feasibility, it is clear that this method is a useful design tool, especially in the performance of design trade-off studies in advance of testing. The limited examination of closed form solutions in Appendix VI illustrates what really is involved in the basic theory. Of course it points out the complexity of the mathematics involved and thus it serves to reemphasize the versatility and economy of a time sharing computer system. The adaptation of the GE time sharing computer for example, to the problem of combining random variables quickly and cheaply, has been one of the most significant outputs of this research effort. We have seen how it can combine probability densities without resort to Monte Carlo methods—it in effect generates discrete approximations to closed form solutions with the capability of reducing approximation errors to any required low level. The examples which have been worked out also demonstrate that, as far as the method is concerned, it is quite unnecessary to attempt to pre-judge the form of the input densities. The method works equally well with density equations, with tables of discrete data, or with any combination thereof.

In summary, then, it seems appropriate to say that the numerical results obtained in this phase of the study are encouraging to the extent that they do validate the R||C method. With respect to methodology, results seem to be quite close to expectation. The major problems involved in combining random variables have been solved but future research can provide even faster and cheaper techniques through proper revision and improvements of the computer programs.

6. CONCLUSIONS

The goals of this study, namely to demonstrate the R||C analyses of certain failure modes on a large solid rocket motor, have been met to a degree that demonstrates the soundness of the technique. The research effort associated with these goals, and described herein covers a) reliability analysis of the large solid rocket motor, and b) technique development. Hence it is appropriate to present the conclusions (and in Section 7 the recommendations) in the two corresponding categories.

1. Conclusions Concerning Estimates of Reliability of the Large Solid Rocket Motor System.
 - 1.1 Failure Modes 1 and 4 cover hoop and meridional stresses of the case welds. The analysis shows that the weld strength parameters of hand welds are by far the most critical—they are used in the rework of defective machine welds. Although only 10% of all welds were done by hand, they greatly predominated the failure probability by many orders of magnitude.
 - 1.2 The insulation burn-through failure mode was found to be critical at four motor stations, 5, 6, 7, and 12. These had undesirable reliability estimates of .984, .863, .989 and .953 respectively. The sensitivity analysis indicated two things: first that these reliabilities could be raised to satisfactory values if the insulation were increased by varying amounts at the critical stations, or if the standard deviation of the insulation erosion rate could be decreased; second, that the insulation erosion rate variability was the most sensitive parameter by far. Some parameters showed little effect on the estimate of reliability even when they were increased an order of magnitude or more (e. g. propellant effective web thickness could be reduced 10 inches and still not affect burn-through significantly).
 - 1.3 Analysis of the forward motor skirt forging in combined compression, shear and bending indicated very low probability of failure.
 - 1.4 Results indicated that the probability of rupture of the nozzle joint bolts was very low.
 - 1.5 Separation of the motor chamber and nozzle flange failure mode showed a reliability of .999 998. However, further attention should be given to the parameters associated with this failure mode because the sensitivity analysis showed that values of about .98 were possible.

- 1.6 The two propellant failure modes 7 and 9 dealing with inner bore hoop strain-storage, and principle stress-storage, appeared to be marginal in terms of their reliability and warrant further study.
- 1.7 The three propellant failure modes 8, 10 and 11, which involve propellant/liner interface radial bond stress—storage, propellant/liner interface shear stress—flight, and propellant inner bore hoop stress—flight, showed relatively low probabilities of failure.
- 1.8 The insulation/motor case interface bond failure mode showed a relatively high reliability.
- 1.9 The auto-ignition failure mode appears to have an insignificant probability of occurrence on the basis of the data and other information currently available from AGC. They reported it to be much less than 10^{-6} .
- 1.10 Study results were distinctly encouraging in that the feasibility of application of the R||C method seemed to be clearly established. Given appropriate support, and necessary input data and transfer functions from AGC, then, GE time sharing (or possibly other computer techniques) has the capacity and flexibility ideally suited for such analyses.
2. Conclusions Relating to the Results of Technique Research.
 - 2.1 A methodology has been developed that can be used directly by the design engineer. The techniques used to implement this methodology have proven to be tractable and economical.
 - 2.2 Very satisfactory progress has been made in the development of computation methods using time sharing computer techniques. For example, the computer programs provided rapid and economical processing of input data when the inputs were assumed to be Gaussian as well as when raw data was used.
 - 2.3 It should be emphasized that the computer technique permits the accomplishment of R||C analysis, no matter what the forms of the input densities, through the use of discrete approximations to continuous densities.

- 2.4 Numerical accuracy is dependent on the accuracy of the input data and on the way in which the continuous density is approximated by the discrete one. Of course, the discrete approximation can be as good as required by forming a sufficiently large number of intervals with sufficiently small widths.
- 2.5 The data, in general, was available but some searching of the files by AGC was necessary.
- 2.6 The discussion of closed form solutions presented in Appendix VI pointed out the fact that input densities of a specified type do not regularly lead to output densities of the same type. Indeed, it is neither easy nor necessary to attempt to guess the form of the output density. The method will generate it without any guess by the analyst.

7. RECOMMENDATIONS FOR FUTURE WORK

Future efforts should be continued in the reliability analysis and technique development categories for solid rocket motor examples. Technique development, which included the mathematics and computer methods for handling the R||C analysis, is further advanced in the present phase of work than is the reliability analysis of the failure modes. It is therefore recommended that greater stress be placed upon the reliability analysis category; however, certain important improvements of the techniques are strongly advised.

1. Recommendations Relating to Reliability Analysis

1.1 The weld strengths were found to be the critical element of failure mode 1. This will require a detailed analysis of the elements that make up weld strengths and their associated variabilities:

- a) Fracture toughness, critical crack length, location, size, etc.
- b) Comparison of an alternative material such HY-160 steels.

Further study of welds that require hand processing should be made because of the predominant effect on reliability of their reduced strengths.

1.2 It is recommended that additional factors associated with the burn-through failure mode, such as the presence of cracks, voids, laps and folds, be considered in the future work. Further analysis of the variability of the insulation erosion rates should be made, since this was found to be a critical element of the analysis of failure mode 2. The time to burn through the case could be considered and its effect upon system failure could also be evaluated.

1.3 The current status of data generated and engineering analysis made by AGC of the bond and tensile stress failure modes associated with the grain was inadequate for a proper R||C analysis. Within the limitations of the data, however, the failure modes appeared to require further analysis because of their relatively low reliability:

- a) the propellant maximum inner bore hoop strain (storage condition), and
- b) the propellant maximum combined stress in shear and tension (storage condition)

It is suggested that further effort be made by AGC to generate additional data and transfer functions required for this analysis.

- 2. Recommendations Relating to Technique Research.
 - 2.1 The theory for handling dependence between failure modes which is merely correlation between transfer functions has been presented. However, the computational techniques for this situation need further refinement and this should be included in future phases of the research program.
 - 2.2 Further study should be made of those subsystems that have not yet been analyzed by the R||C technique (e. g. ignition system, nozzle, etc.)
 - 2.3 Consideration should be given to the problem of appropriately apportioning the reliability required for the total system to each of the individual failure modes.
 - 2.4 The R||C approach is general in its applicability and should be applied to other systems, as well as the large solid motor, such as the small motors, both liquids and solids, the hybrids, other liquid systems, etc.
 - 2.5 Future research should be devoted to further refinement of the computational procedures and to additional study of closed form solutions for more realistic transfer functions.
 - 2.6 Computer program refinements which were made during the course of this study indicate the feasibility of even more significant improvements, specifically in a reduction in the time which must be spent by an engineer in performing an R||C analysis. Research in this area should be pursued.

APPENDIX I

SUMMARY OF INPUT DATA,
RATIONALE AND DESIGN EQUATIONS
OBTAINED FROM AGC

Introduction

This appendix contains the input data received from AGC in the form of data packages and progress reports. This information consists of engineering equations, rationale, and density function data describing the means and variability of the parameters. These data are in general unmodified, with only minor changes and editing done in the interest of conformity to the report format or to prepare the form of the material for R||C analysis. The use of these data and transfer functions in R||C form are discussed in Appendix II, and summarized in Section 5 of the body of the report.

The AGC progress reports and data packages are listed in the references in this report. AGC has also prepared a final report covering these data (Reference 5).

Since it is not the intent to modify any data or comments, much of the following data is only briefly presented and explained. Certain sources referred to in their data packages were deleted. For more details, the reader is referred to the AGC progress reports, work packages, and final report as listed in the references.

Details of AGC Information on the Failure Modes

Failure Mode 1. Failure of Cylindrical Section Longitudinal Weld in Hoop Stress (Location 40" Aft of Forward Equator)

The basic engineering data for this failure mode is covered by AGC Data Pack II-1.

Table I. 1 summarizes the AGC parameter averages, standard deviations, and coefficients of variations for this failure mode.

Table I. 2 consists of the AGC support data, the "batch" data, from which is made up the summary data of Table I. 1. The rationale and engineering discussion in support of these data as supplied by AGC is as follows.

1. Capability Rationale. The formula used is the basic hoop stress formula modified to allow for a reduction due to local bending and discontinuities and for an increase due to biaxial gain. Ultimate, rather than yield parameters are used. The capability is calculated at the exterior surface which theoretically will experience greater stress than the interior. A location 40" aft of the forward equator* was chosen to eliminate the effects of discontinuity stresses associated with the transition from the cylindrical section to the forward head.

During the fabrication of the first two 260-inch diameter short length motors, it was found that manual repair welds had a lower strength than the normal machine welds. It is estimated by AGC that 10% of the total weld length of the 260/S IV-B motor would consist of manual welds. Therefore, the capability distribution should be constructed as the probabilistic sum of both a manual and a machine weld distribution, with the latter encompassing 90% of the total welds and the former 10%. All parameters used in the formula are assumed to be independently and normally distributed. The coefficient of variation, $\frac{\sigma}{\bar{x}}$, is assumed to be constant for varying values of \bar{x} .

Machine and Hand Weld Ultimate Tensile Strength. Data were available for a limited number of sample machine weld and hand weld coupons that were maraged in representative locations on both 260-SL chambers. A variety of weld wire heats are represented since it is this parameter rather than parent metal strength that governs weld strength. As can be

* This region occurs at about motor station 3.

Table I. 1 Summary of Capability Distribution Parameters: Averages, Standard Deviations and Coefficient of Variations for Failure Mode 1: Motor Case Hoop Stress Failure.

Parameter	Avg. or Nominal \bar{x}	Standard Deviation (Est. of Pop Deviation) σ	Coef. of Variation, σ / \bar{x} Non dim.	Source of Values
Machine Weld UTS, S_{umw} , psi	232,000	2516.6	.010847	\bar{x}, σ : 260-SL-1 and 260-SL-2 Maraged weld coupons*
Hand Weld UTS, S_{uhw} , psi	199,333	8641.0	.043350	\bar{x}, σ : 260-SL-1 and 260-SL-2 Maraged weld coupons*
Plate Thickness, t_c in.	.63922	.0095	.0149	\bar{x} : Design nominal σ : 18 plates from 18 heats used in 260-SL-1 and 260-SL-2*
Radius (exterior), R_o in.	130.631	.0261	.0002	\bar{x} : Design nominal σ : Tolerance on radius plus plate thickness variability*
Bending/Discontinuity Reduction Factor, K_{be}	.95845	.00693	.007231	\bar{x}, σ : Est from 260-SL-1 and SL-2 hydrotest strain gage data*
Biaxial Gain, K_{bx} Factor	1.1105	.0312	.0282	\bar{x} : Two PETV subscale hydroburst tests* σ : Nine D6AC 7.25 in dia test vessels*
Web Thickness, b , in.	85.0	.170	.002	\bar{x} : Design nominal σ : 260-SL-1 vs. 260-SL-2 (AGC Report NAS 7-572 PR -2, Figure 3)
Propellant Weight, W_p , lb	3,400,000	6120	.0018	\bar{x} : Design nominal σ : 260-SL-1 vs. 260-SL-2**
Burning Rate, r_b at (80°F), in/sec	.606	.00818	.0135	\bar{x} : Design nominal σ : 260-SL-1 vs. 260-SL-2 plus Scaleup Factor*
Temperature Sensitivity, π_k , %/°F	.16	.00666	.0416	\bar{x} : Design nominal σ : NASA Variability Study, Report 0815-*F, Figure 11
Max Temperature Difference, Δt , °F (Assumes max value)	20	—	—	\bar{x} : Extreme (100°F) Minus Nominal (80°F)
Ratio of Peak to Avg. Pressure, $K_{m/a}$	1.18	.008968	.0076	\bar{x} : Design nominal σ : Avg. of 4 Motor Programs*
Mass Flow Coefficient, C_w , sec ⁻¹	.0062477	.0000190	.00305	\bar{x} : Design nominal σ : Nine 52-in. -dia Motors*
Avg. Throat Area, A_t , in ²	6355	20.9	.00332	\bar{x} : Design nominal σ : 260-SL-1 vs. 260-SL-2*

* AGC routinely used the notation \bar{x} for mean and σ for standard deviation for all parameters in their data presentations even though other letters were used in the equations.

** See Table I. 2

Table I. 2 List of AGC Batch Data for Parameters Summarized in Table I. 1.

Maraged Weld Coupon Ultimate Tensile Strength		
1) <u>Machine Welds</u> , Sumw		
<u>Weld Wire Heat No.</u>	<u>UTS lb/in²</u>	<u>Maraged with Motor No.</u>
63343	231, 000	260-SL-1
8436	235, 000	" "
9035	231, 000	" "
8950	233, 000	" "
9620	228, 000	" "
9624	235, 000	260-SL-2
<u>9994</u>	<u>231, 000</u>	<u>" "</u>
$\bar{x} = 232, 000; \sigma = 2516.6$		
$cv = \frac{\sigma}{\bar{x}} = .010847$		

Maraged Weld Coupon Ultimate Tensile Strength		
2) <u>Hand Welds</u> , Suhw		
63343	189, 000	260-SL-1
63343	195, 000	" "
63343	197, 000	" "
9624	214, 000	260-SL-2
9624	197, 000	" "
<u>9620</u>	<u>204, 000</u>	<u>" "</u>
$\bar{x} = 199,333; \sigma = 8641$		
$cv = \frac{\sigma}{\bar{x}} = .04335$		

Table I.2 Cont

3) Plate Thickness, t_c

<u>Heat No.</u>	<u>Plate Thickness, in. (Avg of 15 Readings)</u>	<u>Within Plate Std Deviation*</u>	<u>Motor No.</u>
50265	.651	.0060	260-SL-2
50264 B1	.637	.0052	"
50338 B2	.640	.0033	"
50210-3	.647	.0057	260-SL-1
24997-1A	.631	.0060	"
24999-1A	.639	.0080	"
3951218-A	.631	.0060	"
25126-1	.638	.0070	"
3951215 B	.653	.0097	260-SL-2
3960819	.635	.0078	260-SL-1
3960832 A	.640	.0080	"
25098-1	.643	.0034	"
25007-1	.642	.0020	"
24998-1	.630	.0026	"
3960829 B	.636	.0092	260-SL-1
3960870 B	.625	.0051	260-SL-2
24996-1A	.642	.0049	"
<u>50234</u>	<u>.646</u>	<u>.0086</u>	<u>"</u>

$$\bar{x} = .63922 \quad \sigma_{\text{within plate}} = .0060 \text{ (avg)}$$

$$\sigma_{\text{plate to plate}} = .0074$$

$$\text{Total variability (any location)} = \sqrt{\sigma_{pp}^2 + \sigma_{wp}^2}; \sigma_t = .0095$$

$$\frac{\sigma_t}{\bar{x}} = .0149$$

* Estimated by range method. AGC used this method routinely for estimating standard deviations from small samples.

Table I. 2 Cont

4) Estimation of Radius Variability, R_o

- (1) Tolerance on radius = .125 in.
- (2) Assuming tolerance = 6σ , $\sigma_{R_o} = .0208$ in.
- (3) Variability of plate thickness $\sigma_{t_c} = .0095$
- (4) Combining plate and radius tolerance, $\sigma = .0228$

(5)
$$cv = \frac{\sigma}{\bar{x}} = \frac{.0228}{130.63} = .0002$$

5) Bending/Discontinuity Strength Reduction Factor, K_{be}

<u>Motor</u>	<u>Location</u>	<u>Net Tensile Stress psi</u>	<u>Bending Stress, psi</u>	$1 - \left(\frac{\text{Bending Stress}}{\text{Net Tensile Stress}} \right)$
260-SL-1	16	151,200	+ 4,850	.9679
"	17	153,500	+ 6,800	.9559
260-SL-2	43	149,400	+ 7,350	.9515
"	44	148,200	+ 6,400	.9585
				$\bar{x} = .95845$
				$\sigma = .00693$
				$cv = \frac{\sigma}{\bar{x}} = .007231$

Table I. 2 Cont

6) Biaxial Gain Factor, K_{bx}

(1) \bar{x} from 36" Dia Subscale Hydroburst Tests (18% Ni Maraged Steel)

<u>Test</u>	<u>Weld Coupon Uniaxial UTS, KSI</u>	<u>Burst Strength, KSI (PR/t)</u>	<u>Biaxial Gain Factor</u>
PETV-1	216	240	1.111
PETV-2	217	241	1.110
			$\bar{x} = 1.1105$

(2) σ from 7.25" Dia Subscale Hydroburst Tests (Ladish D6AC Steel)

<u>Test</u>	<u>Uniaxial UTS, KSI</u>	<u>Burst Strength, KSI (PR/t)</u>	<u>Biaxial Gain Factor</u>
1	233	258	1.107
2	225	262	1.164
3	222	254	1.144
4	230	257	1.117
5	235	256	1.089
6	241	263	1.091
7	241	263	1.091
8	234	252	1.077
9	230	246	1.070
			$\bar{x} = 1.106$
			$\sigma = .0312$
			$cv = \frac{\sigma}{\bar{x}} = .0282$

Table I.2 Cont

7) Propellant Weight, W_p

<u>Motor</u>	<u>Propellant Weight, lb.</u>
260-SL-1	1,676,366
<u>260-SL-2</u>	<u>1,673,000</u>

Range = 3,366 lbs.

$\sigma = 3,000^*$

$cv = \frac{\sigma}{\bar{x}} = \frac{3000}{1,674,683} = .0018$

Thus for 260/S IV-B: $\sigma = 3,400,000 (.0018) = 6120$ lbs.

NOTE: This observed σ/\bar{x} compares well with a figure of .0021 calculated from estimated variability of density, length, and web thickness.

8) Propellant Burning Rate, r_b

<u>Motor</u>	<u>Web Duration sec</u>	<u>Batch Mix Liquid Strand Burning Rate in/sec</u>
260-SL-1	113.7	.444
<u>260-SL-2</u>	<u>114.0</u>	<u>.441</u>

Range = .003 in/sec

$\sigma = .00265^*$

cv = .006

Thus for 260/S IV-B: $\left(\frac{\sigma}{\bar{x}}\right) (2.255)^{**} = .006 (2.255) = .0135$

and $\sigma = (.0135) (.606) = .00818$

* Using the range method

** Special AGC scaleup factor, see text, page I.12

Table I.2 Cont

9) Ratio of Avg. to Peak Pressure, $K_{m/a}$

<u>Program</u>	<u>Average Ratio</u> \bar{x}	<u>Motor to Motor Coefficient of Variation</u>
Minuteman Wing VI	1.17	.0050
Minuteman Wing I	1.08	.0082
Alcor	1.27	.0081
<u>Algol</u>	<u>1.08</u>	<u>.0091</u>
	$\bar{x} = 1.18^*$	$\overline{cv} = \frac{\sigma}{\bar{x}} = .0076^{**}$

For 260/S IV-B: $\sigma = 1.18 (.0076) = .008969$

10) Mass Flow Coefficient, C_w

<u>52-in. -dia Motor no.</u>	<u>C_w /sec</u>
1	.00624583
2	.00628364
3	.00624590
5	.00622264
6	.00626091
7	.00624864
10	.00623781
11	.00622428
<u>RCD-1</u>	<u>.00625999</u>
	$\bar{x} = .00624774$
	$\sigma = .00001904$
	$cv = \frac{\sigma}{\bar{x}} = .003048$

* This reported value was used in this study. (It should be 1.15)

** Average for 4 motor programs (see text).

Table I. 2 Cont.

11) Avg. Throat Area, A_t

<u>Motor No.</u>	<u>Avg. Throat Area, in²</u>
260-SL-1	3991
<u>260-SL-2</u>	<u>3979</u>

$$\text{Range} = 12 \text{ in}^2$$

$$\sigma = 10.65 \text{ (Based on range)}$$

$$cv = \frac{\sigma}{\bar{x}} = .00332$$

$$\text{For 260/S IV-B, } \sigma = 6355 (.00332) = 20.9 \text{ in}^2$$

NOTE: This observed $\frac{\sigma}{\bar{x}}$ value is the same as that obtained when based upon dimensional tolerances and observed linear erosion rate variability.

seen in Table I.2, items 1 and 2, the hand weld strength averaged 86% of the machine weld and it had a coefficient of variation of .04335 compared to the .0108 for the machine weld. The .04335 figure is probably excessive and indicates an area in which additional data is required.*

Plate Thickness. These data came from 18 plates of material that were used in 260-SL-1 and 260-SL-2, shown in Table I.2, item 3. In addition to the plate-to-plate variability, a within-plate component of variance was included to properly estimate the range of thickness possible at any given location. To save computational time, the within-plate component of variance was estimated for each sheet by taking a stratified sample of 15 readings of the 200 or more vidigage measurements actually made, and the average of these 18 within-plate standard deviations was squared and combined with the plate-to-plate variance to obtain an estimate of the total thickness variability.

Exterior Radius Variability. The exterior radius variability was estimated as the sum of two components of variance: the tolerance on the inside diameter and the variability of the plate thickness. As shown on Table I.2, item 4, the coefficient of variation derived from this combination of these two sources is an almost negligible .0002.

Bending/Discontinuity Strength Reduction Factor. While it is well known that local contour deviations and material discontinuities can result in bending stresses above that normally predicted, data as to the magnitude and variability of the amount of reduced strength that can be expected is extremely limited. The best data that can be obtained was derived from strain gage measurements taken during the hydrotest of the two 260-inch diameter motors. Table I.2, item 5, shows the bending stress estimated at four locations in the two motors. The locations were in the middle of the plates in the cylindrical section and were chosen as control gages to compare with readings at other locations where the effects of thin material, inclusions, and known contour deviations were being assessed. The strength reduction factor, calculated as one minus the ratio of bending stress to net tensile stress, was calculated for each of the four locations. The computed coefficient of variation, .0072, was assumed to represent the variability to be encountered.

Biaxial Gain Factor. The average level of biaxial gain in the cylindrical section was estimated at 1.1105 based upon the results obtained in two burst tests of 18% maraging steel 36-inch-diameter chambers. The coefficient of variation was determined to be .0282 for nine 7.5-inch-diameter Ladish D6aC test chambers. It is not known whether this value

* This is especially true since sensitivity analysis indicates that this parameter's variability is the critical element of this failure mode.

reflects heat-to-heat variability or whether the welds or parent metal coupons were used in the uniaxial tests. (Table I.2, item 6)

2. Requirement Data Rationale. The requirement distribution is that of the maximum chamber pressure expected when operating at the upper specified pre-firing propellant temperature limit of 100° F.

Propellant Weight. The standard deviation of the first two 260-inch-diameter motors was estimated by dividing the observed difference by a factor of 1.128.* The resulting coefficient of variation of .0018 agreed well with a figure of .0021 calculated by estimating the grain weight variability from the variability of an equivalent cylindrical grain whose density, length, inside diameter and outside diameter variabilities can be estimated. (Table I.2, item 7)

Propellant Burning Rate. The motor-to-motor variability of average propellant liquid strand burning rate was estimated from the average batch mix liquid strand burning rate cast in 260-SL-1 and SL-2 motors. The standard deviation estimated by the range method was .00265 in/sec, from which we obtained the coefficient variation, $.00265/.4425 = .006$. While the two motors were actually targeted for slightly different averages, the difference between the two for batch mix propellant was felt to be a conservative estimate of what could be attained if motors were actually targeted for the same averages.

Experience in a variety of programs has shown that the variability of web action time is significantly greater than can be accounted for by liquid strand burning rate variability. As a result, an adjustment or scale up factor is used to account for this discrepancy. An average adjustment factor of 2.255 was determined from eight different motor designs and it was used to compensate between liquid strand burning rate data and the 260/S IV-B motor estimate of burning rate. Multiplying this factor times .006 yields a value of .0135 for $\frac{\sigma}{\bar{x}}$. (Table I.2, item 8).

* Aerojet prefers to use the more conservative range method for estimating standard deviations when the sample size is extremely small (i. e., 2, 3, etc.). For a sample of two, this will result in a standard deviation 25.3% higher than that estimated by the conventional method. Reference: (1) Bennet & Franklin, Statistical Analysis in Chemistry and the Chemical Industry, 1954. Table 5.5, Page 165. (2) Grant, E. L., Statistical Quality Control, 1952, Table 3, Page 512, Factors for Estimating σ from R.

Ratio of Average to Peak Pressure. This factor is included to reflect the effects of additional burning surface variability due to separations, voids and manufacturing deviations. The average value is the design ratio of maximum to average pressure for a nominal 80° F firing. The variability was estimated as the average coefficient of variation measured in four motor programs. (Table I.2, item 9)

Mass Flow Coefficient. The most accurate measurement of C_w variability was obtained in a 52-inch-diameter motor program where the most advanced computer data reduction techniques were employed. The estimated motor-to-motor $\frac{\sigma}{\bar{x}}$ for these motors was found to be .00305. (Table I.2, item 10)

Average Throat Area. A $\frac{\sigma}{\bar{x}}$ of .00332 was estimated by the range method using the average of prefire and postfire throat areas in the first two 260-inch-diameter motor firings. (Table I.2, item 11)

3. AGC Design Equations* for FM 1 Requirement. The formula for instantaneous chamber pressure P_c is derived from the steady state mass balance equation

$$P_c = \frac{r_b A_p \rho}{C_w A_t} \quad (1)$$

where

r_b = propellant burning rate at nominal temperature, in./sec.

A_p = burning surface, in.²

ρ = propellant density, lb/in.³

C_w = mass flow coefficient, sec.⁻¹

A_t = average throat area, in.²

This formula was judged not to be an optimum one for use in estimating the distribution of maximum pressures since the variability of burning surface at time of maximum pressure cannot be measured. The following

* These data are found in Data Package II-1, reference 4.

formula, which substitutes propellant weight and web thickness for the density and surface area terms, was used to gain a better evaluation:

$$P_{c \max} = \frac{W_p r_b K_{m/a} e^{\pi_k \Delta t}}{b C_w A_t} \quad (2)$$

where

- W_p = propellant weight, lb.
- $K_{m/a}$ = ratio of peak to average web pressure, (ND)
- C_w = propellant mass flow coefficient, sec.^{-1}
- A_t = average throat area, in.^2
- b = propellant web thickness, in.
- π_k = temperature sensitivity coefficient of pressure, $\%/\text{°F}$

Capability. The ultimate burst pressure, P_{mw} , due to machine welding may be expressed by

$$P_{mw} = \frac{S_{umw} t_c K_{be} K_{bx}}{R_o} \quad (3)$$

where

- P_{mw} = ultimate burst pressure machine welds, psi.
- S_{umw} = machine weld ultimate tensile strength, psi.
- t_c = case plate thickness, in.
- R_o = radius (to exterior), in.
- K_{be} = bending/discontinuity strength reduction factor (ND)
- K_{bx} = biaxial gain factor (ND)

Ten percent of the time the weld strength will be reduced due to the necessity to make local repairs by hand welding. The same formula applies with S_{uhw} hand weld ultimate tensile strength, substituted for S_{umw} .

Failure Mode 2. Data, Motor Case Insulation Burn-Through

Data used for this failure mode supplied by AGC is covered in Reference 3. Failure was defined as the occurrence of erosion through the insulation to any part of the case prior to the end of action time. Although additional time would be required to burn through the steel and cause the chamber to rupture, this extra margin was not considered.

Capability. It was defined then that the capability at any section of the motor is

$$T_{bt} = \frac{b}{r_b} + \frac{t_i}{e_r} \quad (4)$$

where

T_{bt} = time to burn through insulation, second

b = propellant web thickness, in.

r_b = propellant burning rate, in. per second

t_i = insulation thickness, in.

e_r = erosion rate, in. per second

This failure mode involves both the insulation and propellant subsystems and is an excellent example of why failure rates cannot be calculated separately for the propellant or insulation subsystems of solid rocket motors.

Requirement for this failure mode is total action time, or the maximum time of burning. This is derived by the formula

$$T_a = \frac{b'}{r'_b} \quad (5)$$

where

T_a = total action time (maximum time of burning), second

b' = propellant web thickness, where the maximum T_a occurs (generally where propellant web is a maximum), in.

r'_b = average burning rate for maximum action time, in. per second

The maximum web thickness for the 260/S IV-B motor occurs in the forward part of the cylindrical section (Station 4) where the nominal value for b' is 87.5 inches. Although the design nominal propellant burning rate is 0.606 inches per second, the average burning rate for the maximum web thickness section is less than this because the section nearest the sidewall burns during the tail-off period when the motor pressure is decreasing rapidly. Since the design nominal total action time is 148.5 seconds, the nominal average burning rate for maximum web thickness is 0.590 inches per second, and occurs at motor station 4.

The nominal thickness and burning rate for the insulation and propellant at other sections of the motor are tabulated in Table I. 3. The assumed nominal maximum erosion rates, based upon the estimated maximum Mach number of the gas stream at that section are also shown in the table.

Estimation of Parameter Variability

Propellant Burning Rate, r'_b . The variability of the propellant burning rate was assumed to be the same as the variability of the 12-pot increments for motors 260-SL-1 and 260-SL-2. As discussed earlier, the increment-to-increment variability was used because a certain amount of mixing of propellant occurs in successive pots as the motor is cast. Table I. 4 summarizes the burning rate data for both motors and shows the distribution of individual values and the distribution of the 12-pot averages. Because different target values were used for the nominals of these first 260-inch motors, the data was rationalized to provide coincidental average values.

The value of $\frac{\sigma}{\bar{x}}$, (12-pot increment to 12-pot increment) was found to be .0067 for Motor SL-1 and .0052 for Motor SL-2. The combined average of .00595 was selected for this study.

Table I.3 260/SIVB Design Parameters, Mean (Nominal)
Values for Insulation Burn Thru Failure Mode.

Location Station	Web Thickness (b) in.	Propellant Burning rate (r_b) in/sec	Insulation* Thickness (t_1) in.	Insulation Erosion rate (e_r) in/sec
① Igniter Boss	0	-	1.125	.003
② Fwd Head (Igniter Boss to Equator)	24.5	.606	1.125	.003
3. 35" Aft of Fwd Equator	86.7	.606	1.125	.003
④ 120" Aft of Fwd Equator	87.5	.590	.11	.003
⑤ 274" Fwd of Aft Equator	85.0	.606	.11	.005
⑥ 47" Fwd of Aft Equator	71.85	.606	.250	.005
⑦ Aft Equator	70.57	.606	.430	.006
8. 12.5 in. Aft of Aft Equator	70.57	.606	.470	.00625
9. Aft Head at 240" Dia	52.5	.606	.750	.00725
10. Aft Head at 220" Dia	31.9	.606	1.10	.00825
11. Aft Head at 200" Dia	15.5	.606	1.80	.0105
⑫ Aft Head at Nozzle Joint	0	-	3.60	.0168

* V44 Silica Asbestos

△ These seven station have been used in the R||C analysis for this failure mode.
(See Figure 1 of this report for motor schematic)

Table I. 4 Distribution Data* for Design Parameter r_b
Propellant Burning Rate.

Propellant Burn Rate In/Sec for 260-SL-1 Motor	Propellant Burn Rate In/Sec for 260-SL-2 Motor
0.4369	0.4408
0.4391	0.4435
0.4426	0.4423
0.4401	0.4395
0.4446	0.4377
0.4427	0.4426
0.4443	0.4425
0.4447	0.4422
0.4461	0.4388
0.4443	0.4417
0.4477	0.4431
0.4460	0.4388
0.4477	0.4365
0.4459	0.4402
0.4449	0.4450
$\bar{x}_1 = 0.4438$	$\bar{x}_2 = 0.4410$
$\sigma_1 = 0.00299 \text{ in/sec}$	$\sigma_2 = 0.00229 \text{ in/sec}$
$cv_1 = \frac{\sigma_1}{\bar{x}_1} = 0.0067$	$cv_2 = \frac{\sigma_2}{\bar{x}_2} = 0.0052$
$cv_{260/SIVB} \cong \left(\frac{cv_1 + cv_2}{2} \right)^{**} = 0.00595$	

* LSBR-BATCH MIX DATA from 260-SL-1 and 260-SL-2 motors,
based on 12 pot averages.

** See comments in Appendix II, page II.2 which discuss the averaging
of two coefficients of variation.

Propellant Web Thickness. The formula for web thickness for the cylindrical grain was assumed to be given by the formula

$$b = \frac{(D_c - D_b)}{2}$$

where

b = web thickness

D_c = inside diameter of the insulated case

D_b = bore diameter

A value of .002 was obtained for $\frac{\sigma_b}{\bar{x}}$ for the propellant web thickness, based on 260-SL-1 and 260-SL-2 motor data. From these data and nominal web thickness for the 260/S IV-B motor, the standard deviation is equal to .002(85) = 0.170 .

Insulation Thickness. The standard deviation of insulation thickness was estimated from drawing tolerances. Assuming that the difference between the upper and lower limits equals six standard deviations, a value of 0.0033 in. was adopted for the cylindrical section (0.100/0.120 in. - thick stock) and 0.0167 in. for the varying thickness sections of the forward and aft ends.

Insulation Erosion Rate. The variability of the erosion rate was estimated from the maximum erosion distance observed at four circumferential locations for four longitudinal stations in a sample of 24 Polaris A3 motors as shown in Table I.5. The coefficient of variation ranged from .12026 at the nozzle base to .1890 at the equator, with a high value of .23914. The average of the eleven stations was .1631 which was chosen for use in the study since data for other motors indicated no consistent trend for higher $\frac{\sigma}{\bar{x}}$ variability at one station as opposed to another. The maximum value of the four circumferential locations was used rather than the average since the design nominal thickness was based on nominal maximum erosion rates and not on the average.

Table I.6 shows the distribution of sidewall erosion data for 20 Minuteman Wing II motors. This data results in a considerably higher figure for the coefficient of variation, .51714 instead of .1631 for Polaris data.

Table I. 5 Distribution, Polaris Insulation Erosion Data from 24 Motors, Readings at Four Stations 90° Apart (V52 Silica Asbestos Insulation).

Station No.	Total Erosion, Inches				
	Read 1	Read 2	Read 3	Read 4	X max from Read 1 → 4
26 (Nozzle Base)	.17	.36	.27	.29	.36
	.34	.28	.26	.28	.34
	.36	.28	.29	.26	.36
	.31	.29	.37	.37	.37
	.33	.33	.35	.40	.40
	.30	.30	.32	.30	.32
	.33	.38	.35	.42	.42
	.30	.35	.34	.28	.35
	.42	.27	.30	.26	.42
	.37	.37	.39	.39	.39
	.39	.30	.27	.38	.39
	.40	.28	.34	.31	.40
	.36	.38	.35	.25	.38
	.42	.27	.36	.25	.42
	.36	.35	.29	.35	.36
	.25	.28	.25	.26	.28
	.29	.34	.24	.31	.34
	.34	.35	.37	.40	.40
	.24	.25	.41	.26	.41
	.30	.17	.38	.23	.38
	.40	.42	.40	.43	.43
	.27	.28	.31	.30	.31
	.20	.24	.23	.23	.24
	.29	.27	.32	.37	.37
27	.22	.40	.27	.30	.40
	.37	.33	.35	.28	.37
	.33	.29	.28	.28	.33
	.27	.33	.36	.36	.36
	.37	.29	.39	.36	.39
	.30	.27	.33	.33	.33
	.34	.29	.25	.43	.43
	.31	.34	.23	.35	.35
	.41	.28	.29	.29	.41
	.32	.30	.40	.37	.40
	.41	.32	.28	.35	.41
	.34	.33	.32	.31	.34
	.35	.37	.35	.25	.37
	.43	.29	.40	.25	.43

Table I.5 Cont

Station No.	Total Erosion, Inches					
	Read 1	Read 2	Read 3	Read 4	X max from Read 1 → 4	
27 (Cont)	.30	.36	.32	.37	.37	
	.24	.29	.26	.26	.29	
	.27	.32	.22	.40	.40	
	.32	.37	.34	.38	.38	
	.30	.21	.38	.29	.38	
	.28	.17	.33	.21	.33	
	.42	.43	.40	.39	.43	
	.26	.25	.29	.26	.29	
	.18	.26	.28	.21	.28	
	.26	.32	.25	.30	.32	
	28	.17	.41	.24	.27	.41
		.28	.33	.36	.25	.36
		.34	.29	.27	.25	.34
.26		.34	.30	.35	.35	
.37		.32	.37	.36	.37	
.27		.25	.31	.30	.30	
.34		.25	.21	.36	.36	
.30		.33	.21	.32	.33	
.38		.28	.27	.27	.38	
.25		.27	.31	.33	.33	
.33		.28	.31	.30	.33	
.34		.33	.31	.34	.34	
.33		.31	.36	.29	.36	
.39		.24	.38	.29	.39	
.26		.35	.32	.37	.37	
.23		.28	.21	.25	.28	
.24		.28	.22	.36	.36	
.31		.33	.32	.39	.39	
.31		.24	.32	.27	.32	
.21	.12	.28	.18	.28		
.42	.40	.39	.39	.42		
.24	.24	.27	.24	.27		
.20	.23	.27	.14	.27		
.23	.29	.18	.24	.29		
29	.21	.41	.34	.25	.41	
	.32	.30	.28	.23	.32	

Table I. 5 Cont

Station No.	Total Erosion, Inches				
	Read 1	Read 2	Read 3	Read 4	X max from Read 1 → 4
29 (Cont)	.30	.24	.25	.23	.30
	.22	.31	.31	.30	.31
	.37	.29	.34	.34	.37
	.25	.24	.28	.28	.28
	.31	.19	.18	.36	.36
	.28	.30	.20	.37	.37
	.40	.24	.29	.31	.40
	.25	.28	.26	.28	.28
	.28	.27	.29	.29	.29
	.34	.33	.29	.33	.34
	.27	.27	.31	.23	.31
	.34	.19	.40	.23	.40
	.27	.37	.29	.37	.37
	.21	.24	.18	.19	.24
	.20	.26	.29	.33	.33
	.28	.27	.31	.42	.42
	.21	.21	.29	.29	.29
	.28	.12	.29	.21	.29
	.36	.37	.33	.35	.37
	.22	.27	.30	.20	.30
.19	.22	.28	.16	.28	
.17	.26	.16	.24	.26	
30	.17	.36	.30	.27	.36
	.25	.25	.24	.23	.25
	.25	.24	.23	.25	.25
	.18	.30	.27	.28	.30
	.27	.28	.36	.36	.36
	.24	.23	.24	.30	.30
	.32	.21	.16	.35	.35
	.27	.28	.25	.18	.28
	.37	.21	.31	.29	.37
	.23	.25	.25	.33	.33
	.30	.31	.26	.29	.31
	.29	.30	.28	.35	.35
	.29	.25	.32	.24	.32
	.33	.17	.39	.24	.39
	.25	.36	.29	.36	.36
.16	.25	.17	.18	.25	

Table I.5 Cont

Station No.	Total Erosion, Inches				
	Read 1	Read 2	Read 3	Read 4	X max from Read 1 → 4
30 (Cont)	.11	.24	.38	.32	.38
	.25	.24	.27	.38	.38
	.19	.19	.35	.36	.36
	.32	.15	.29	.21	.32
	.36	.34	.29	.42	.42
	.24	.24	.40	.19	.40
	.18	.24	.24	.18	.24
	.16	.26	.18	.23	.26
31	.16	.31	.27	.24	.31
	.23	.20	.23	.27	.27
	.20	.24	.22	.23	.24
	.16	.28	.24	.27	.28
	.27	.28	.36	.33	.36
	.26	.20	.25	.29	.29
	.29	.23	.16	.38	.38
	.25	.28	.25	.20	.28
	.32	.19	.31	.28	.32
	.18	.28	.23	.31	.31
	.30	.31	.25	.25	.31
	.26	.29	.29	.30	.30
	.29	.25	.36	.25	.36
	.30	.15	.36	.25	.36
	.26	.33	.29	.31	.33
	.15	.24	.19	.19	.24
	.14	.21	.37	.29	.37
	.20	.23	.25	.38	.38
	.19	.15	.34	.35	.35
	.29	.20	.31	.18	.31
.29	.32	.25	.37	.37	
.20	.26	.39	.21	.39	
.17	.27	.24	.18	.27	
.11	.27	.21	.24	.27	
32	.17	.28	.24	.20	.28
	.25	.14	.27	.29	.29
	.18	.20	.22	.21	.22
	.12	.24	.24	.25	.25

Table I.5 Cont

Station No.	Total Erosion, Inches				
	Read 1	Read 2	Read 3	Read 4	X max from Read 1 → 4
32 (Cont)	.27	.25	.31	.27	.31
	.19	.22	.23	.27	.27
	.29	.28	.17	.31	.31
	.26	.27	.24	.16	.27
	.25	.17	.30	.30	.30
	.16	.26	.19	.26	.26
	.27	.29	.20	.21	.29
	.24	.27	.24	.25	.27
	.27	.29	.35	.22	.35
	.29	.15	.32	.22	.32
	.28	.28	.25	.36	.36
	.21	.21	.21	.20	.21
	.17	.13	.30	.27	.30
	.20	.23	.25	.34	.34
	.19	.16	.29	.31	.31
	.25	.17	.30	.16	.30
	.19	.29	.25	.25	.29
	.20	.23	.32	.20	.32
	.15	.23	.20	.13	.23
	.12	.25	.20	.22	.25
33	.17	.26	.21	.18	.26
	.22	.15	.23	.27	.27
	.20	.16	.24	.17	.24
	.11	.21	.22	.24	.24
	.25	.16	.24	.23	.25
	.23	.21	.20	.21	.23
	.28	.29	.17	.22	.29
	.29	.23	.25	.18	.29
	.13	.17	.27	.29	.29
	.12	.27	.16	.21	.27
	.24	.20	.19	.13	.24
	.26	.27	.24	.24	.27
	.22	.27	.32	.23	.32
	.24	.13	.28	.23	.28
	.25	.27	.21	.37	.37
	.24	.19	.16	.16	.24
.15	.09	.25	.28	.28	
.21	.25	.23	.45	.45	

Table I. 5 Cont

Station No.	Total Erosion, Inches				
	Read 1	Read 2	Read 3	Read 4	X max from Read 1 → 4
33 (Cont)	.23	.13	.26	.25	.26
	.25	.16	.22	.15	.25
	.15	.22	.24	.18	.24
	.14	.19	.31	.15	.31
	.10	.16	.09	.12	.16
	.11	.25	.16	.15	.25
34	.12	.21	.13	.20	.21
	.20	.16	.22	.19	.22
	.21	.19	.22	.18	.22
	.15	.18	.23	.24	.24
	.18	.17	.18	.22	.22
	.19	.21	.21	.16	.21
	.25	.25	.16	.21	.25
	.25	.23	.21	.17	.25
	.11	.14	.23	.25	.25
	.07	.28	.16	.17	.28
	.21	.21	.19	.11	.21
	.21	.28	.22	.27	.28
	.17	.24	.39	.25	.39
	.22	.14	.26	.25	.26
	.13	.24	.16	.26	.26
	.21	.21	.15	.17	.21
	.16	.09	.23	.25	.25
	.22	.32	.24	.39	.39
	.19	.12	.19	.24	.24
	.25	.12	.20	.15	.25
.06	.18	.21	.16	.21	
.12	.14	.29	.18	.29	
.10	.12	.05	.13	.13	
.12	.24	.13	.18	.24	
35	.11	.22	.11	.20	.22
	.15	.14	.20	.13	.20
	.20	.17	.21	.15	.21
	.13	.17	.21	.23	.23
	.18	.13	.13	.21	.21
	.13	.13	.15	.17	.17

Table I. 5 Cont

Station No.	Total Erosion, Inches					
	Read 1	Read 2	Read 3	Read 4	X max from Read 1 → 4	
35 (Cont)	.21	.19	.17	.18	.21	
	.18	.20	.17	.20	.20	
	.14	.12	.21	.19	.21	
	.08	.21	.15	.16	.21	
	.23	.19	.16	.15	.23	
	.16	.20	.16	.18	.20	
	.18	.19	.24	.18	.24	
	.20	.12	.24	.18	.24	
	.18	.19	.12	.20	.20	
	.13	.18	.15	.16	.18	
	.17	.10	.15	.21	.21	
	.19	.34	.17	.35	.35	
	.15	.11	.15	.15	.15	
	.17	.19	.14	.16	.19	
	.06	.13	.07	.14	.14	
	.13	.11	.37	.15	.37	
	.13	.08	.08	.15	.15	
	.18	.23	.09	.16	.23	
	36 (Equator)	.10	.20	.11	.16	.20
		.12	.11	.20	.15	.20
.15		.17	.15	.08	.17	
.12		.12	.17	.21	.21	
.15		.10	.08	.20	.20	
.12		.12	.13	.17	.17	
.15		.20	.14	.16	.20	
.16		.17	.18	.18	.18	
.10		.11	.14	.15	.15	
.06		.23	.16	.19	.23	
.23		.18	.13	.16	.23	
.17		.21	.14	.12	.21	
.17		.15	.23	.20	.23	
.14		.12	.21	.20	.21	
.10		.18	.09	.15	.18	
.15		.14	.11	.19	.19	
.19		.15	.15	.14	.19	
.17		.27	.16	.32	.32	
.09		.06	.13	.14	.14	
.13		.22	.16	.16	.22	

Table I. 5 Cont

Station No.	Total Erosion, Inches				
	Read 1	Read 2	Read 3	Read 4	X max from Read 1 → 4
36 (Equator) (Cont)	.09	.08	.10	.15	.15
	.15	.14	.22	.11	.22
	.16	.08	.13	.17	.17
	.16	.12	.08	.15	.16

Table I. 6 Distribution of Sidewall Erosion Data 20 Minuteman Wing II Motors (V44 Silica Asbestos).

Maximum Sidewall* Erosion, Inches	Number of Samples
.005 - .006	2
.009 - .010	4
.010 - .011	1
.011 - .012	3
.012 - .013	1
.015 - .016	5
.017 - .018	1
.030 - .031	3
	Total 20
Calculations for MM Wing II data:	
\bar{x}	= .01465
σ	= .00738
$cv = \frac{\sigma}{\bar{x}}$	= .51714

* These data are maximum values obtained in the cylindrical region of the motor, from a population sample of 20 motors. They were used to compute σ and $\frac{\sigma}{\bar{x}}$ for the cylindrical region of the 260/SIVB motor (stations 4 and 5).

The validity of using this data is questionable because: (1) it is more difficult to measure sidewall than aft head erosion, (2) it was derived from motors using a bi-propellant grain that might have had more variability in burning rate than a mono-propellant grain, (3) sidewall erosion is mainly a function of tailoff time, which is usually more variable than the web burning time that primarily governs the fore and aft head insulation erosion rates.

These factors make the applicability of the .51714 value doubtful for $\frac{\sigma}{x}$ and indicate that the variability of the V-44 erosion rate in sidewall locations should be given additional study. (However, for purposes of preliminary analysis this value was used for stations 4 and 5 in the motor.)

Failure Mode 3. Failure of the Forward Skirt
Forging in Combined Compression, Shear, and Bending Loads.

Requirement versus Capability Relationship. When combined loads are present, as in the case of the forward skirt which is subjected to combined compressive, shear, and bending forces, it is the opinion of AGC that the correct estimation of failure cannot be obtained by separately comparing the requirement and capability of each type of loading and then combining the total failure. The non-validity of such an approach, they feel, is due to the fact that the combination of different types of loads interact to reduce the material capabilities to levels below that which they exhibit for single types of loads. As a consequence, stress engineers have derived empirical relationships to account for the amount of interaction between various types of combined loads. In these relationships, the ratios of the requirement of each type of load to their corresponding allowables are combined in an interaction formula such that if the sum of the ratios is greater than unity, failure is assumed to occur. The transfer function used for the combined compression, shear and bending in the skirts of solid rocket motors is

$$R_c + \left(R_b^3 + R_s^3 \right)^{1/3} \quad (6)$$

where

R_c = the ratio of axial compressive load requirements to material capability.

R_s = the ratio of transverse shear load requirement to material capability

R_b = the ratio of pure bending load requirement to material capability

This function can be used in the R||C analysis to describe the requirement, or more specifically the requirement ratio. The capability distribution is assumed to be the single value of 1.000, with no variability.

Expanding the interaction formula to account for the geometry of the 260/S IV-B vehicle, we obtain:

$$\text{Requirement Ratio} = \frac{L_c}{2\pi R_i t_s K_c E_s} + \sqrt[3]{\left(\frac{L_b}{\pi R_i^2 t_s K_b E_s}\right)^3 + \left(\frac{L_s}{\pi R_i t_s K_s E_s}\right)^3}$$

These parameters are defined in Table I.7, and a summary of the mean values and standard deviations are also given.

Engineering Data for Failure Mode 3. Failure of the forward motor skirt forging in combined compression, shear and bending, is discussed and the rationale and data used in this study follow.

L_c , L_b , L_s ; Axial Compression, Pure Bending, Transverse Shear Loads.

The axial compression, pure bending, and transverse shear loads are single limit values with zero variability.

Assumptions: The loads used in this analysis were specified by the launch vehicle systems designer, Douglas Missile and Space Systems Division. In actuality, the maximum axial compression load occurred at 116 sec while the maximum shear and bending moment occurred at 59 sec. However, lacking data for shear and bending at 116 sec, the 59 sec values were used instead since this produced a conservative estimate. The values used are maximum requirements based in part on a 95% probability quasi-steady state winds, plus associated wind shears, wind speed changes and gusts. In addition, the TVC portion of the loads also reflected a root-sum-square combination of the maximum expected variability of thrust misalignment, motor thrust, and vehicle weight. The probability of failure calculated from these loads is therefore a maximum one in the same sense that the hoop stress failure rate was evaluated at the maximum temperature requirement. To obtain the skirt failure probability for normal use would require the vehicle designer to furnish variability estimates for these loads.

Table I. 7. Summary of Parameter Average and Standard Deviations.

	Nominal Value \bar{X}	Standard Deviation Units σ	Coefficient of Variation $\frac{\sigma}{\bar{X}}$	Source of Data
Maximum Axial Compressive Load, L_c , lb.	2, 200, 000	0	0	Figure 4-17, <u>Saturn IB Improvement Study</u> , Douglas Missile & Space Systems Div., 3/30/66 (Douglas Rpt SM-51896, Vol. II) Contract NAS8-20242.
Maximum Pure Bending Load, L_b , in. -lb.	94, 000, 000	0	0	Fig. 4-15, Same report as above.
Maximum Transverse Shear Load, L_s , lb.	60, 000	0	0	Fig. 4-15, Same report as above .
Skirt Radius (interior), R_1 , in.	129, 903	.0208	.00016	\bar{X} : Design nominal σ : Assuming design tolerance = 6 sigma.
Modulus of Elasticity, E_s , psi	27, 500, 000	54, 725	.00199	\bar{X} : Design nominal σ : Est. from plate-to-plate variability of material composition.
Ratio of Axial Compression Strength to Mod. of Elasticity, K_c	.0036	.000685	.190	\bar{X} , σ : <u>Development of design curves for stability of thin pressurized and unpressurized circular cylinders</u> , Report AZS-27.275, 3/8/59, Convair Astronautics Div., General Dynamics Corp.
Ratio of Pure Bending Strength to Mod. of Elasticity, K_b	.0050	.000968	.193	\bar{X} , σ : " " " " .
Ratio of Transverse Shear Strength to Mod. of Elasticity, K_s	.00288	.000334	.116	\bar{X} , σ : " " " " .
Skirt Thickness, t_s , in.	.728	.0093	.0128	X : Design Nominal σ : Assuming design tolerance = 6 sigma.

R_i, Skirt Radius Distribution

1. The tolerance on the interior skirt radius = 0.125
2. Assuming the tolerance equals 6σ , $\sigma = 0.0208$
3. $\frac{\sigma}{\bar{x}} = \frac{0.0208}{129.903} = 0.00016$
4. The population is assumed to be normally distributed.

Assumptions: Engineering judgment supports the statement that such tolerances could be held in production motors.

Experience with similar manufacturing parameters in smaller motors indicate a normal distribution.

t_s, Skirt Thickness Distribution

1. The tolerance on the skirt thickness is 0.056 inches.
2. Assuming the tolerance equals 6σ , $\sigma = 0.0093$
3. $\frac{\sigma}{\bar{x}} = \frac{0.0093}{0.728} = 0.0128$
4. The population is assumed to be normally distributed.

Assumptions: Engineering judgment supports the statement that such tolerances could be held in production motors.

Experience with similar manufacturing parameters in smaller motors indicate a normal distribution.

E_s, Modulus of Elasticity Distribution

Table I. 8 lists the data for E_s. Twenty-four heat number values are shown.

Assumptions: No data were available for the plate-to-plate variability of modulus of elasticity. However, the chemical composition data available for each plate made possible an estimate of the modulus of elasticity.

Table I. 8. E_s , Modulus of Elasticity Distribution

Heat No.	Estimated Modulus of Elasticity lb/in ² x 10 ⁻⁶
50265	29.138
50264	29.087
50338	29.138
50210	29.189
24997	29.248
24999	29.138
3951218A	29.036
25126	29.146
3951215	29.240
3960819	29.138
3920781	29.129
2500	29.189
392077	29.078
25064	29.104
3960832	29.104
25098	29.180
25007	29.163
24998	29.129
3960829	29.036
50187	29.180
3960870	29.061
25050	29.036
24996	29.155
50234	29.138
	$\bar{x} = 29.132 \times 10^6$
	$\sigma = 0.058 \times 10^6$
	$cv = \frac{\sigma}{\bar{x}} = 0.00199$

This was done by obtaining handbook values for modulus of elasticity of each of the ingredients and obtaining a weighted average estimate of the modulus of each plate. While the true modulus of elasticity is probably affected by other factors than composition, this method is felt to be sufficiently accurate for variability estimating purposes. The average value obtained by this method was 29,132,000 which is within 5% of the design nominal value of 27,500,000.

The assumptions of a normal distribution and the constancy of the coefficient of variation apply to this parameter.

Ratio of Strengths to Modulus of Elasticity Distribution. The variability of axial compressive strength, pure bending strength and transverse shear strength was obtained from a study performed by Convair Astronautics Division, wherein data from unstiffened circular cylinders in compression, bending and shear from numerous studies were analyzed and summarized. The results were calculated for various radius/thickness relationships as well as length/radius relationships. In addition to showing average values, results were portrayed for 90% probability with 95% confidence levels which made possible direct estimation of standard deviation. The results are summarized as follows:

Assumptions:

$$\text{Radius/Thickness} = 129.903/728 = 180$$

$$\text{Length/Radius} = 30/129.903 = 0.23$$

Function	Ratio of Strength to Modulus of Elasticity		(No. of σ between \bar{x} & 90% prob. 95% C. L. based on sample size)	Standard Deviation σ	Coef. of variation $\frac{\sigma}{\bar{x}}$
	Avg. Value	90% Prob. 95% C. L.			
Axial Compressive Strength, K_c	.0036	.0026	1.459	.000685	.190
Pure Bending Strength, K_b	.0050	.0035	1.548	.000968	.193
Transverse Shear (1.25 x torsion), K_s	.00288	.00238	1.497	.000334	.116

The data in the Convair study were shown only in summary form and it was assumed that populations are normally distributed. It is interesting to note

that coefficients of variation obtained, which ranged from .116 to .193 are considerably larger than the .025 obtained for the tensile strength of the plates maraged in 260-SL-1 and 260-SL-2. This is to be expected, since the initiation of buckling failures is more susceptible to local discontinuities and contour deviation than is the case of simple tensile tests. As such, this data can be considered to include the bending/discontinuity factor that was evaluated separately in the hoop stress failure mode.

Failure Mode 4. Data, Failure of Forward Head
Circumferential Weld in Meridional
Stress (Location: Weld Between
Igniter Boss Forging and Upper
Gore, 35" from Center Line)*

Capability Distribution:

90% of time weld strength is

$$P_{mw} = \frac{2S_{umw} t_c (K_{be})}{R_o} \quad (8)$$

where

P_{mw} = Ultimate burst pressure of machine welds, psi,

S_{umw} = Ultimate tensile strength of machine welds, psi,

t_c = Plate thickness, in. ,

R_o = Radius (to exterior surface), in. ,

K_{be} = Bending/discontinuity strength reduction factor, ND.

10% of time weld strength is reduced due to the necessity of making local hand weld repairs. The same formula applies except S_{uhw} is substituted for S_{umw} .

S_{uhw} = Ultimate tensile strength of hand welds, psi.

* Motor Station 3

As shown in Table I. 9, the same values for average and standard deviations for cylindrical welds as was used for FM 1 apply to the forward head welds with the exception of plate thickness and radius.

Requirement Distribution. The requirement distribution of maximum chamber pressure for this failure mode is the same as for the failure of longitudinal welds* in hoop stress. Tables I. 10 and I. 11 support the plate thickness and exterior radius variabilities.

Failure Mode 5. ** Data, Rupture of the
Nozzle Joint Bolts

Failure of nozzle joint bolts in tension due to combined loads of pressure ejection, and TVC bending moments.

Requirement Distribution. The requirement distribution is the sum of three distributions: the tension due to pretorquing, a portion of the ejection load due to internal and external pressure and inertia, and the added tension effect due to the thrust vector control moment.

The portion of the total ejection load that is felt as tension in the bolt can be approximated by the ratio of the cross sectional area of a bolt to the area of flange per bolt. Since this results in a load that is less than . 1% of the pretorque load for the 260/S IV-B design, the ejection load effects were not considered in this failure mode. The resulting requirement transfer function is then that the Bolt Tensile Load = Pretorque Load + Thrust Vector Control Load.

The thrust vector control load results from the side force load of the liquid injection TVC system. It acts at right angles to the longitudinal axis at the TVC ports in the exit cone and results in a bending stress at the nozzle joint. The basic formula for the load/bolt at the joint is:

$$P_b = \frac{(F_{\max}) (\tan \alpha) (d)}{\frac{n}{2} \left(\frac{D_j}{2} \right)} \quad (9)$$

* Ref. Data Package II-1 and equation (2) of this Appendix.

** Ref. 4, Data Package II-4.

Table I.9. Summary of Parameter Averages and Standard Deviations, FM-4.

Parameter	Parameter Average Value, \bar{X}	Parameter Standard Deviation in Units, σ	Coefficient of Variation $\frac{\sigma}{\bar{X}}$	Source of Values
Machine Weld UTS, S_{umw} , psi	232,000	2,516	.0109	\bar{X}, σ : 260-SL-1 and 260-SL-2 Maraged weld coupons (see Data Package II-1, Table 2).
Hand Weld UTS, S_{uhw} , psi	199,333	8,641	.0433	\bar{X}, σ : " " " "
Plate Thickness, t_c , in.	.428	.0108	.0250	\bar{X} : Design nominal. σ : 18 plates from 18 heat used in 260-SL-1 and SL-2
Radius (exterior), R_o , in.	130.428	.0456	.00035	\bar{X} : Design nominal. σ : Tolerance on radius r plate thickness variable
Bending/Discontinuity Reduction Factor, K_{be} (ND)	.9585	.00693	.72	\bar{X}, σ : Est. from 260-SL-1 and SL-2, Hydrotest strain gauge data. See Data Package II-1 Table 5.

Table I.10. Plate Thickness Variability

Heat No.	Plate Thickness Average of 15 Readings	Within-Plate Standard Deviation	Used In Motor Number
3920778-B	.414	.0089	260-SL-1
25000-6A	.429	.0050	250-SL-1
25064-1	.434	.0069	260-SL-1
25050-1	.435	.0023	260-SL-1
3960870-C	.436	.0023	260-SL-2
50187-2T	.443	.0032	260-SL-2
24996-1	.446	.0059	260-SL-2
50187-2B	.441	.0065	260-SL-2

$t_c \text{ avg.} = .434$
 $\sigma_{\text{plate to plate}} = .0095$ $\sigma_{\text{within plate}} = .0051 \text{ (avg.)}$

$\sigma = \text{Estimated Total Variability (any location)} = \sqrt{\sigma_{pp}^2 + \sigma_{wp}^2}$

$\sigma = .0108$

$cv = \frac{\sigma}{\bar{x}} = .0250$

Table I. 11. Estimation of Exterior Radius Variability.

(1) Tolerance on interior radius	=	.26
(2) Assuming tolerance = 6σ ,	σ	= .0433
(3) Variability of plate Table 1.1 σ_t	=	.0108
(4) Combining plate and radius variability by RSS,	σ	= .0456
(5) Coefficient of variation		
	$\frac{\sigma}{\bar{x}}$	= $\frac{.0456}{130.428}$ = .00035

where:

- P_b = load per bolt, lb.
 F_{\max} = maximum longitudinal thrust, lb.
 α = TVC side force deflection angle, degrees.
 d = longitudinal distance between TVC port and joint, in.
 n = number of bolts
 D_j = diameter at nozzle joint, in.

However, the maximum longitudinal thrust can be expressed in terms of maximum chamber pressure which is the requirement parameter for other failure modes. The relationship is:

$$F_{\max} = P_{sn} A_{ti} C_{f \text{ vac}} K_f + (P_e - P_a) A_{ti} \epsilon \quad (10)$$

where:

- P_{sn} = chamber stagnation pressure, psi.
 P_a = atmospheric pressure, psi.
 A_{ti} = initial throat area, in²
 $C_{f \text{ vac}}$ = nozzle thrust coefficient in vacuum, (ND)
 K_f = nozzle efficiency factor, (ND)
 ϵ = nozzle expansion ratio, (ND)
 P_e = nozzle exit pressure, psi

Constant values for α , $C_{f \text{ vac}}$, K_f , and ϵ , are used in the following formula for the bolt tensile load:

$$Q_{BT} = K_p F_{by} + \left[\frac{(\tan \alpha)(d)(.8538 P_{cmax})(A_{ti}) \left(1.66642 - \frac{11.0 P_a}{.8538 P_{cmax}} \right)}{\left(\frac{n}{2} \right) \left(\frac{D_j}{2} \right)} \right] \quad (11)$$

where:

Q_{BT} = total tensile load per bolt, lb.

K_p = fraction of bolt minimum yield strength to which bolt is pretorqued, %/100.

F_{by} = minimum tensile load per bolt, lb.

α = 3.6° (TVC side force deflection angle)

d = longitudinal distance between TVC port and joint, in.

P_{cmax} = maximum chamber pressure, psi

P_a = atmosphere pressure, psi

A_{ti} = initial nozzle throat area, in²

n = number of bolts, 220

D_j = diameter at nozzle joint, in.

Capability Distribution. The load capability parameter, P_y is based on the tensile strength of the nozzle attachment bolts. The nominal value for bolt load capability is estimated at 15% greater than the specified minimum of 213, 310 lbs per bolt, or 245, 307 lb/bolt. The coefficient of variation is .0081 as shown in Table I. 12 thus $\sigma = (cv) P_y = 1987$ psi.

A summary of the averages and standard deviations characterizing these parameters, is presented in Table I. 12. Table I. 13 shows distribution data and rationale for the parameters shown in Table I. 9.

Table I. 12. Summary of Parameters for FM-5.

Symbol	Parameter	Nominal Value \bar{x}	Standard Deviation Units σ	Coefficient of Variation σ/\bar{x}	Source of Data
K_P	Pretorque fraction of minimum yield strength, %/100	.60	.077	.128	\bar{x} : design nominal σ : measured variability for tensile strength for six $1\frac{1}{4}$ -in. -dia EWB bolts all pretorqued to same 1000 ft. lb. load. See Table 1.13
F_{by}	Bolt minimum yield strength, lb/bolt	213,310	0	0	\bar{x} : design nominal σ : included in pretorque data
d	Distance between TVC port and nozzle joint, in.	178.84	0	0	\bar{x} : design nominal σ : no data available
P_{cmax}	Maximum chamber pressure, psi	-	-	-	A parameter expressed as a function of other parameters. (See equation (I. 2))
P_a	Atmospheric pressure, psi	14.696	.0735	.0049	\bar{x} and σ : Handbook of Geophysics for Air Force Design. Data is for sea level. 30°N latitude.
A_{ti}	Initial nozzle throat area, in ²	6235	0	0	\bar{x} : design, nominal σ : negligible (one sigma equals .045%, assuming dia. dwg. tolerance equal to 6 sigma (see Table I. 13))
n	Number of bolts	220	-	-	\bar{x} : design nominal
D_j	Diameter of nozzle joint, in.	180	0	0	\bar{x} : design nominal σ : negligible (.001% assuming dwg. tolerance equal to 6 sigma. See Table I. 13)
P_y	Bolt Load Capability lbs/bolt.	245,307	1987	.0081	

Table I.13. Distribution Data for FM-5.

Pretorque Distribution

Pretorque design nominal is set at 60% of minimum bolt tensile strength; the pretorque variability is estimated from 6 tests performed on 1.25 in. dia. EWB bolts similar to LWB used in 260-in./SIVB design were torqued to 1000 ft-lbs (lubricated). The imposed tensile loads were measured as follows:

<u>Test</u>	<u>Tensile load, psi</u>
1	124,000
2	133,000
3	147,000
4	153,000
5	167,000
6	<u>174,000</u>
	Avg. 149,667
	$\sigma = 19,210$
	$cv = \frac{\sigma}{\bar{x}} = 0.128$

Assumptions: It was assumed that the $\frac{\sigma}{\bar{x}}$ observed in these tests would apply to 260/SIVB bolts when torqued to 60% of their minimum yield. It was also assumed that the pretorque variability represented both the variability of the inherent tensile strength and the variability resulting from pretorquing itself.

Initial Throat Area

This parameter is assumed to be normally distributed with the tolerance on initial throat area equal to 6 standard deviations. The 0.060 inches total tolerance on the 89.1 inch diameter becomes the equivalent of 0.045% for one sigma of initial throat area. This small magnitude can be neglected.

TABLE L.13 continued

Diameter of Nozzle Joint

This parameter is assumed to be normally distributed with the tolerance on the joint diameter equal to 6 standard deviations. Thus, the 0.015 inches total tolerance on the 180 in. diameter of the bolt circle becomes 0.00139%. This small magnitude can be neglected.

Summary of Bolt Tensile Strength Data

Only summarized data were available. The following were obtained from AGC reports, reflecting strength measured in Aerojet acceptance tests:

<u>Type of Bolt</u>	<u>Material</u>	<u>Average Ultimate Tensile Strength, psi</u>	<u>Standard Deviation psi</u>	<u>Coefficients of Variation σ / \bar{x}</u>
-	8735	190,950	1667	0.00873
-	8740	181,600	1718	0.00946
NAS626 H4	-	214,900	1310	0.00610
				cv Avg. = 0.00810

Assumptions: The average of the coefficients of variation, σ / \bar{x} was used as the best estimate of the population coefficient of variation. The assumption is also made that yield strength σ / \bar{x} is the same as ultimate tensile strength σ / \bar{x} .

Failure Mode 6. Data, Separation of Motor Chamber and Nozzle Flange

1. Relationship of Requirement and Capability. *

The longitudinal compression of the flange due to pretorque can be described by the formula:

$$\epsilon_c = \frac{Q_{pt}}{A_F E_F}$$

where:

- ϵ_c = fractional compression (ND)
- Q_{pt} = pretorque load per bolt, lb/bolt
- A_F = area of flange/bolt, in.²
- E_F = modulus of elasticity of flange, psi.

Similarly, the longitudinal elongation of the flange due to the ejection load can be described by the formula:

$$\epsilon_e = \frac{Q_{ej}}{A_F E_F}$$

where:

- ϵ_e = fractional elongation (ND)
- Q_{ej} = ejection load per bolt due to internal pressure, external pressure, and inertia, lb/bolt

The joint will separate when the elongation due to ejection load exceeds the compression due to pretorque. This occurs when: $\epsilon_c = \epsilon_e$ or:

* Ref. AGC Data Package II-4, 5

$$\frac{Q_{pt}}{A_F E_F} = \frac{Q_{ej}}{A_F E_F}$$

This reduces to $Q_{pt} = Q_{ej}$ at time of failure. Thus the ejection load becomes the requirement and the pretorque load the capability.

Requirement distribution. The ejection load on the nozzle in flight is made up of three components:

a. The force on the entrance to the nozzle minus the reacting forces in the exit cone:

$$P_{180} A_{180} (1 + \gamma M_{180}^2) - P_e A_{ei} (1 + \gamma M_e^2)$$

where:

P_{180} = pressure at 180" joint diameter, psi,

A_{180} = area at 180" joint diameter, in²,

γ = ratio of propellant specific heats (ND),

M_{180} = Mach number of gas stream at joint diameter, (ND),

P_e = gas pressure at exit diameter, psi,

A_{ei} = initial exit area, in²,

M_e = Mach number at exit plane, (ND).

b. The drag on the exterior surface of the nozzle due to ambient air pressure:

$$P_a (A_{ei} - A_{180})$$

where:

P_a = atmospheric air pressure.

c. The inertial load on the nozzle:

$$\frac{W_{ni} + W_{veh}}{F}$$

where:

- W_{ni} = initial weight of the nozzle, lb,
 W_{veh} = total weight of the launch vehicle, lb,
 F = thrust, lb.

As in the case of the failure mode due to bolt pretorque and TVC loads the thrust term has been replaced by chamber pressure, throat area and other parameters. The final formula for the ejection load per bolt is then:

$$R_6 = Q_{ej} = \left[\left(.9981 P_{cmax} A_{180} (1 + \gamma M_{180}^2) - .014092 P_{cmax} A_{ei} (1 + \gamma M_e^2) \right) + \left(P_a (A_{ei} - A_{180}) \right) + \left(\frac{W_{ni} (W_p + W_{vi})}{.8538 P_{cmax} A_{ti} \left(1.66642 - \frac{11 P_a}{.8538 P_{cmax}} \right)} \right) \right] \frac{1}{n} \quad (12)$$

where:

- Q_{ej} = ejection load per bolt, lb/bolt,
 P_{max} = maximum chamber pressure, psi (see Equation II.22, Appendix II),
 γ = ratio of propellant specific heats, (ND),
 M_{180} = Mach number of gas stream at joint diameter, (ND),
 M_e = Mach number of gas stream at exit plane, (ND),
 P_a = atmospheric pressure, psi,

- A_{ei} = initial exit area, in.²,
 A_{180} = area at nozzle joint, in.²,
 W_{ni} = initial weight of nozzle, lb,
 W_p = propellant weight (first stage), lb,
 W_{vi} = initial weight of launch vehicle (less first stage propellant), lb,
 A_{ti} = initial throat area, in.²,
 n = number of bolts.

A preliminary evaluation indicates that load Q_{ej} or the requirement, will be at a maximum immediately after ignition.

Capability Distribution. The formula for the pretorque load/bolt is:

$$C_6 = Q_{pt} = K_p F_{by} \quad (13)$$

where:

- Q_{pt} = pretorque load on bolt, lb,
 K_p = fraction of bolt minimum yield strength to which bolt is pretorqued, %/100,
 F_{by} = bolt minimum load capability based on yield strength, lb.

Table I. 14 presents the FM 6 parameters giving estimates of the means, standard deviations, coefficient of variations, and data sources. Table I. 15 summarizes the rationale for those parameters assumed to have $\sigma = 0$.

Table I. 14. Summary of Parameter Data FM-6.

Parameter	Nominal Value \bar{x}	Standard Deviation σ	Coefficient of Variation σ/\bar{x}	Source of Data
Ratio of propellant specific heats, γ (ND)	1.2	0	0	\bar{x} : design nominal σ : is negligible .00167% per Report 0815-81F "Survey of Existing Solid Propellant Ballistic Data", Contract NAS8-11033, 4-29-64.
Mach number at joint diameter, M_{180} (ND)	0.0576	0	0	\bar{x} design nominal σ : negligible. (A one sigma change in A_{ti} produces only .04% change in M_{180} . See Table II).
Mach number at exit plane, M_e (ND)	3.205	0	0	\bar{x} design nominal σ : negligible (one sigma equals .0039% based on .04% for A_{ti} and .01796% for A_{ei} . See Table II).
Atmospheric Pressure, psi P_a	14.696	.0735	.0049	x : and σ . Handbook of Physics for Air Force Design. Data is for sea level, 20°N latitude.
Initial Exit Area, A_{ei} in ²	56,116	0	0	\bar{x} : design nominal σ : negligible (one sigma equals .01796% based on assumption that exit dia tolerance is 6 sigma. See Table II).
Area at Nozzle Joint, A_{180} in ²	25,447	0	0	\bar{x} : design nominal σ : negligible (one sigma equals .00343% based on assumption that joint dia. tolerance equals 6 sigma. See Table II).
Initial Nozzle Weight, W_{ni} lb	58,428	0	.0134	\bar{x} : design nominal σ : same source as for sigma of γ .
Propellant Weight, W_p lb (1st Stage)	3,400,000	6120	.18	See Data Package II-1, AGC
Initial Launch Vehicle Weight, W_{vi} lb (Less First Stage Propellant)	726,466	4085	.70	\bar{x} : design nominal σ : Saturn IB Improvement Study, Douglas Missile and Space Systems Division. (Douglas Report SM-51896 Vol. II, 3-30-66).
Initial Throat Area, A_{ti} in ²	6,235	0	0	\bar{x} : design nominal σ : negligible (sigma equals .045% based on assumption that dwg. tolerance equals 6 sigma. See Table II).
Number of Bolts, n	220	-	-	--
Fraction of Bolt Min. Yield Strength to Which Bolt is pretorqued, K_p	0.6	.077	.1283	

Table I.15. Summary for Parameters Assumed Without Variance FM-6.

<u>Symbol</u>	<u>Requirement Formula Parameter</u>	<u>Related Primary Parameter</u>	<u>Equation for Requirement Formula Parameter</u>	<u>Variability of Related Parameters</u>	<u>Corresponding Formula Parameter Variability</u>	<u>Assumption</u>
M_{180}	Mach number at throat diameter	A_{ti}	Complex	.045% ($\sigma_{A_{ti}}$)	.04%	Negligible effect on requirement variability
M_e	Mach number at exit diameter	A_{ti} and A_{ei}	Complex	.045% ($\sigma_{A_{ei}}$) .01796% ($\sigma_{A_{ei}}$)	.0039%	"
A_{ei}	Exit Area	Exit Area Radius	$2\pi R_{ei} \sigma_{R_{ei}}$.012 ($\sigma_{R_{180}} = \frac{tol}{6}$)	.01796%	"
A_{180}	Nozzle Joint Area	Nozzle Joint Dia	$2\pi R_{180} \sigma_{R_{180}}$.00125 ($\sigma_{R_{180}} = \frac{tol}{6}$)	.00343%	"
A_{ti}	Throat Area	Throat Radius	$2\pi R_{ti} \sigma_{R_{ti}}$.010 ($\sigma_{R_{ti}} = \frac{tol}{6}$)	.045%	"

DATA FOR PROPELLANT STRESS FAILURE MODES, * FM7-11 INCLUSIVE

These five failure modes are a representative group related to propellant stress problems. They will be discussed together because only a small amount of input data applicable for R||C analysis was made available. However, this data collection effort represented a sizeable computer and study program on the part of AGC. It did, however, show that R||C analysis can still be a valuable tool when data supply is marginal. The five failure modes are as follows.

Failure Mode 7. Propellant Max, Inner Bore
Hoop Strain Failure Mode,
Storage Condition

Innerbore grain failure in hoop stress due to cool down and storage (undetected) critical station-center region of motor.

Failure Mode 8. Propellant/Liner Interface Maximum
Radial Bond Stress Failure Mode,
Storage Condition

Propellant/Liner interface bond fails radially during cool down and storage (undetected), critical station-aft end of motor.

Failure Mode 9. Propellant Maximum Combined
Stress (Principal Stress), Shear
and Tension Failure Mode, Storage
Condition

Failure of propellant due to combined shear and tension stress during cool down and storage (undetected), critical station-aft end of motor.

Failure Mode 10. Propellant/Liner Interface Maximum
Shear Stress Failure Mode, Flight
Condition

Propellant/Liner interface bond fails due to shear stress during cool down and storage (undetected), critical station-forward end of motor.

* Data covered by AGC Progress Report No. 6, NAS 7-572. (Phase I study).

Failure Mode 11. Propellant Maximum Inner Bore
Hoop Strain Failure Mode, Flight
Condition

Inner bore grain failure in hoop stress due to pressurization and flight acceleration, critical station-aft end of motor.

Requirement Distribution. Data received from AGC and used for the R||C analysis for the failure modes 7 through 11 was given in the form of output R and C density parameters. AGC said that these functions were Gaussian and therefore TEMPO used closed formed solutions.

Detailed input and output data from the computer grain stress analysis performed by AGC are covered here. Input variables for the eight storage and eight flight simulations were used in the AGC analysis. Only the storage modulus of elasticity, the coefficients of thermal expansion, and the case wall thickness were varied, however, for the simulation storage conditions. For the flight simulations, the flight modulus was substituted for storage modulus and the propellant density and initial chamber pressure were added to the parameters varied in each run. A sample run is shown in Table I. 16.

The corresponding output data which are the grain stress and strain requirements are presented in a sample run, Table I. 17, which is the result of one of the eight simulation runs made by AGC. No Requirements are shown for inner bore strain in the forward part of the motor since it is non-axisymmetric, and would require special analytical treatment. The assumption was made that the grain design in this forward end could be so modified as to ensure that the maximum bore strain requirements would occur in the cylindrical section. AGC 260/S IV-B Propellant success criteria is as follows:

SATISFACTORY PERFORMANCE OF PROPELLANT/
LINER SUBSYSTEM

- Grain does not auto-ignite prior to planned ignition.
- Propellant burns without producing overpressure, burn-through, or structural damage. (Does not include performance failure wherein structure remains intact, but delivered thrust, ignition delay, tail off, etc., are out of specification.)

TIME PERIOD

- From start of countdown to end of motor total action time.

Table I. 16 Sample* AGC Run #2, Input Variables
for Propellant Stress Failure Modes.

Section	Propellant Modulus of Elasticity, psi		Coef. of Thermal Exp., %/°F		Case Wall Thickness, Inches	Prop. Density, lb/in ³	Initial Chamber Pressure, psi
	Storage	Flight	Prop. (X10 ⁵)	Case (X10 ⁶)			
1-3	55	857	5.3996	5.594	.425	.06328	528.1
4	63	1084	5.4003	"	"	.06332	539.8
5	54	838	5.3995	"	"	.06331	549.8
6	63	1071	5.4005	5.590	.433	.06331	547.8
7	58	954	5.4000	5.605	.641	.06330	561.6
8	63	1095	5.4019	"	"	.06327	567.4
9	64	1121	5.4008	5.595	.650	.06329	591.3
10	62	1053	5.3992	5.514	.625	.06330	586.8
11	60	990	5.3988	5.606	.637	.06332	588.0
12	62	1049	5.4007	"	"	.06332	601.0
13	62	1063	5.4001	"	"	.06331	596.5
14	57	923	5.3992	5.618	.618	.06328	608.6
15	70	1269	5.4018	"	"	.06328	613.4
16	61	1028	5.3984	"	"	.06330	615.4
17	62	1049	5.4014	5.594	.641	.06334	608.1
18	60	1003	5.3992	"	"	.06329	612.4
19	53	817	5.3980	"	"	.06332	621.9
20	64	1097	5.4001	5.589	.621	.06331	619.2
21	57	929	5.4002	"	"	.06330	619.8
22	62	1063	5.3993	"	"	.06331	628.0
23	57	923	5.4007	"	"	.06330	644.6
24	58	956	5.3985	5.600	.648	.06329	639.6
25	60	993	5.3987	"	"	.06333	659.4
26	50	734	5.3974	"	"	.06329	647.3
27	58	948	5.3984	5.584	.647	.06331	635.9
28	60	993	5.3998	"	"	.06329	646.1
29	64	1109	5.3996	"	"	.06330	659.5
30	61	1014	5.4003	5.585	.645	.06331	658.1
31	54	823	5.3983	"	"	.06328	653.8
32	60	1165	5.3987	"	"	.06330	672.1
33-37	58	946	5.3991	5.619	.637	.06330	679.0
38-39	66	1154	5.4015	"	"	.06330	661.0
40-41	54	829	5.4010	"	"	.06329	683.7
42-43	57	920	5.4002	5.602	.432	.06331	689.1
44	67	1185	5.3989	5.598	.432	.06329	690.3
45	57	913	5.3997	5.597	.426	.06332	701.8

* 8 Simulation computer runs were made by AGC.

Table I. 17 Sample* AGC Run #2, Output (Requirements)
for Propellant Stress Failure Modes.

Section	Flight		Storage		
	Inner Bore Strain, %	Bond Shear Stress, lb/in ²	Inner Bore Strain, %	Radial Bond Stress, lb/in ²	Prop. Principle Stress, lb/in ²
1-3	2.76	17.7	1.80	2.35**	5.26**
4	3.15	4.9	1.75	1.03	1.88
5	3.50	8.7	1.13	.40	.91
6	5.00	7.9	2.16	1.05	1.61
7	5.79	9.1	2.60	.93	1.44
8	6.08	11.7	2.99	1.41	1.95
9	7.70**	14.3	3.53	1.42	1.93
10	7.23	16.0	3.48	1.79	2.28
11	6.58	14.8	3.44	1.41	1.88
12	6.29	12.3	3.45	1.77	2.25
13	6.32	17.2	3.47	1.54	2.03
14	6.26	12.4	3.38	1.78	2.23
15	6.20	18.2	3.32	1.51	2.04
16	6.15	15.1	3.38	1.82	2.30
17	5.91	15.6	3.44	1.49	1.97
18	6.11	20.7	3.54**	1.78	2.25
19	6.32	13.5	3.54**	1.52	1.94
20	5.95	16.7	3.44	1.69	2.18
21	5.65	15.9	3.40	1.51	1.96
22	5.96	18.5	3.38	1.64	2.13
23	6.42	17.3	3.38	1.48	1.93
24	6.66	27.1	3.36	1.57	2.04
25	6.92	16.7	3.38	1.36	1.85
26	6.70	13.0	3.43	1.55	1.98
27	5.84	16.6	3.31	1.25	1.74
28	5.53	18.3	3.09	1.38	1.90
29	5.58	21.8	2.91	1.11	1.72
30	5.51	24.4	2.84	1.22	1.85
31	5.77	20.8	2.86	.92	1.53
32	NA	28.4**	NA	.76	1.44
33-37	"	20.5	"	.81	1.46
38-39	"	24.4	"	.53	1.23
40-41	"	15.1	"	.35	.85
42-43	"	9.0	"	.47	.73
44	"	10.4	"	.46	.69
45	"	17.3	"	.56	1.09

* 8 simulation computer runs were made by AGC.

** Maximum Value

PRE COUNTDOWN ENVIRONMENTAL CONDITIONS

- Post cast cool down from 140° to 60° F.
- Horizontal storage 3 years prior to use.
- Handling and shipping maximum, 1.3 g's longitudinal, 3.0 g's lateral.
- Countdown and launch at ETR, 2 g's axial load maximum.

EXCLUSIONS*

- Grain cracks and flaws, slump, deformation, and propellant/liner separations that can be visually detected prior to countdown.
- All failures originating due to human error in manufacturing, inspection, assembly, transport, etc., that result in material strength or capability far below that normally considered in design.
- Failures resulting from the inability of quality control tests run on samples of case, liner, insulation and propellant to accurately reflect motor conditions.

Data for the input parameters used by AGC in the grain stress analysis, is given in Table I. 18. Table I. 19 summarizes the results of the AGC computer runs, which, although inadequate for a high confidence** in the results, do show a relatively small variability for so few runs.

* It should be pointed out that some of the performance irregularities of the last 260 inch SL-3 motor firing might include failure modes associated with some of these exclusions.

** Note that these data which represent maximum stress strain data, have standard deviations of from 10% to about 30% of the means. Only because the capability is so much greater does this data appear reasonable. From the few runs made, even if the data is representative of one of the "tails" of a distribution curve, our estimate is that R||C analysis would still yield useful results.

Table I.18 . Propellant Stress Data
for Failure Modes 7 through 11.

Requirement Parameter	Capability Parameter	Average Value	Coefficient of Variation $\frac{\sigma}{x}$	Standard Deviation, σ
Inner Bore Strain, in/in	Critical Storage Strain	.242	.153	.037
Radial Bond Stress, psi	Tensile Strength	18.3	.097	.018
Propellant Principle Stress, psi	Tensile Strength	18.3	.097	.018

Table I. 19. Summary of AGC Computer Output, Showing Maximum Stress and Strain Requirements For Eight Flight and Eight Storage Simulation Runs

Propellant Flight Conditions						
Run No.	Max Inner Bore Hoop Strain		Max Bond Shear Stress			
	in/in	Section Location	lb/in ²	Section Location		
1	.0747	31	24.5	32		
2	.0770*	9	28.4*	32		
3	.0746	9	34.0	32		
4	.0743	9	25.3	36		
5	.0746	9	24.7	30		
6	.0667	26	31.8	36		
7	.0731	9	29.7	37		
8	.0845	9	52.8	39		
$\bar{x} = .0749 (= R_{11})^{**}$ $\sigma = .00489 \text{ in/in}$ $\frac{\sigma}{\bar{x}} = .065$			$\bar{x} = 30.62 (= R_{12})^{**}$ $\sigma = 9.52 \text{ lbs/in}^2$ $\frac{\sigma}{\bar{x}} = .311$			
Propellant Storage Conditions						
Run No.	Max Inner Bore Hoop Strain		Max Radial Bond Stress		Max Propellant Principle Stress	
	in/in	Section Loc.	lb/in ²	Section Loc.	lb/in ²	Section Loc.
1	.0354	18	2.26	2	5.16	2
2	.0354*	18 + 19	2.35*	2	5.26*	2
3	.0356	13	2.34	2	5.29	2
4	.0353	21	2.14	2	4.93	2
5	.0361	16	2.89	2	6.25	2
6	.0362	14	2.34	2	5.24	2
7	.0363	17	2.58	2	5.67	2
8	.0457	14	2.88	2	6.26	2
$\bar{x} = .0370(=R_7)^{**}$ $\sigma = .00374$ $\frac{\sigma}{\bar{x}} = .101$		$\bar{x} = 2.47(=R_8)^{**}$ $\sigma = 0.282 \text{ lbs/in}^2$ $\frac{\sigma}{\bar{x}} = .114$		$\bar{x} = 5.51(=R_9)^{**}$ $\sigma = 0.604 \text{ lbs/in}^2$ $\frac{\sigma}{\bar{x}} = .091$		

* Note max values in sample Table I. 17.

** The \bar{x} values are also the requirement average values.

It should also be pointed out that, the \bar{x} values are also the Requirements: R_7 , R_8 , R_9 , R_{10} , and R_{11} . The following list the relationship for R and C parameters, as given by AGC:

Measurement of Requirement Parameters for Storage Condition:

- Inner-bore Hoop Strain, in/in
- Radial Bond Stress, lbs/in²
- Propellant Principal Stress, lbs/in²

Measurement of Corresponding Capability Parameters for Storage Conditions:

- Measured Critical Storage Strain, in/in
- Measured Tensile Strength, lb/in²
- Measured Tensile Strength, lb/in²

Measurement of Requirement for Firing and Flight Conditions:

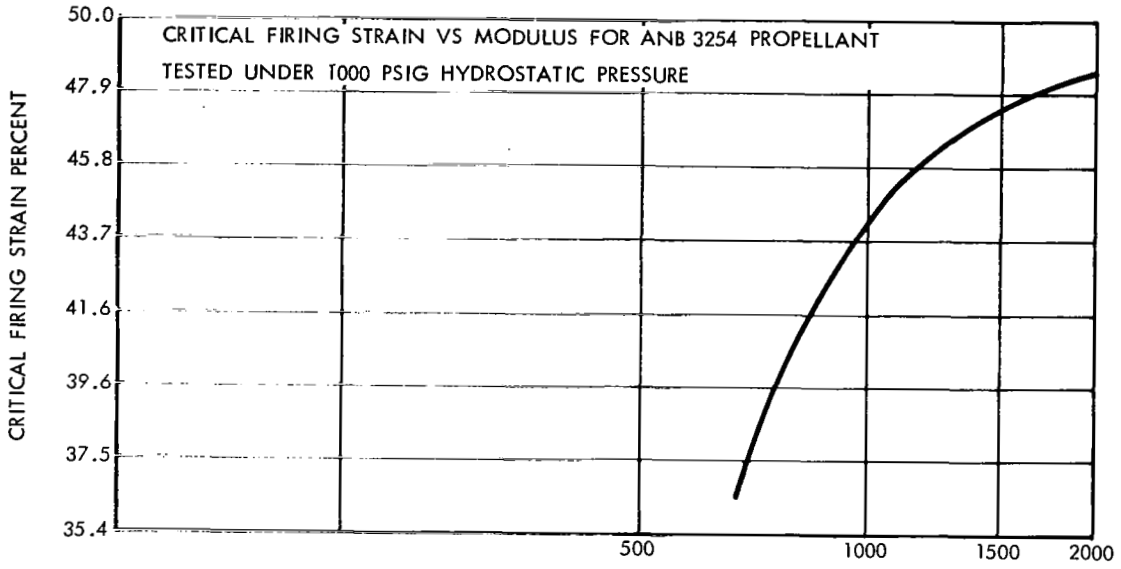
- Bond Shear Stress, lbs/in²
- Inner-bore Hoop Strain, in/in

Measurement of Corresponding Capability Parameters for Firing and Flight Conditions:

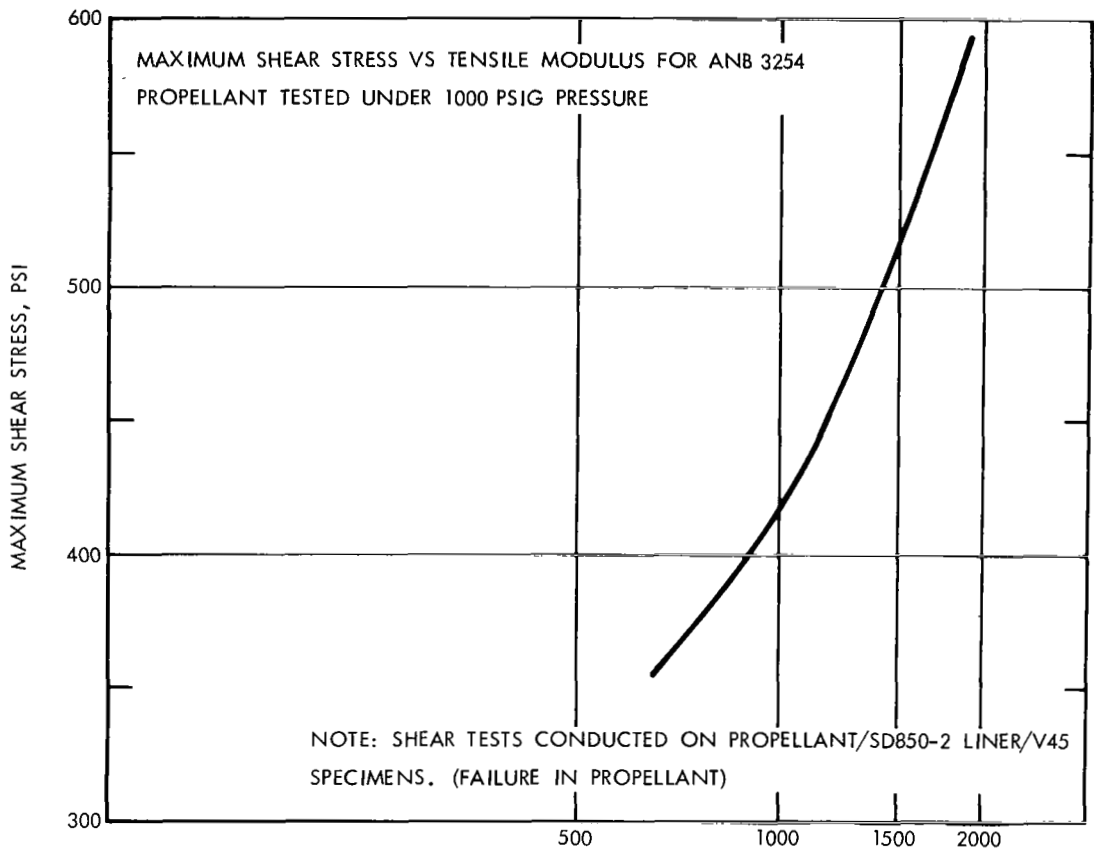
- Measured Shear Stress Under Pressure, lb/in²
- Measured Critical Firing Strain, in/in

Capability Distribution. Data relative to propellant capability is given in Figures I. 1 and I. 2, and those relating propellant modulus to critical firing strain and shear strength are used in determining the capability for flight failure modes for each section of the motor. No such correlation is assumed to exist for storage failure modes. Therefore, the capability to resist storage inner bore strain, radial bond stress, and propellant principle stress is considered normally distributed in accordance with the parameter distribution data shown in Table I. 20.

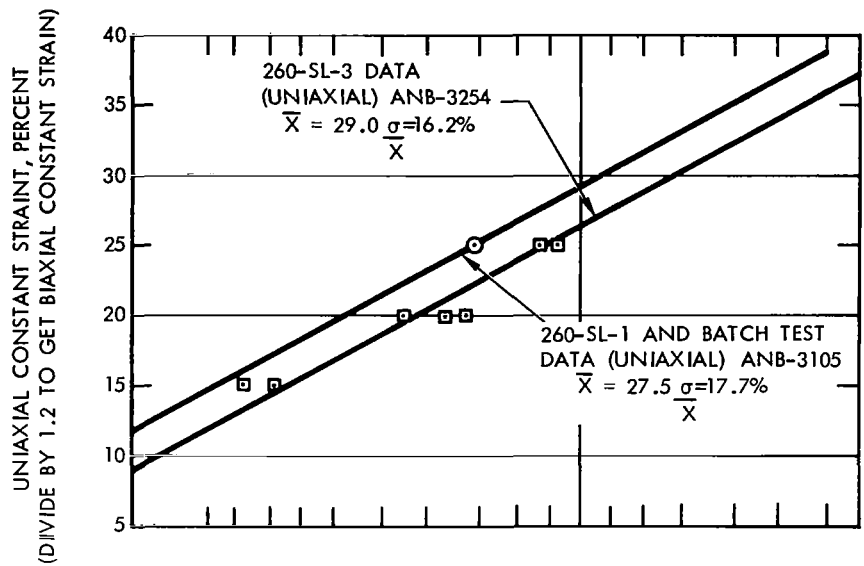
A summary of AGC capability data is shown in Table I. 21. These data are obtained from Figures I. 3 through I. 6. Appendix II discusses how this data is used.



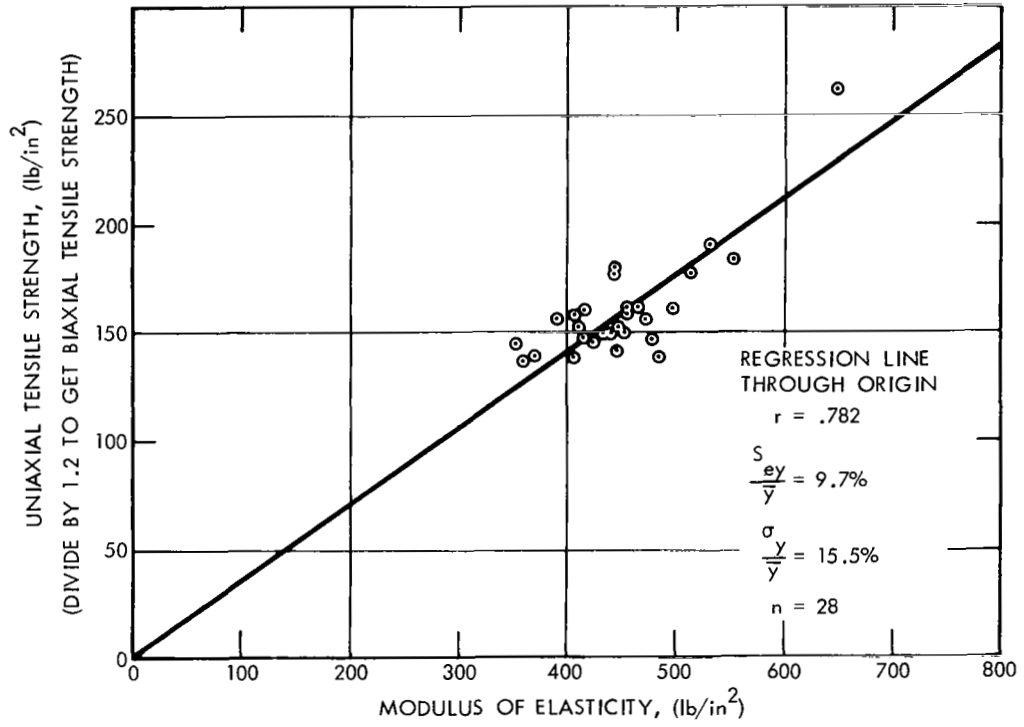
Modulus of Elasticity
Figure I.1



Modulus of Elasticity, Psi
Figure 1.2

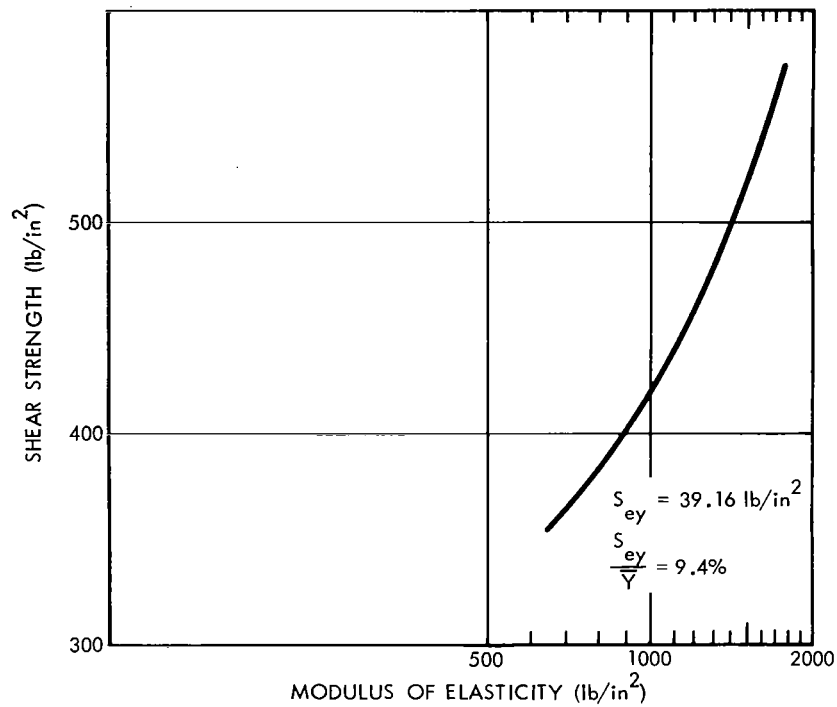


Constant Strain Data For ANB-3105 and ANB-3254 Propellant
Figure 1.3



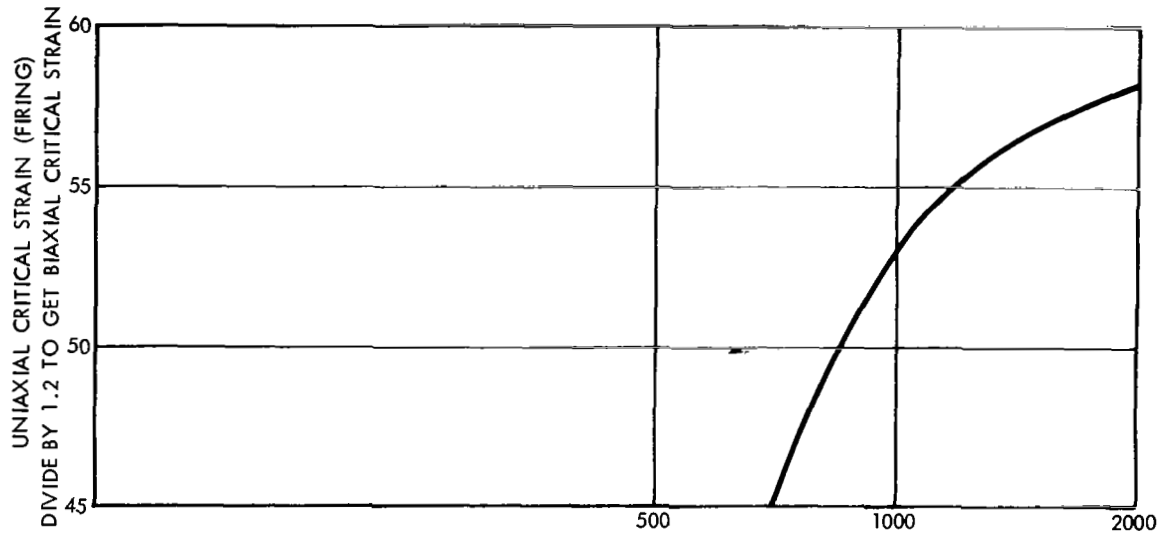
Bond Tensile Strength vs Modulus of Elasticity
for ANB-3254 Propellant From 260-SL-3.

Figure 1.4



Modulus of Elasticity vs Shear Strength for ANB-3254 Propellant Tested under 1000 psig Pressure.

Figure 1.5



Modulus of Elasticity vs Critical Strain (Firing) - ANB-3254 Prop.
 Tested under 1000 psig Pressure.

Figure 1.6

Table I. 20. Summary of Capability Parameter Data for FM-7 through FM-11.

<u>Storage Conditions</u>	Average Value, \bar{x}	Source of Average Value	Standard Deviation	Coefficient of Variation $\frac{\sigma}{\bar{x}}$	Source of Standard Deviation
Critical storage strain, (C_7) in/in.	.242	Extrapolated strain at which 50% of ANB-3254 samples from 260-SL-3 would fail. (Figure I. 3)	.0392	.162	σ assumed to be same as 260-SL-1 data (Figure I. 3)
Tensile strength, (C_8, C_9) psi	18.3	Value corresponds to modulus of 60 extrapolated from tensile stress vs modulus data for 28 batches of ANB-3254 from 260-SL-3 (Figure I. 4)	2.84	.155	$\frac{\sigma}{\bar{x}}$ from same 260-SL-3 and data used in Figure I. 4.
<u>Firing Conditions</u>					
Inter-face shear strength, (C_{10}) psi	418	Value corresponding to modulus of 1000 lb/in ² from graph of shear strength vs modulus based on one batch of ANB-3254 (Figure I. 5)	39.2	.094	S_{e_y} from correlation between modulus and shear strength for one batch of ANB-3254 (Figure I. 5)
Critical firing strain, (C_{11}) in/in.	.44	Value corresponding to modulus of 1000 lb/in ² from graph of strain vs modulus single batch of ANB-3254 (Figure I. 6)	.0674	.153	S_{e_y} from correlation between modulus and maximum strain for one batch of ANB-3254
* eg: .0392 = (.242) (.162)					

Table I. 21. Propellant and Case Input Parameters Varied by AGC in Grain Design Computer Simulation Runs.

Parameter	\bar{x}	σ	σ / \bar{x}
Propellant Modulus-Storage, psi (3 year relaxation 60° to 100° F)	60	4.67	.078
Propellant Modulus-Storage, psi (Initial)	1000	59.3	.138
Propellant Density, lb/in. ³	0.06330	0.0000147	.000231
Propellant Linear Coefficient of Thermal Expansion in/in °F	5.4×10^{-5}	0.00132×10^{-5}	.00231
Case Coefficient of Thermal Expansion	5.6×10^{-6}	0.014×10^{-6}	.0025
Case Modulus of Elasticity, E _c (200 grade marage steel), psi	27,500,000	—	—
Case Thickness-Fwd and Aft Heads, in.	0.428	0.00482	.0115
Case Thickness-Cyl Section, in.	0.631	0.0118	.0187
Initial Chamber Pressure- Fwd End* psi.	700	10	.0143
Initial Chamber Pressure- Aft End* psi.	530	7.6	.0143

* Varies Linearly between fwd and aft end

Failure Mode 12. Data, Insulation/Motor Case
Interface Bond Maximum Shear
Stress, Flight Condition

The requirement distribution is the calculated maximum shear stress at the chamber wall for a 2.0 g maximum launch acceleration. It was assumed that the Insulation/Motor case interface maximum bond shear stress can be conservatively approximated by the maximum bond shear stress of the propellant. Thus from the 8 computer simulation runs made (as discussed in FM's 7-11), from Table I.19, the mean value for the bond shear stress is 30.62 psi and the standard deviation is 9.52 psi. Although the sample size is small, the standard deviation based upon this sample data is probably conservatively high—the 52.8 psi obtained in the 8th run appears to be abnormally large.

For the Capability distribution, no data was available for the distribution of the shear strength of V44/Epon 948/Steel Bond. However, engineering judgment indicates that the data given in Table I.22 for shear strength of V45/SC 48:68 Epoxy Anhydride/Glass could be used as a conservative estimate.

Failure Modes 13 and 14. Data, Propellant Auto Ignition
due to Static Discharge; and
Auto Ignition due to Self Heating.

The data for these failure modes is discussed in AGC report NAS 7-572, Progress Report 6. Because of the extremely low probability of failure based on the limitations of data, the following AGC summary is given:

PROPELLANT AUTOIGNITION DUE TO STATIC DISCHARGE

Summary for distribution, R and C. Autoignition of a 260-in. -diameter motor propellant grain because of a static electrical discharge is considered to be unlikely because of the normally followed safety precautions and the large amount of energy required to ignite the grain. The requirement (in Joules) is assumed to be the single point value fixed by the U.S. Bureau of Mines as being "a reasonable value under not too extreme conditions." The capability distribution of the propellant is derived from ignition threshold tests.

The AGC report yielded the following data: $R_{13_{\max}} = .013$ Joules charge energy, with $\sigma_{R_{13}} \cong 0$ and $\bar{C}_{13} = 12.8$ Joules charge energy, with $\sigma_{C_{13}} = .188$ Joules.

Table I. 22. Distribution of Bond Strength of
V45/SC 58:68 Epoxy-Anhydride/Glass

Specimen	Bond Shear Strength, @ 77°F, psi
9	373
10	356
11	490
12	402
13	316
14	435
15	328
16	303
$\bar{x} = 375$ $\sigma = 64.13$ $\frac{\sigma}{\bar{x}} = .170$	

PROPELLANT AUTOIGNITION DUE TO AMBIENT AIR TEMPERATURE

Requirement Distribution. The requirement is established as a single maximum value specified by the procuring activity. In the case of the 260-in. -diameter motor, this has been set at 100°F for the ambient air at the surface of the propellant grain. With some propellants, the temperature at the interior of the grain may be more than this because of propellant self-heating. For ANB-3105 in an 87.5-in. web, the estimated temperature rise is of a 0.1°F order of magnitude and can be overlooked.

Capability Distribution. The capability of ANB-3105 to resist autoignition is determined by heating small propellant samples until they ignite. A value of 480°F was established for the ANB-3105 propellant. As is ordinarily the case where the capability is far in excess of the requirement, there is usually little effort made to determine a variability for the capability parameter. A limited amount of data for a similar propellant (ANB-3066) indicated a $\frac{\sigma}{\bar{x}}$ value of .0094. Since this represented only a single batch of propellant, it is recommended that a $\frac{\sigma}{\bar{x}}$ value of .02 be used instead. This assumption is based on engineering judgment and reflects experience with the batch-to-batch variability of other propellant parameters.

The AGC report yielded the following data:

$$R_{14_{\max}} = 100.1^{\circ}\text{F}, \text{ with } \sigma_{R_{14}} \cong 0$$

and

$$C_{14} = 586^{\circ}\text{F}, \text{ with } \sigma_{C_{14}} = 5.5^{\circ}\text{F}.$$

APPENDIX II

**DETAILS OF APPLICATION OF
LARGE SOLID ROCKET MOTOR**

Introduction

This appendix contains the details of the analysis and results that were summarized in Section 5 of this report. It is based upon the ground rules, data and rationale set up by AGC as given in Appendix I of this report. Computer programs and sample printouts are shown in the appendices which follow. A description of variability and sensitivity is also given in this appendix. This is followed by a discussion of the R|C analyses for the fourteen failure modes.

Discussion of Variability and Sensitivity Analysis

Standard Deviations, σ

It is appropriate to include a brief comment on the manner in which variances are computed and used in this report. The basic formulas are as follows. Consider a set of n observations of a variable, say x_1, x_2, \dots, x_n . (These n values are in effect what we have called "batch data"). The sample mean is

$$\bar{x} = \frac{1}{n} \sum_{i=1}^{i=n} x_i \quad (1)$$

and the sample variance is

$$s^2 = \frac{1}{n} \sum_{i=1}^{i=n} (x_i - \bar{x})^2 \quad (2)$$

The sample standard deviation is s , the positive square root of the variance. Denote the unknown population variance by σ^2 , σ being the population standard deviation. An unbiased estimate of σ^2 , denoted by $\hat{\sigma}^2$, computed from the sample is

$$\hat{\sigma}^2 = \frac{1}{n-1} \sum_{i=1}^{i=n} (x_i - \bar{x})^2 \quad (3)$$

Coefficient of Variation, cv

The coefficient of variation* is defined as the ratio of the standard deviation to the mean. In this case, we can speak of two such ratios based on computations from the n observations, namely

$$\frac{s}{\bar{x}} \text{ and } \frac{\hat{\sigma}}{\bar{x}}$$

We can describe s/\bar{x} as the coefficient of variation of the sample and $\hat{\sigma}/\bar{x}$ as an estimate of the coefficient of variation of the population.

Following a regrettably all too common practice, both TEMPO and AGC have used an inexact notation—we have used σ to mean s sometimes and to mean $\hat{\sigma}$ at others. This means that throughout this report, σ represents our estimate of the population standard deviation which may be either s or $\hat{\sigma}$. Of course there is little difference between s and $\hat{\sigma}$ for large n and we have regularly used the preferred one, $\hat{\sigma}$, where n is small. In the subsequent discussion, we will use this σ notation.

AGC has indicated that their data and their engineering analysis leads them to believe that the coefficient of variation is a key parameter and that it tends to remain constant over a rather wide range of designs. In other words, they can extrapolate coefficients of variation without adjustment—the scaling factor is nearly unity. This is an engineering property and not a statistical characteristic of σ/\bar{x} so at this point we can make no comment as to the validity of the AGC belief.

It often happens that various data sources yield a variety of estimates of σ/\bar{x} . As an example, one might observe a design characteristic for each of a number of different motors. AGC has chosen to combine these estimates of σ/\bar{x} by computing their arithmetic mean. Perhaps they consider that this is an appropriate method in view of their belief in the constancy of the coefficient of variation. We are not prepared to take issue with this method on theoretical statistical grounds. It should be noted, however, that it is an unusual procedure.

* AGC frequently obtains an estimate of a standard deviation for a new parameter of interest, by multiplying estimates of the mean value of the parameter of interest (e. g., 260/S IV. B), by the coefficient of variation based on similar systems data. Thus

$$\sigma \cong \bar{x}_{\text{std}} \text{ cv} \quad (4)$$

Variability Factor, V_f

The factor V_f is used to test the sensitivities of the failure probabilities to the values of the standard deviations of the input parameters. This was accomplished by multiplying the unadjusted standard deviation of the parameter, σ , by a variability factor V_f

$$\sigma = V_f \sigma_{\text{std}} \quad (5)$$

where

$$V_f > 0.$$

If $V_f > 1$, we are analyzing the effect of increased parameter variability on the failure probability—an increase is expected. If $V_f < 1$, we would anticipate a decrease in the failure probability. Sensitivity analysis thus provides an indication of the motor characteristics which can be adjusted through design changes or modifications in production methods to effect desired changes in reliability.

Detailed Analysis of the Failure Modes

The fourteen failure modes discussed herein were selected for analysis according to the provisions of the contract work statement given in Section 2, Study Objectives. The first six failure modes are in general those itemized under Task VIII, with some changes as suggested by AGC. They wished to cover the aft closure and bolt failure modes (numbers 5 and 6) instead of the forward areas because better design data was available.

Failure modes 7 through 11 were propellant stress failure modes. Failure mode 12 covered the interface bond stress of case and insulation, and the final two, 13 and 14, dealt with auto ignition failures.

In order to gain further insight into the rocket motor failures, special analyses were made in some cases of the fourteen listed failure modes. Parameter variability is based upon the AGC data and rationale shown in Appendix I. AGC has determined that as a good preliminary approximation, for this study, all parameters will be assumed normally distributed. The reader is reminded, however, that the R|C analysis works equally well if the data is used as any other

closed form or if discrete sets of data are used. A discussion of the failure modes follows.

Failure Mode 1. Hoop Stress Case Rupture Failure Mode

- 1a) Rupture with 90% of welds by machine 40" Fwd of equator, station 3.
- 1b) Rupture with 10% of welds by hand. 40" Fwd. of equator, station 3.

For purposes of this analysis, motor station 3, Figure 1, Section 5, was selected by AGC as being the critical one to consider. Since the analysis is made before fabrication it is not known exactly where hand welds will occur and hence AGC had to provide this selection. Past experience by AGC shows, however, that about 10% of the welds will have detectable flaws that must be reworked by hand welding. AGC data shows that the hand welds tend to be weaker and have more strength variability than those done by machine. For this analysis, we assumed that 90% of the welds would be by machine and the 10% remaining by hand. It was further assumed that these proportions would hold throughout the motor case. The critical region of the motor case, section 3, is a logical choice since it is where the transformation of a thin walled spherical region joins the thicker walled cylindrical section of the motor.

1. Requirement Function. The basic engineering equation was described in Appendix I. To fit the R||C analysis format better, both sides of the requirement equation are multiplied by R_o/t_c , giving

$$R_1 = \frac{P_{cmax} R_o}{t_c} = \frac{W_p r R_o K_m / a e^{\pi_k \Delta t}}{C_w A_t b t_c} \tag{6}$$

where

π_k = propellant temperature sensitivity coefficient, %/°F

Δt = ambient temperature difference between nominal and an upper specified limit prior to motor firing, °F.

- W_p = propellant weight, lb.
 b = nominal web thickness, in.
 $K_{m/a}$ = the ratio of peak to average web time pressure. (ND)

The factor $e^{\pi_k \Delta t}$ was put in to allow for estimating the maximum chamber pressure at the specified upper limit. π_k is a random variable but Δt is a single valued or fixed (maximum) design limit.

The factor $K_{m/a}$ is the ratio of the design maximum pressure to the design average web pressure. The variability of this factor, observed from data on other motor programs, was used to reflect the effects of burning surface variability due to non-homogeneous burning, propellant linear separations, voids, etc. AGC values are tabulated in Table II. 1.

2. Capability Function. The capability of the case to withstand the stresses imposed can be divided into two parts. The first part consists of those stresses that are the result of the machine welds, which is assumed to constitute 90% of all the case welds. The second part consists of the remaining 10% which are hand welds. To fit the R|||C analysis format, both sides of the equation are multiplied by R_o/t_c and the resulting capability equations become

$$C_{1m} = \frac{P_{mw} R_o}{t_c} = S_{umw} K_{be} K_{bx} \quad (7)$$

for the machine welds and

$$C_{1h} = S_{uhw} K_{be} K_{bx} \quad (8)$$

for the hand welds. *

The R|||C equation for failure mode 1, for the probability of failure is

$$P[F]_1 = P\{(C_1 - R_1) \leq 0\} \quad (9)$$

* The subscript designation is m for machine and h for hand welds.

which becomes, for 90% welds:

$$P_m[F]_{1m} = P\{C_{1m} - R_1 \leq 0\}; \quad (10)$$

and for 10% of the welds:

$$P_h[F]_{1h} = P\{(C_{1h} - R_1) \leq 0\}; \quad (11)$$

and for 100% of the welds:

$$P[F]_1 = .9P_m[F]_{1m} + .1P_h[F]_{1h} \quad (12)$$

Finally, using Equations 6 through 12, we obtain

$$P[F]_1 = .9\left\{P_m \left[K_{be} K_{bx} S_{umw} - \frac{W_p r_b R_o K_{m/a} e^{\pi_k \Delta t}}{C_w A_t b t_c} \right] \leq 0 \right\} +$$

$$.1\left\{P_h \left[K_{be} K_{bx} S_{uhw} - \frac{W_p r_b R_o K_{m/a} e^{\pi_k \Delta t}}{C_w A_t b t_c} \right] \leq 0 \right\} \quad (13)$$

The machine and hand weld portions shown in Equation 13 were calculated in separate computer runs.

The program used for failure mode one, RELFM1, is given as an example in Appendix V. Sample runs are shown for FMI_m for the standard case ($V_f = 1$ for all parameters), and for FMI_h for case 2 ($V_f = 4$ for the standard deviation of the parameter S_{uhw}). Over 30 computer runs were made for this failure mode to cover the standard case and the sensitivity analysis.

Table II.2 summarizes the results of the solution to Equations 10 and 11. Based on the data supplied by AGC, the standard computer runs were made for the 90% and 10% cases. For the 90% case, only when the value for one standard deviation for S_{umw} is increased from 2516.6 psi to 20,132.8 psi ($V_f = 8$) does the probability of failure increase from virtually zero to .00007567 ($V_f = 1$ for all other parameters). From the table, the critical ranking of the parameters was obtained, and is: S_{uhw} , S_{umw} , r_b , K_{be} and $K_{m/a}$. The remaining parameters are relatively insensitive to increases in variability. If more detailed sets of computer runs were to be made such as using other weld ratios (namely, 80/20 or 95/05 etc.) the remaining insensitive parameters A_t ,

Table II.1. Summary Data for Failure Mode-1

Symbol	Parameter Description	Mean Value \bar{x}	Parameter Standard Deviation
S_{umw}	Ultimate weld strength, psi. — Machine weld — Hand weld	232,000	2516.6
S_{uhw}		199,000	8641
K_{be}	Bending/discontinuity factor, (ND)	.95845	.00693
K_{bx}	Biaxial Gain Factor, (ND)	1.106	.0312
W_p	Propellant weight, lb.	3,400,000	6120
C_w	Mass flow coefficient sec^{-1} .	.0062477	.0000190
r_b	Propellant burn rate, in/sec.	.606	.00818
A_t	Average Throat area, in.^2	6355	20.9
$K_{m/a}$	Ratio of Avg to peak chamber pressure (ND)	1.18	.008968
b	Web thickness propel- lant, in.	85	.17
R_0	External motor radius, in.	130.631	.0261
t_c	Case wall thickness, in.	.6392	.0095
π_k	Temperature sensi- tivity, $\%/^{\circ}\text{F}$.	.16	.00676
Δt	Maximum temperature difference, $^{\circ}\text{F}$.	20	---

Table II. 2. Summary of Results of Computer Runs for Failure Mode-1

RUN	Variable	\bar{x}	V_f	σV_f	$P[F]_{1m, 1h}$
<u>FOR MACHINE WELDS (90%)</u>					
Std.	*	*	*	*	<<.000 000 01
1	Sumw	232,000	4	10,066.4	<.000 000 01
2	Sumw	232,000	8	20,132.8	.000 075 67
3	r_b	.606	4	.03272	<<.000 000 01
4	r_b	.606	8	.06544	.000 009 47
5	K_{be}	.95845	~5	.03	<<.000 000 01
6	K_{be}	.95845	~10	.06	.000 000 13
7	$K_{m/a}$	1.18	5	.04485	<<.000 000 01
8	$K_{m/a}$	1.18	~10	.1	.000 000 04
9	A_t	6355	~5	100	<<.000 000 01
10	t_c	.6392	~2	.01	<<.000 000 01
11	C_w	.0062477	5	.000095	<<.000 000 01
12	WP	3,400,000	3	18,360	<<.000 000 01
13	R_0	130.631	~5	.125	<<.000 000 01
14	π_k	.16	~3	.0002	<<.000 000 01
15	b	85	~50	8.5	<<.000 000 01
<u>FOR HAND WELDS (10%)</u>					
Std.	*	*	*	*	.000 000 81
1	Suhw	199,333	2	17,282	.002 283 40
2	Suhw	199,333	4	34,564	.049 484 70
3	r_b	.606	2	.01636	.000 012 04
4	r_b	.606	4	.03272	.000 219 25
5	K_{be}	.95845	5	.03465	.000 050 83
6	K_{be}	.95845	~10	.06	.001 684 02
7	$K_{m/a}$	1.18	5	.04485	.000 006 19
8	$K_{m/a}$	1.18	~10	.1	.001 145 91

* V_f , the variability factor, is varied for one parameter at a time.

For the standard run, $V_f = 1$ for all parameters.

Table II. 3. Summary of R|C Analyses
for Failure Mode-1

Parameter	Variability Factor V_f	σ	$V_f \sigma$	$P[S]**$
Standard run*	1	*	*	>.999999
S_{umw}	4	2516.6	10,066.4	.999772
S_{uhw}	2	8641.	17,282.	
S_{umw}	8	2616.6	20,132.8	.994983
S_{uhw}	4	8641.	34,564.	
r_b	4	.00361	.01444	.999781
K_{be}	5	.00693	.03465	.999995
K_{be}	10	.00693	.0693	.999832
$K_{m/a}$	5	.00897	.04485	.999999
$K_{m/a}$	10	.00897	.0897	.999885

* The standard run uses the unadjusted data supplied by AGC for all parameters and, consequently, the variability factor is unity.

** The $P[S]$ is obtained by combining the data of Table II. 2 for 90% and 10% welds, using Equation 13; and noting that $P[S] = 1 - P[F]$.

t_c , C_w , W_p , R_o , π_k and b could be treated as constants to greatly reduce computer time, and determine the sensitivity of ratio of machine welds to hand welds.

It can be seen from Table II. 2 and II. 3 that, as the variability factor (V_f) increases, the probability of failure increases significantly. The most significant of these increases in probability of failure are a result of the welds made by hand techniques.

Table II. 3 summarizes the results of some of the combinations of the Table II. 2 run results for 90% machine and 10% hand welds. We note that for the standard run ($V_f = 1$ for all parameters) the reliability is in excess of .999999. An illustration of a somewhat critical case for the present design of the 260/S IV B welds arises if the V_f is as great as 8 for machine welds and 4 for hand welds. This is shown by the third calculation in Table II. 3 with a value of $P[S]$ equal to .994983. The table considers variability factors for one parameter at a time except for the second and third calculations. The "90/10" ratio of welds should be investigated further and also the variability of S_{uhw} , S_{umw} , r_b . Possibly K_{be} and K_m/a should also be investigated to check if these in fact have significant influence for realistic values of V_f 's.

Failure Mode 2. Motor Case Insulation Burn Through Failure Mode

- 2a) Burn-through of the insulation to case wall at stations with propellant.
- 2b) Burn-through of the insulation to case wall at stations that have no propellant.

Many motor stations are being considered in studying this failure mode since it is not obvious which is critical—for purposes of this analysis, AGC suggested that we examine stations 1, 2, 4, 5, 6, 7 and 12 as are shown in Figure 1, Section 5.

Transfer Function. Four basic parameters enter in the transfer functions for this failure mode. These four parameters are as follows.

- b = nominal propellant web thickness, in.
- r_b = propellant burning rates, in. per second.

t_i = insulation thickness, in.

e_r = insulation erosion rate, in. per second.

The capability transfer function, C , is $(b/r_b + t_i/e_r)$. This function represents the total time it takes to burn through the propellant and insulation at any motor station.

The requirement transfer function, R , is b'/r'_b . This function represents the time it takes to burn through the propellant to the insulation at that motor station, where the propellant web thickness, b' , divided by the propellant burning rate, r'_b , is greatest. The resulting transfer function for FM2 becomes

$$(C - R)_2 = (b/r_b + t_i/e_r) - b'/r'_b \quad (14)$$

The requirement term involving primed parameters occurs at station 4—it is compared to the capability function at each motor station using the equation

$$P[S]_2 = 1 - P \left[\left(\frac{b}{r_b} + \frac{t_i}{e_r} - \frac{b'}{r'_b} \right) \leq 0 \right] \quad (15)$$

Parameter Variability. The analysis for FM2, follows.

Propellant Burning Rate, r_b . The burning rate variability is estimated from the coefficient of variation based on LSBR batch mix data for 260-SL-1 and 260-SL-2 motors. Table II.4 lists the burning rate data from which the coefficient of variation for the propellant burning rate is estimated at 0.00595 for the 260/S IV-B motor. Using the propellant burning rate as 0.606 in/sec at motor stations 2, 5, 6 and 7, and 0.590 in/sec at motor station 4, we can estimate the respective standard deviations for the propellant burning rates as follows:

At Motor stations 2, 5, 6 and 7

$$\sigma_{std} = 0.00595 (0.606) = \underline{0.00361}$$

At motor station 4

$$\sigma_{std} = 0.00595 (0.590) = \underline{0.00351}$$

Propellant Web Thickness, b. AGC assumed the coefficient of variation is .002 and constant throughout the propellant. This then resulted in the values for one standard deviation* at the various motor stations and summarized in Table II.4.

Insulation Thickness, t_i . The insulation thickness variability is estimated by AGC to be ± 0.010 inches for $\pm 3\sigma$ in the thin section of the motor (stations 4 and 5, where $t_i = 0.110$ inches), and ± 0.050 inches for $\pm 3\sigma$ in the remainder of the motor.

At motor stations 4 and 5

$$\sigma_{\text{std}} = \frac{0.01}{3} = \underline{0.0033}$$

At motor stations 1, 2, 6, 7 and 12

$$\sigma_{\text{std}} = \frac{0.05}{3} = \underline{0.01667}$$

Table II. 5 shows this data as it will be used in the R | C analysis. For the first set of data, standard runs will use the above data with the nominal design values for t_i . The second set of values are used in the sensitivity analysis, where insulation thicknesses were doubled in the thin sections (stations 4 and 5) and increased by a factor that was less than double in the thicker sections. The results of this analysis are discussed in Section 5 of the report.

Insulation Erosion Rate, e_p . The insulation erosion rate variability is estimated from the coefficient of variations based on Polaris and Minuteman (MM) data since these also use V-44 type Silica Asbestos insulation on the motor case. AGC suggested that the MM data may be used in the cylindrical sections of the motor as a preliminary estimate, but they feel that the high variability of the data may lead to an over conservative analysis. Polaris data is to be used in the remaining sections of the motor. Table II. 5 of Appendix I lists distribution data for 11 Polaris motor stations and are assumed by AGC to be comparable to the hemispherical ends of the 260/S IV-B motor. Table II. 6 lists the MM data estimated by AGC as conservatively comparable to the thin wall section of the 260/S IV-B, at motor station 5.

* The assumption of a normal distribution for the propellant web thickness, b, is based upon a homogeneous propellant not having voids, cracks, laps, folds, etc. This assumption appears to be less realistic than some others. A more reasonable one would consider a skewed distribution.

Table II. 4. Variability Data for Propellant Web Thickness,
Parameter b

Motor Station	σ_{std}
2	0.049
4	0.175
5	0.170
6	0.1437
7	0.1411
1	(no propellant)
2	(no propellant)

Notes: Based on AGC judgment it is assumed that the coefficient of variation , $\sigma/\bar{x} = 0.002$, is constant for the entire propellant grain. (AGC report 0815-81F on 260 SL1 and 260 SL2 motors.)

Table II. 5. Variability Data for Insulation Thickness
Parameter, t_i

Motor Station	Standard Runs			Sensitivity Runs		
	t_i	σ_{std}	Run No.	t_i	σ_{std}	Run No.
1	1.125	0.01667	1	(not required)		--
2	1.125	0.01667	2	(not required)		--
4	0.110	0.00333	(all)*	(not apply) ⁽¹⁾		--
5	0.110	0.00333	3, 5	0.220	0.005	4
6	0.250	0.01667	6	0.375	0.025	7
				0.500	0.025	8
7	0.430	0.01667	9	0.516	0.025	10
				0.645	0.025	11
12	3.60	0.01667	12	4.32	0.025	13
				5.4	0.025	14

* Station 4 is the station by which the requirement is generated.

Thus, from the Polaris data, the coefficient of variation is estimated as being the "average" * of the 11 station maximums. Using a computer program to compute the means, standard deviations, and coefficient of variations for "batch" data, values obtained for \bar{x} and cv are calculated and summarized in Table II.6. Thus:

$$cv_{POL} = 0.16310 \approx cv_{260/S IV-B}; \text{ at stations 1, 2, 6, 7 and 12.}$$

Table II. 6. Summary of Polaris Data

<u>Station</u>	<u>Mean, \bar{x}</u>	<u>cv, $\frac{\sigma}{\bar{x}}$</u>
26	.368333	.123837
27	.366250	.120264
28	.341667	.123079
29	.328750	.151663
30	.328750	.157890
31	.318750	.140394
32	.283333	.143245
33	.272917	.194025
34	.248333	.214555
35	.214583	.239135
36	.197083	.184974

$$cv_{POL} = 0.16310$$

Similarly, for Minuteman data based on 20 motor firings and shown in Table I. 6 of Appendix I the coefficient of variation was calculated, to be

$$cv_{MM} = 0.51714$$

and this was used as the cv for stations 4 and 5. Thus, the estimates of the standard deviations for the insulation erosion to be used in this analysis for 260/S IV-B are as follows.

*

This is an engineering judgement rather than a statistical one. See beginning of this appendix for comments on coefficients of variations. (If the total population of 264 \bar{x} maximum values were averaged, the total mean would have been .297159 and $cv_{264} = .245477$).

At motor stations 1 and 2 (cv = .16310)

$$\sigma_{\text{std}} = \text{cv}_{\text{POL}} \bar{e}_r = 0.16310 (0.003) = \underline{0.0004893}$$

At motor station 5 (cv = 0.51714)

$$\sigma_{\text{std}} = \text{cv}_{\text{MM}} \bar{e}_r = 0.51714 (0.005) = \underline{0.002586}$$

At motor station 6 (cv = 0.16310)

$$\sigma_{\text{std}} = \text{cv}_{\text{POL}} \bar{e}_r = 0.16310 (0.005) = \underline{0.000816}$$

At motor station 7 (cv = 0.16310)

$$\sigma_{\text{std}} = \text{cv}_{\text{POL}} \bar{e}_r = 0.16310 (0.006) = \underline{0.000979}$$

At motor station 12 (cv = 0.16310)

$$\sigma_{\text{std}} = \text{cv}_{\text{POL}} \bar{e}_r = 0.16310 (0.0168) = \underline{0.002740}$$

Results of Failure Mode 2 Analysis. The parameters, standard deviations and summary of results are tabulated in Table II. 7. Fourteen computer runs were made, including six standard runs for the six motor stations. This resulted in critical values of .862888 at station 6; .953370 at station 12; .983907 at station 5; and .988810 at station 7. The sensitivity analysis showed that by increasing the insulation thickness at these stations reliability values greater than .999999 resulted, except for station 5 where even for an increase of from .110 to .220 inches (cylindrical region) the P[S] was only .999988. This represents the conservative AGC estimate based on MM variability data for the erosion rate of the insulation. It was noted that if Polaris variability data were used instead of the MM data in the cylindrical region of the motor, this would effectively amount to a V_f value of .316 on the standard deviation. Thus, for the thin wall region; $t_i = .110$, and this would have increased P[S] at station 6 from .86288 to .998. This is still too low, but coupled with increased insulation thickness, the P[S] will exceed .999999 at this critical station. A major effort may be required to accomplish this gain. If further analysis indicates that the MM data is in fact about the "best estimate" of σ , then the only course open is to increase the insulation thickness about 120% at station 5.

Table II.7. Summary for Failure Mode FM-2; Motor Insulation Burn-Through.

Computer Run	Motor Station	Variability Sensitivity	CAPABILITY ⁽¹⁾								REQUIREMENT [Station 4]				P[S] ₂
			Web, b, ins		Burn Rate, r _b (ins/sec)		Ins. Thick., t _i ins		Eros. Rate, e _r (in/sec.)		Web, b, ins		Burn Rate, r _b (in/sec.)		
			\bar{X}	σ	\bar{X}	σ	\bar{X}	σ	\bar{X}	σ	\bar{X}	σ	\bar{X}	σ	
1	1	Standard Run	No Propellant				1.125	.1667	.003	.000489	87.5	.175	.59	.00351	> .999 999
2	2	Standard Run	24.5	.049	.606	.00361	"	"	"	"	"	"	"	"	> .999 999
3	5	Standard Run	85	.170	"	"	0.110	.0033	.005	.002586	"	"	"	"	.983 907
4	5	Double Insulation	"	"	"	"	0.220	.005	"	"	"	"	"	"	.999 988
5	5	Decr. V _f ⁽³⁾ for e _r	"	"	"	"	0.110	.0033	"	.000816	"	"	"	"	.998 001
6	6	Standard Run	71.85	.1437	"	"	0.25	.01667	"	"	"	"	"	"	.862 888
7	6	50% Incr. Insul.	"	"	"	"	0.375	.025	"	"	"	"	"	"	.993 235
8	6	Double Insul.	"	"	"	"	0.50	.025	"	"	"	"	"	"	> .999 999
9	7	Standard Run	70.57	.1411	"	"	0.43	.01667	.006	.000979	"	"	"	"	.988 810
10	7	Incr. Insul. 20%	"	"	"	"	0.516	.025	"	"	"	"	"	"	.995 213
11	7	Incr. Insul. 50%	"	"	"	"	0.645	.025	"	"	"	"	"	"	> .999 999
12	12	Standard Run	No Propellant				3.6	.01667	.0168	.00274	"	"	"	"	.953 370
13	12	Incr. Insul 50%	No Propellant				4.32	.025	"	"	"	"	"	"	.983 565
14	12	Incr. Insul 50%	No Propellant				5.4	"	"	"	"	"	"	"	> .999 999

(1) $C = (b/r_b + t_i/e_r)$.

(2) $R = b'/r'_b$.

(3) $V_f = 1/3$; POLARIS Standard deviation used at this station instead of MM standard deviation.

II-17

**Failure Mode 3. Failure of the Forward Motor Skirt
Forging in Combined Compression, Shear,
and Bending.**

This failure mode involves consideration of the interaction ratios of axial compression, transverse shear and pure bending load requirements to their respective material capabilities. The mode is associated with only one region of the motor case, namely the forward motor skirt forging. The engineering data and rationale to be used for analysis will be found in Appendix I.

The transfer function for this failure mode was given in Equation 6 of Appendix I. It was transformed into R||C form as follows.

$$P[F]_3 = P \left[(R_c + \sqrt[3]{R_b^3 + R_s^3}) \geq 1.000 \right]. \quad (16)$$

By expanding the interaction transfer function, and by substitution we have for the 260/SIV-B motor, in R||C form, the following:

$$P[F]_3 = P \left\{ \left[\frac{L_c}{2\pi R_i t_s K_c E_s} + \sqrt[3]{\left(\frac{L_b}{\pi R_i^2 t_s K_b E_s} \right)^3 + \left(\frac{L_s}{\pi R_i t_s K_s E_s} \right)^3} \right] \geq 1.000 \right\}. \quad (17)$$

where

- L_c = Axial compressure load, lb.
- L_b = Pure bending load, lb.
- L_s = Transverse shear load, lb.
- R_i = Radius to inner surface of skirt, in.
- t_s = Thickness of skirt, in.
- E_s = Modules of elasticity, psi
- K_c = Ratio of axial compressure strength to Modulus of Elasticity.

K_b = Ratio of pure bending strength to Modulus of Elasticity.

K_s = Ratio of transverse shear strength to Modulus of Elasticity.

A summary of the averages and standard deviations characterizing the distribution of these parameters is shown in Table I. 7 of Appendix I. Based on this data, the computations indicated that the probability of failure was very remote. Hence, with $P[S]_3 > .999\ 999$ no sensitivity analysis was made for this failure mode.

Failure Mode 4. Meridional Stress Case

Rupture Failure Mode:

- 4a) Rupture with 90% of welds machine welded, Fwd head circumferential weld, Meridional stress, spherical section.
- 4b) Rupture with 10% of welds, hand welded. Fwd head circumferential weld, Meridional stress, spherical section.

The general analysis for this failure mode is similar to Failure Mode 1. However, because of the spherical shape in the forward region of the motor, the pressure capacity is twice as great for the same thickness of material. In practice, the hemispherical motor ends are made thicker than half that of the cylindrical sections; hence, this region tends to be much less critical, all things being equal (weld strengths, etc.).

The Requirement is the same, so Equation 3 is used.
Hence,

$$R_3 = R_1$$

The Capability, again as with FM-1, is assumed to have 90% of welds machine welded, and 10% hand welded. Because of the spherical shape, there is no K_{bx} , bi-axial gain factor. Hence the capability for 90% of the welds becomes

$$C_{4m} = \frac{P_{mw} R_0}{2t_c} = S_{umw} K_{be} \quad (19)$$

and for 10% of the welds

$$C_{4h} = \frac{P_{hw} R_0}{2t_c} = S_{uhw} K_{be} \quad (20)$$

In similar fashion to FM-1, these reduce to

$$P[F]_4 = .9 \left\{ P_m \left[K_{be} S_{umw} - \frac{W_p r_b K_{m/a} e^{\pi_k \Delta t}}{2C_w A_t b t_c} \right] \leq 0 \right\} + \quad (21)$$

$$.1 \left\{ P_h \left[K_{be} S_{uhw} - \frac{W_p r_b K_{m/a} e^{\pi_k \Delta t}}{2C_w A_t b t_c} \right] \leq 0 \right\} .$$

Computations for machine and hand welds were made separately. Data and rationale appear in Appendix I for FM-4. Table I. 9 of Appendix I summarizes the data for the runs which were made. The plate thickness parameter, t_c , uses the thinner plate (mean of .428) together with its associated standard deviation. The standard runs yielded the following results.

$$P[S]_4 = 1 - [.9(<.000\ 001) + .1 (<.000001)] = > .999\ 999.$$

Since this failure mode has a considerably lower criticality than FM-1, no sensitivity analysis was made.

Failure Mode 5. Rupture of the Nozzle Joint Bolts

The requirement Equation 11 was given in Appendix I. The term P_{cmax} is contained within that expression, but P_{cmax} is also a function of several other variables, which also appear in FM-1 as:

$$P_{cmax} = \frac{W_p r_b K_{m/a} e^{\pi_k \Delta t}}{C_w A_t b} \quad (22)$$

Substituting (22) in the R_5 function and using Equation 23

$$P[F]_5 = P[C_5 - R_5 \leq 0] \quad (23)$$

we can write the probability of failure for this failure mode as *

$$P[F]_5 = P \left\{ P_y - \left[K_p F_{by} + \frac{5.6912(\tan \alpha) A_{ti} W_p r_b K_{m/a} e^{\pi_k \Delta t}}{n D_j C_w A_t b} - \frac{51.534(\tan \alpha) d A_{ti} P_a}{n D_j} \right] \leq 0 \right\} \quad (24)$$

Equation 24 could have been simplified by factoring, so that the P_{cmax} terms transfer function would match those of FM-1. This would be better if we were considering correlated parameters of different failure modes and if all the terms were variables. In this analysis, however, since many of the variables are constants, Equation 24 was reduced to the following:

$$P[F]_5 = P \left\{ P_y - \left[213\,310 K_p + \frac{10.08146 W_p r_b K_{m/a} e^{20\pi_k}}{C_w A_t b} - 77.9427 P_a \right] \leq 0 \right\} \quad (25)$$

Table II-8 lists the variables and their deviations, the last six being constants in this example. Equation 25 was used in the computer run and the results showed a very low probability of failure. The sensitivity analysis used variability factors to approach a low limit of reliability.

Four of the variables that showed some sensitivity, namely, W_p , r_b , A_t and $K_{m/a}$, were varied together by using factors, V_f , which ranged from 2 to 10. Resulting probabilities of failure were still much less than .000001. Reliability for this failure mode is estimated as $P[S]_5 > .999999$.

* The numerical constants appearing in the Equations 11 and 24 are the result of various computations performed by AGC—they were not described in their reports.

Table II. 8. Summary for FM-5

Parameter	\bar{X}	Standard	Sensitivity	
		σ_{std}	V_f	σV_f
W_p	3,400,000	6120	4	24,480
C_w	.0062477	.000019	1	.000019
r_b	.606	.00818	2	.01636
A_t	.6355	20.9	4	83.6
$K_{m/a}$	1.18	.00897	10	.0897
b	85	.17	1	.17
π_k	.16	.00676	1	.00676
P_a	14.696	.0735	1	.0735
K_p	0.6	.077	1	.077
P_y	245,307	1987	1	1987
F_{by}	213,310	0	1	0
α	3.1	0	1	0
d	178.84	0	1	0
A_{ti}	6235	0	1	0
n	220	-	-	-
D_j	180	0	1	0
$P[F]_5$	=	<.0000001	<.0000001	

Note: only 10 of the 15 parameters had a distribution, and of these all

but three are correlated with FM-1

Failure Mode 6. Separation of Motor Chamber and Nozzle Flange.

This failure mode deals with the separation of the motor chamber from the nozzle flange caused by the ejection load per bolt exceeding the pretorque load per bolt.

Requirement Analysis. The requirement Equation 12 given in Appendix I, may be rewritten as:

$$R_6 = P_{cmax} \left[.9981 A_{180} (1 + \gamma M_{180}^2) - .014092 A_{ei} (1 + \gamma M_e^2) \right] \frac{1}{n} + P_a \left[A_{ei} - A_{180} \right] \frac{1}{n} + \left[\frac{W_{ni} (W_p + W_{vi})}{1.42279 A_{ti} P_{cmax} - 11 A_{ti} P_a} \right] \frac{1}{n} \quad (26)$$

Then, by substituting Equation 22 for P_c ; we obtain the equation in terms of all of the variables:

$$R_6 = \frac{W_p r_b K m/a e^{\pi_k \Delta t}}{C_w A_t b} \left[.9981 A_{180} (1 + \gamma M_{180}^2) - .014092 A_{ei} (1 + \gamma M_e^2) \right] \frac{1}{n} + P_a \left[A_{ei} - A_{180} \right] \frac{1}{n} + \left[\frac{W_{ni} (W_p + W_{vi})}{1.42279 A_{ti} \frac{W_p r_b K m/a e^{\pi_k \Delta t}}{C_w A_t b} - 11 A_{ti} P_a} \right] \frac{1}{n} \quad (27)$$

Since for this study many variables appearing in the above equation are constants ($\sigma = 0$), Equation 27 was reduced to the following:

$$R_6 = \left(\frac{68.0064 W_p r_b K m/a e^{\pi_k \Delta t}}{C_w A_t b} \right) + 139.405 P_a + \frac{59428 (W_p + 726466)}{\left(\frac{1,951,640 W_p r_b K m/a e^{\pi_k \Delta t}}{C_w A_t b} \right) - 15,088,700 P_a} \quad (28)$$

Capability Analysis. The capability is the pretorque load per bolt. This may be expressed simply as

$$C_6 = K_p F_{by} \quad (29)$$

where

- C_6 = the capability of one bolt to withstand the flange separation, lb.
- K_p = the fraction of bolt minimum yield strength to which the bolt is pretorqued, (ND)
- F_{by} = the minimum tensile load per bolt, lb/bolt.

Failure, then is

$$P[F]_6 = P \left\{ \left[K_p F_{by} \right] - \left[\frac{68.0064 W_p r_b K_m / a e^{\pi_k \Delta t}}{C_w A_t b} + 139.405 P_a \right] + \frac{59,428 (W_p + 726,466)}{P} \right\} \leq 0 \quad (30)$$

$$+ \left(\frac{1,951,640 W_p r_b K_m / a e^{\pi_k \Delta t}}{C_w A_t b} - 15,088,700 P_a \right)$$

A program was written for Equation 30 in which the last ratio, to be denoted by "B", before the inequality sign was treated as a constant. This was done after a sensitivity analysis showed that the effect of the last term, B, was negligible. It was found that even if the standard deviation of the parameter of the last term were chosen at the values of $\pm 3 \sigma$ that would cause the term to be a maximum ($B_{max} = 228,653$), the effect on $P[F]$ was negligible. Had this not been so, a more complicated program would have to have been written to account for the correlation of the parameters.* Table II. 9 contains the data and results. Note the effect of the B term when comparing two sets of identical runs. Standard runs 1 and 2 yielded a reliability of .999 998 for both $B = 0$, and $B = 228.653$. Runs 6 and 7 were also unaffected in the 6th place. The variability of K_p , the pretorque factor, is somewhat sensitive. Perhaps a 100% increase in variability is unreasonable (which produces a joint reliability of .983 695); but for a 20% increase in variability, reliability is .999 949. This analysis has about the same effect as Run 8,

* This is an example of parameter correlation within a failure mode. The sensitivity analysis also showed that there was no need to over-complicate the problem with a more exact treatment, since the results would have been nearly the same for all runs.

Table II. 9. Summary for FM-6.

Parameter	\bar{X}	Standard Deviation σ_{std}	Sensitivity Runs ⁽²⁾ , for Values of V_f .							
			1	2	3	4	5	6	7	8
W_p	3,400,000	6,120	1	1	1	1	1	1	1	2
C_w	.0062477	.000019	1	1	1	1	4	4	4	4
r_b	.606	.00818	1	1	1	1	1	1	1	10
A_t	.6355	20.9	1	1	1	1	1	2	2	2
$K_{m/a}$	1.18	.00897	1	1	1	1	1	2	2	2
b	85	.17	1	1	1	1	1	1	1	10
π_k	.16	.00676	1	1	1	1	1	1	1	1
P_a	14.696	.0735	1	1	1	1	1	1	1	1
K_p	0.6	.077	1	1	2	1.2	1	1	1	1
A_{180}	25,477	0	0	0	0	0	0	0	0	0
A_{ei}	56,116	0	0	0	0	0	0	0	0	0
A_{ti}	6,235	0	0	0	0	0	0	0	0	0
γ	1.2	0	0	0	0	0	0	0	0	0
M_{180}	.0576	0	0	0	0	0	0	0	0	0
M_e	3.205	0	0	0	0	0	0	0	0	0
n	220	0	0	0	0	0	0	0	0	0
W_{ni}	58,428	0	0	0	0	0	0	0	0	0
W_{vi}	726,466	0	0	0	0	0	0	0	0	0
$B^{(1)}$	—	—	0	228	0	0	0	0	228	0
$P[S]_6 = 1 - P[F]_6 =$.999998	.999998	.983695	.999949	.999998	.999993	.999993	.999951

(1) B = Maximum value, within $\pm 3 \sigma$, for all variables in the last term of Equation 30. When max, $B = 228.653$; when the term is ignored, $B = 0$. (This term should not be confused with the general notation of \bar{X} for mean value of a parameter).

(2) Eight runs were made. Values in the table are V_f values ($\sigma = V_f \sigma_{std}$); zero values of V_f or σ have no variance, or their estimates are assumed near zero.

where the combined variabilities of propellant weight, mass flow coefficient, burning rate, throat area, maximum to average peak pressure ratio, and propellant web thickness, produces about the same reliability, namely .999951.

Failure Modes 7 through 11 inclusive. Propellant Stress Failure Modes

The propellant stress relationships are perhaps the most complex and least understood of all the solid rocket motor failure modes. For the requirement function, AGC ran a rather complex computer program on a limited propellant stress analysis, using sets of randomly selected input parameter values for each computer run to gain some feel for $R|C$ variability, for those seven failure modes. Within the constraints of the analysis made (see Appendix I for success criteria), and the relatively few computer runs made by AGC (high computer run costs), their outputs gave reasonable preliminary estimates for the mean values of the requirement functions, \bar{R} , for Failure Modes 7 through 11.

For the capability functions, AGC used values based on their curves (see Appendix I) from which \bar{C} estimates were made. These data for \bar{R} and \bar{C} are summarized in Table II.10 together with the estimates for standard deviations, σ . For \bar{R} , the estimate of σ was obtained from the variability of the 8 computer runs. For \bar{C} , the rationale is given in Table I.20 of Appendix I.

AGC did not supply the transfer function equations and input parameter densities. Rather, they gave the R and C output means and standard deviations, stating that R and C had Gaussian densities. Closed form solutions were used to solve for the probability of success for these failure modes. The difference of two Gaussian random variables, $C - R$, is also Gaussian. Thus, the probability of failure is obtained from tables of the normal function as the area in one tail of the normal curve with zero mean and unit variance beyond the point

$\frac{\bar{C} - \bar{R}}{\sqrt{\frac{\sigma_C^2}{2} + \frac{\sigma_R^2}{2}}}$. Table II.10 also summarizes these calculations, and

the last column gives the $P[S]$. A sensitivity analysis was made on two of the failure modes that yielded low estimates of $P[S]$, FM-9 and FM-11. Note that when the principle stress, storage condition, has its standard deviation doubled, $P[S]$ is markedly reduced to .972. Certainly FMs 9 and 11 deserve closer inspection of the input data and the rationale used herein.

Table II.10 Summary of Propellant Stress/Strain Failure Modes in Storage and Flight Conditions

FM	FM Description	\bar{R}	$\hat{\sigma}$	\bar{C}	$\hat{\sigma}$	$\bar{C} - \bar{R}$	P[S]
						$\sqrt{\sigma_C^2 + \sigma_R^2}$	
7	Inner bore hoop strain, storage. in/in	.037	.00374	.242	.0392	5.20595	.999999
8	Prop/Liner radial bond stress, storage. #/in ²	2.47	.282	18.3	2.84	7.61397	>.999999
9a	Principle stress, storage, #/in ²	5.51	.604	18.3	2.84	4.405	.999989
9b	Principle stress, storage, #/in ²	5.51	1.208 ⁽¹⁾	18.3	5.68 ⁽¹⁾	2.2025	(.972360) ⁽¹⁾
10	Prop/liner interface shear stress, flight #/in ²	30.62	9.52 ⁽²⁾	418	39.2	9.60301	>.999999
11a	Inner bore hoop strain, flight, in/in.	.0749	.00489	.441	.0674	5.41751	>.999999
11b	Inner bore hoop strain,	7.49	.978 ⁽³⁾	44.1	8.9 ⁽³⁾	4.08887	(.999956) ⁽³⁾

(1) $V_f = 2$ for σ_R and σ_C .

(2) At less than -3σ value of R becomes negative, truncation required.

(3) $V_f = 2$ for σ_R , and ~ 1.3 for σ_C .

Failure Mode 12. Insulation/Motor Case Interface Bond Max. Shear Stress Failure Mode, Flight Condition

Insulation/Motor Case interface bond fails in shear for a 2g maximum launch acceleration.

The failure mode requirement is that the shear stress at the chamber wall of the motor for a 2g maximum launch acceleration will also be a maximum. From the 8 grain stress computer runs that were made by AGC, a mean value for R_{12} of 30.62 psi maximum shear stress with a standard deviation of 9.52 psi was obtained (see Table I.19 of Appendix I).

No data was available from AGC on the capability distribution of shear strength for V44/Epon 948/steel bond. AGC did report, however, that the shear strength of V45/SC 58:68 epoxy-anhydride/glass could be used as a conservative estimate. From Appendix I, Table I.22, the mean bond shear strength is given as 375 psi, with a value of 64.13 psi for one standard deviation.

Since \bar{R} and \bar{C} are assumed Gaussian, the probability of success is obtained from the closed form Gaussian solution. Thus, for FM-12

$$\frac{\bar{C} - \bar{R}}{\sqrt{\frac{\sigma_C^2}{2} + \frac{\sigma_R^2}{2}}} \text{ is } 5.31182; \text{ and for this value, the table of the normal}$$

function yields $P[S]_{12} < .999999$. Because of the relatively small value of the failure probability, a sensitivity analysis was made. It showed that if $V_f = 2$ for σ_{C12} and σ_{R12} , then $P[S] < .99$. Again, this failure mode data and rationale should be more closely analyzed.

Failure Mode 13. Propellant Auto Ignition Due to Static Discharge.

Premature ignition of the motor due to propellant self-ignition from static electrical discharges, and

Failure Mode 14. Propellant Auto Ignition Due to Self-Heating.

Premature ignition of the motor due to propellant self-ignition from endothermal self-heating within the propellant, caused by propellant internal reactions.

These two failure modes are somewhat similar in that they involve premature ignition of the propellant from other than a normal

ignition sequence. From the data of Appendix I, and again the assumption of Gaussian distributions for C and R for both FM13 and FM14, solution for P[S] indicates an extremely high probability of success. Thus:

$$P[S]_{13} > .999\ 999$$

and

$$P[S]_{14} > .999\ 999 \ .$$

APPENDIX III

COMPUTER PRINTOUTS

Introduction

This appendix contains copies of a sample of computer runs for failure modes 1 through 6. (Modes 7 through 14 were handled as closed form solutions as discussed in Section 5 of this report.) Each run contains a heading which identifies the failure mode. This is followed by the computer run output in a three-column tabular format. The first column, FROM, lists the lower bound of the (C-R) interval; the second column, TO, lists the upper bound of the interval; and the third column, PROB, shows the probability that (C-R) falls within the interval. The probability of failure by this mode is shown below the three column table, identified by the symbol P[F]. This probability is computed by linear interpolation as the probability that (C-R) is less than zero. Computer running time is shown just below the failure probability. Note that some of the times are listed as fractions, the charge unit being one-sixth of a second. Running times on time sharing computer are of course longer than batch computers but time sharing costs are much less. Data is given at the bottom of the runs. This first number in each line is the mean and the second number is the standard deviation. Recall that a Gaussian assumption is made throughout these runs on all input parameters. The remaining numbers in each line are included for purposes of the program operation.

For failure mode 2, runs using unadjusted data are referred to in the headings as nominal or standard runs. Sensitivity runs were made in runs 4, 5, 7, 8, 10, 11, 13 and 14. Eight runs are shown for FM6, and results are tabulated in table II.9. Two types of sensitivity runs were made. Runs 2 and 6 were made with $B = 228.653$ (see page II.24 for explanation). Table II.9 shows the variability factors used for the various runs, for the second type of sensitivity analysis.

REL FM1 13:20 SB WED 03/20/68

HOOP STRESS FAIL MODE FWD CYL SECT, FM-1, MOTOR CASE
9/10 OF TIME
STANDARD RUN

FROM	TO	PROB
<-397.334	-397.334	0
-397.334	8961.05	3.40275 E-34
8961.05	18319.4	1.36223 E-23
18319.4	27677.8	3.21347 E-17
27677.8	37036.2	2.37702 E-12
37036.2	46394.6	1.21983 E-8
46394.6	55753.	4.02486 E-6
55753.	65111.4	4.41090 E-4
65111.4	74469.8	1.26742 E-2
74469.8	83828.2	.123791
83828.2	93186.6	.368434
93186.6	102545.	.358558
102545.	111903.	.12009
111903.	121262.	1.50104 E-2
121262.	130620.	9.82185 E-4
130620.	139979.	1.49434 E-5
139979.	149337.	5.48731 E-8
149337.	158695.	3.23650 E-11
158695.	168054.	1.95549 E-15
168054.	177412.	6.70829 E-21
177412.	186770.	1.20673 E-27
186770.	> 186770.	0

PLF]= 1.44472 E-35

TIME: 1 MINS. 33 SECS.

LISTNH5000

5010 DATA 232000, 2516.6, 1258.3, 10
5020 DATA .95845, .00693, .003465, 10
5030 DATA 1.106, .0312, .0156, 10
5040 DATA 3.4E6, 6120, 3060, 10
5050 DATA 6.2477E-3, 1.9E-5, 9.5E-6, 10
5060 DATA .606, .00818, .00409, 10
5070 DATA 6355, 20.9, 10.45, 10
5080 DATA 1.18, .00897, .004485, 10
5090 DATA 85, .17, .085, 10
5100 DATA 130.631, .0261, .01305, 10
5110 DATA .6392, .0095, .00475, 10
5120 DATA .0016, 6.676E-5, 3.38E-5, 10

HOOP STRESS FAIL MODE FWD CYL SECT, FM-1, MOTOR CASE

1/10 OF TIME

RUN 2

1.

FROM	TO	PROB

<-169692.	-169692.	0
-169692.	-143875.	7.02443 E-17
-143875.	-118057.	1.20510 E-6
-118057.	-92240.1	2.08646 E-5
-92240.1	-66422.9	2.39351 E-4
-66422.9	-40605.6	2.36905 E-3
-40605.6	-14788.4	1.51561 E-2
-14788.4	11028.8	.055338
11028.8	36846.1	.159163
36846.1	62663.3	.295196
62663.3	88480.6	.25941
88480.6	114298.	.127791
114298.	140115.	6.36229 E-2
140115.	165932.	1.80443 E-2
165932.	191750.	3.27235 E-3
191750.	217567.	3.60149 E-4
217567.	243384.	1.48032 E-5
243384.	269201.	3.16083 E-7
269201.	295018.	3.91324 E-9
295018.	320836.	4.28898 E-12
320836.	346653.	4.02567 E-19
346653.	> 346653.	0

P[F]= 4.94847 E-2

TIME: 1 MINS. 31 SECS.

LISTNH5000

- 5010 DATA 199333, 34564, 17282, 10
- 5020 DATA .95845, .00693, .003465, 10
- 5030 DATA 1.106, .0312, .0156, 10
- 5040 DATA 3.4E6, 6120, 3060, 10
- 5050 DATA 6.2477E-3, 1.9E-5, 9.5E-6, 10
- 5060 DATA .606, .00818, .00409, 10
- 5070 DATA 6355, 20.9, 10.45, 10
- 5080 DATA 1.18, .00897, .004485, 10
- 5090 DATA 85, .17, .085, 10
- 5100 DATA 130.631, .0261, .01305, 10
- 5110 DATA .6392, .0095, .00475, 10
- 5120 DATA .0016, 6.676E-5, 3.38E-5, 10

REL2 17:38 SB THU 04/11/68

INSUL BURN THRU FM-2, MOTOR CASE

NOMINAL RUN

STA 1

1.

FROM	TO	PROB

< 36.9237	36.9237	0
36.9237	136.809	3.48628 E-2
136.809	236.694	.561804
236.694	336.579	.338034
336.579	436.464	4.85317 E-2
436.464	536.349	1.48401 E-2
536.349	636.234	8.68104 E-4
636.234	736.12	8.56160 E-4
736.12	836.005	1.64879 E-4
836.005	935.89	1.14193 E-5
935.89	1035.78	5.16168 E-7
1035.78	1135.66	2.33383 E-5
1135.66	1235.55	4.83562 E-9
1235.55	1335.43	0
1335.43	1435.32	3.06095 E-9
1435.32	1535.2	2.11915 E-6
1535.2	1635.09	3.92546 E-7
1635.09	1734.97	0
1734.97	1834.86	0
1834.86	1934.74	0
1934.74	2034.63	0
2034.63	> 2034.63	0

P[F]= 0

RAN 179/6 SEC
LISTNH5000

5020 DATA 1.125,.01667,.008335,10
5030 DATA .003,.000489,.0002445,10
5040 DATA 87.5,.175,.0875,10
5050 DATA .59,.00351,.001755,10

REL FM2 17:32 SB WED 04/10/68

INSULATION BURN THRU FAILURE MODE-2, MOTOR CASE
NOMINAL CASE

STA 2

1.

FROM	TO	PROB

75.7907	75.7907	0
75.7907	175.837	3.48628 E-2
175.837	275.883	.561804
275.883	375.929	.338034
375.929	475.975	4.85317 E-2
475.975	576.021	1.48401 E-2
576.021	676.067	8.68104 E-4
676.067	776.114	8.56160 E-4
776.114	876.16	1.64879 E-4
876.16	976.206	1.14193 E-5
976.206	1076.25	5.16168 E-7
1076.25	1176.3	2.33383 E-5
1176.3	1276.34	4.83562 E-9
1276.34	1376.39	0
1376.39	1476.44	3.06095 E-9
1476.44	1576.48	2.11915 E-6
1576.48	1676.53	3.92546 E-7
1676.53	1776.57	0
1776.57	1876.62	0
1876.62	1976.67	0
1976.67	2076.71	0
2076.71	> 2076.71	0

PLF] = 0

RAN 278/6 SEC
LISTNH5000

5000 DATA 24.5, .049, .0245, 10
5010 DATA .606, .00361, .001805, 10
5020 DATA 1.125, .01667, .008335, 10
5030 DATA .003, .000489, .0002445, 10
5040 DATA 87.5, .175, .0875, 10
5050 DATA .59, .00351, .001755, 10

REL FM2 17:50 SB WED 04/10/68

INSULATION BURN THRU FAILURE MODE-2, MOTOR CASE
NOMINAL CASE

STA 5

1.

FROM	TO	PROB

<-14.0866	-14.0866	0
-14.0866	-9.98349	5.46581 E-12
-9.98349	-5.88037	4.57727 E-7
-5.88037	-1.77725	7.17910 E-4
-1.77725	2.32587	3.54963 E-2
2.32587	6.42899	.147657
6.42899	10.5321	.199825
10.5321	14.6352	.187377
14.6352	18.7383	.156787
18.7383	22.8415	8.24432 E-2
22.8415	26.9446	4.30062 E-2
26.9446	31.0477	6.70429 E-2
31.0477	35.1508	6.32103 E-3
35.1508	39.2539	.03741
39.2539	43.3571	3.27667 E-2
43.3571	47.4602	3.13296 E-3
47.4602	51.5633	1.73846 E-5
51.5633	55.6664	1.57849 E-9
55.6664	59.7695	0
59.7695	63.8726	0
63.8726	67.9758	0
67.9758	67.9758	0

PCF= 1.60934 E-2

RAN 270/6 SEC
LISTNH5000

5000 DATA 85, .170, .085, 10
5010 DATA .606, .00361, .001805, 10
5020 DATA .11, .0033, .00165, 10
5030 DATA .005, .002586, .00076, 4
5040 DATA 87.5, .175, .0875, 10
5050 DATA .59, .00351, .001755, 10

RELFM2 10:46 SB THU 04/11/68

INSULATION BURN THRU FAILURE MODE-2, MOTOR CASE
INCREASED INSULATION THICKNESS

STA 5

1.

FROM	TO	PROB

<-8.17169	-8.17169	0
-8.17169	-1.34136	4.34000 E-8
-1.34136	5.48898	5.98296 E-5
5.48898	12.3193	6.69687 E-3
12.3193	19.1496	8.15602 E-2
19.1496	25.98	.201266
25.98	32.8103	.207558
32.8103	39.6406	.171833
39.6406	46.471	8.64536 E-2
46.471	53.3013	6.38087 E-2
53.3013	60.1316	7.46558 E-3
60.1316	66.962	9.27011 E-2
66.962	73.7923	2.19805 E-3
73.7923	80.6226	2.44819 E-3
80.6226	87.453	3.28294 E-2
87.453	94.2833	4.01691 E-2
94.2833	101.114	2.95299 E-3
101.114	107.944	1.37432 E-7
107.944	114.774	0
114.774	121.605	0
121.605	128.435	0
128.435	> 128.435	0

P[F]= 1.17929 E-5

RAN 276/6 SEC
LISTNH5000

5000 DATA 85,.17,.085,10
5010 DATA .606,.00361,.001805,10
5020 DATA .22,.005,.0025,10
5030 DATA .005,.002586,.00076,4
5040 DATA 87.5,.175,.0875,10
5050 DATA .59,.00351,.001755,10

RELFM2 10:55 SB THU 04/11/68

INSULATION BURN THRU FAILURE MODE-2, MOTOR CASE
POL DATA FOR EROS RATE AT 5030
STA 5
1.

FROM	TO	PROB

<-9.23797	-9.23797	0
-9.23797	-1.72932	1.98411 E-5
-1.72932	5.77932	8.59162 E-3
5.77932	13.288	.219643
13.288	20.7966	.589701
20.7966	28.3053	.16963
28.3053	35.8139	1.16532 E-2
35.8139	43.3226	5.71658 E-4
43.3226	50.8312	1.60487 E-4
50.8312	58.3398	3.35618 E-6
58.3398	65.8485	1.96193 E-5
65.8485	73.3571	3.72613 E-6
73.3571	80.8658	3.04620 E-9
80.8658	88.3744	2.60923 E-7
88.3744	95.8831	1.63801 E-6
95.8831	103.392	6.05777 E-7
103.392	110.9	7.65812 E-9
110.9	118.409	0
118.409	125.918	0
125.918	133.426	0
133.426	140.935	0
140.935	> 140.935	0

P[F]= 1.99858 E-3

RAN 281/6 SEC
LISTNH5000

5000 DATA 85,.17,.085,10
5010 DATA .606,.00361,.001805,10
5020 DATA .11,.0033,.00165,10
5030 DATA .005,.000816,.000408,10
5040 DATA 87.5,.175,.0875,10
5050 DATA .59,.00351,.001755,10

RELFM2 10:04 SB THU 04/11/68

INSULATION BURN THRU FAILURE MODE-2, MOTOR CASE
NOMINAL CASE

STA 6

1.

FROM	TO	PROB

<-22.0431	-22.0431	0
-22.0431	-3.78184	1.41237 E-2
-3.78184	14.4794	.59387
14.4794	32.7407	.343887
32.7407	51.002	4.27197 E-2
51.002	69.2633	4.46839 E-3
69.2633	87.5245	7.34970 E-4
87.5245	105.786	1.43720 E-4
105.786	124.047	3.41082 E-5
124.047	142.308	1.30332 E-5
142.308	160.57	3.64074 E-6
160.57	178.831	4.75038 E-7
178.831	197.092	8.65461 E-7
197.092	215.353	1.09449 E-6
215.353	233.615	1.48392 E-7
233.615	251.876	1.39853 E-8
251.876	270.137	5.09671 E-10
270.137	288.399	0
288.399	306.66	0
306.66	324.921	0
324.921	343.182	0
343.182	> 343.182	0

PIF]= .137112

RAN 281/6 SEC
LISTNH5000

5000 DATA 71.85,.1437,.07185,10
5010 DATA .606,.00361,.001805,10
5020 DATA .25,.01667,.008335,10
5030 DATA .005,.000816,.000408,10
5040 DATA 87.5,.175,.0875,10
5050 DATA .59,.00351,.001755,10

RELFM2 11:28 SB THU 04/11/68

INSULATION BURN THRU FAILURE MODE-2, MOTOR CASE
INCREASED INSULATION RUN

STA 6

1.

FROM	TO	PROB

<-12.8636	-12.8636	0
-12.8636	13.9958	1.41251 E-2
13.9958	40.8551	.593872
40.8551	67.7145	.343883
67.7145	94.5739	4.27197 E-2
94.5739	121.433	4.46839 E-3
121.433	148.293	7.34970 E-4
148.293	175.152	1.43720 E-4
175.152	202.011	3.41082 E-5
202.011	228.871	1.30332 E-5
228.871	255.73	3.64074 E-6
255.73	282.589	4.75038 E-7
282.589	309.449	8.65461 E-7
309.449	336.308	1.09449 E-6
336.308	363.168	1.48392 E-7
363.168	390.027	1.39853 E-8
390.027	416.886	5.09671 E-10
416.886	443.746	0
443.746	470.605	0
470.605	497.464	0
497.464	524.324	0
524.324	> 524.324	0

P[F]= 6.76484 E-3

RAN 284/6 SEC
LISTNH5000

5000 DATA 71.85,.1437,.07185,10
5010 DATA .606,.00361,.001805,10
5020 DATA .375,.025,.0125,10
5030 DATA .005,.000816,.000408,10
5040 DATA 87.5,.175,.0875,10
5050 DATA .59,.00351,.001755,10

RUN

RELFM2 11:06 SB THU 04/11/68

INSULATION BURN THRU FAILURE MODE-2, MOTOR CASE
INCREASED INSULATION RUN
STA 6
1.

FROM	TO	PROB

< .902925	.902925	0
.902925	33.8674	.020274
33.8674	66.832	.581951
66.832	99.7965	.344343
99.7965	132.761	.046933
132.761	165.726	5.34132 E-3
165.726	198.69	9.36390 E-4
198.69	231.655	1.40368 E-4
231.655	264.619	5.43655 E-5
264.619	297.584	1.16281 E-5
297.584	330.548	1.14136 E-5
330.548	363.513	5.29968 E-7
363.513	396.477	3.78680 E-7
396.477	429.442	1.35102 E-6
429.442	462.406	7.16786 E-7
462.406	495.371	5.38941 E-8
495.371	528.335	5.09671 E-10
528.335	561.3	0
561.3	594.264	0
594.264	627.229	0
627.229	660.193	0
660.193	> 660.193	0

P[F]= 0

RAN 279/6 SEC

*** OFF AT 11:20 ELAPSED TERMINAL TIME = 87 MIN.

RELFM2 10:13 SB THU 04/11/68

INSULATION BURN THRU FAILURE MODE-2, MOTOR CASE
NOMINAL CASE

STA 7

1.

FROM	TO	PROB

<-10.6096	-10.6096	0
-10.6096	12.0817	2.39327 E-2
12.0817	34.773	.574877
34.773	57.4643	.341176
57.4643	80.1556	5.17988 E-2
80.1556	102.847	6.92150 E-3
102.847	125.538	1.02544 E-3
125.538	148.23	1.53648 E-4
148.23	170.921	8.79634 E-5
170.921	193.612	3.90992 E-6
193.612	216.303	1.85895 E-5
216.303	238.995	1.54487 E-6
238.995	261.686	5.49667 E-8
261.686	284.377	7.16786 E-7
284.377	307.069	1.58068 E-6
307.069	329.76	1.59826 E-7
329.76	352.451	3.06095 E-9
352.451	375.143	0
375.143	397.834	0
397.834	420.525	0
420.525	443.216	0
443.216	> 443.216	0

PIF]= .01119

RAN 286/6 SEC
LISTNH5000

5000 DATA 70.57,.1411,.07055,10
5010 DATA .606,.00361,.001805,10
5020 DATA .43,.01667,.008335,10
5030 DATA .006,.000979,.0004895,10
5040 DATA 87.5,.175,.0875,10
5050 DATA .59,.00351,.001755,10

RELFM2 10:36 SB THU 04/11/68

INSULATION BURN THRU FAILURE MODE-2, MOTOR CASE
INCREASED INSULATION THICKNESS

STA 7

1.

FROM	TO	PROB

<-6.5389	-6.5389	0
-6.5389	21.7249	2.06893 E-2
21.7249	49.9887	.581536
49.9887	78.2525	.344271
78.2525	106.516	4.70051 E-2
106.516	134.78	5.24869 E-3
134.78	163.044	1.02904 E-3
163.044	191.308	1.40368 E-4
191.308	219.571	5.43655 E-5
219.571	247.835	1.16281 E-5
247.835	276.099	1.14136 E-5
276.099	304.363	5.29968 E-7
304.363	332.626	3.78680 E-7
332.626	360.89	1.35102 E-6
360.89	389.154	7.16786 E-7
389.154	417.418	5.38941 E-8
417.418	445.682	5.09671 E-10
445.682	473.945	0
473.945	502.209	0
502.209	530.473	0
530.473	558.737	0
558.737	> 558.737	0

P[F]= 4.78651 E-3

RAN 285/6 SEC
LISTNH 5000

5000 DATA 70.57,.1411,.07055,10
5010 DATA .606,.00361,.001805,10
5020 DATA .516,.025,.0125,10
5030 DATA .006,.000979,.0004895,10
5040 DATA 87.5,.175,.0875,10
5050 DATA .59,.00351,.001755,10

RELFM2 10:30 SB THU. 04/11/68

INSULATION BURN THRU FAILURE MODE-2, MOTOR CASE
INCREASED INSULATION THICKNESS
STA 7
1.

FROM	TO	PROB

< 5.3014	5.3014	0
5.3014	38.8103	2.39327 E-2
38.8103	72.3191	.574877
72.3191	105.828	.341176
105.828	139.337	5.17988 E-2
139.337	172.846	6.92150 E-3
172.846	206.355	1.02544 E-3
206.355	239.864	1.53648 E-4
239.864	273.372	8.79634 E-5
273.372	306.881	3.90992 E-6
306.881	340.39	1.85895 E-5
340.39	373.899	1.54487 E-6
373.899	407.408	5.49667 E-8
407.408	440.917	7.16786 E-7
440.917	474.426	1.58068 E-6
474.426	507.934	1.59826 E-7
507.934	541.443	3.06096 E-9
541.443	574.952	0
574.952	608.461	0
608.461	641.97	0
641.97	675.479	0
675.479	> 675.479	0

P[F]= 0

RAN 277/6 SEC
LISTNH5000

5000 DATA 70.57,.1411,.07055,10
5010 DATA .606,.00361,.001805,10
5020 DATA .645,.025,.0125,10
5030 DATA .006,.000979,.0004895,10
5040 DATA 87.5,.175,.0875,10
5050 DATA .59,.00351,.001755,10

REL F2 11:41 SB THU 04/11/68

INSUL BURN THRU FM-2, MOTOR CASE
STANDARD CASE
STA 12

1.

FROM	TO	PROB

<-39.0822	-39.0822	0
-39.0822	15.1613	.06472
15.1613	69.4049	.465459
69.4049	123.648	.405049
123.648	177.892	4.31387 E-2
177.892	232.135	1.58754 E-2
232.135	286.379	4.54125 E-3
286.379	340.622	1.01452 E-3
340.622	394.866	2.14589 E-7
394.866	449.109	1.76083 E-4
449.109	503.353	0
503.353	557.597	2.33432 E-5
557.597	611.84	5.16170 E-7
611.84	666.084	0
666.084	720.327	0
720.327	774.571	0
774.571	828.814	2.51475 E-6
828.814	883.058	0
883.058	937.301	0
937.301	991.545	0
991.545	1045.79	0
1045.79	> 1045.79	0

P[F]= 4.66304 E-2

RAN 178/6 SEC
LISTNH 5000

5020 DATA 3.6, .01667, .008335, 10
5030 DATA .0168, 2.7401E-3, 1.37005E-3, 10
5040 DATA 87.5, .175, .0875, 10
5050 DATA .59, .00351, .001755, 10

READY.

RUN

REL2 11:47 SB THU 04/11/68

INSUL BURN THRU FM-2, MOTOR CASE
INCREASED INSUL. RUN
STA 12
1.

FROM	TO	PROB

< 18.5677	18.5677	0
18.5677	99.6375	.06472
99.6375	180.707	.465459
180.707	261.777	.405049
261.777	342.847	4.31387 E-2
342.847	423.917	1.58754 E-2
423.917	504.987	4.54125 E-3
504.987	586.057	1.01452 E-3
586.057	667.126	2.14589 E-7
667.126	748.196	1.76083 E-4
748.196	829.266	0
829.266	910.336	2.33432 E-5
910.336	991.406	5.16171 E-7
991.406	1072.48	0
1072.48	1153.55	0
1153.55	1234.62	0
1234.62	1315.69	2.51475 E-6
1315.69	1396.76	0
1396.76	1477.83	0
1477.83	1558.89	0
1558.89	1639.96	0
1639.96	> 1639.96	0

P[F]= 0

RAN 178/6 SEC

RELF2 11:51 SB THU 04/11/68

INSUL BURN THRU FM-2 MOTOR CASE
INCREASED INSUL. RUN

STA 12

1.

FROM	TO	PROB

<-16.8416	-16.8416	0
-16.8416	48.5766	6.38392 E-2
48.5766	113.995	.49545
113.995	179.413	.375939
179.413	244.831	4.31391 E-2
244.831	310.249	1.61639 E-2
310.249	375.667	4.25228 E-3
375.667	441.085	1.01452 E-3
441.085	506.504	1.14192 E-5
506.504	571.922	1.64879 E-4
571.922	637.34	0
637.34	702.758	2.37218 E-5
702.758	768.176	1.37526 E-7
768.176	833.594	0
833.594	899.012	0
899.012	964.431	0
964.431	1029.85	2.51475 E-6
1029.85	1095.27	0
1095.27	1160.69	0
1160.69	1226.1	0
1226.1	1291.52	0
1291.52	> 1291.52	0

P[F]= 1.64351 E-2

RAN 178/6 SEC
LISTNH5000

5020 DATA 4.32,.025,.0125,10
5030 DATA .0168,2.7401E-3,1.37005E-3,10
5040 DATA 87.5,.175,.0875,10
5050 DATA .59,.00351,.001755,10

COMBINED STRESSES FWD SKIRT FM-3,
MOTOR CASE.

1.

FROM	TO	PROB
< 2.62092 E-2	2.62092 E-2	0
2.62092 E-2	9.63239 E-2	.992361
9.63239 E-2	.166439	7.60727 E-3
.166439	.236553	2.64528 E-5
.236553	.306668	2.64137 E-6
.306668	.376783	1.23014 E-7
.376783	.446898	2.39640 E-6
.446898	.517012	1.03689 E-8
.517012	.587127	2.34873 E-11
.587127	.657242	9.08492 E-13
.657242	.727356	0
.727356	.797471	0
.797471	.867586	0
.867586	.937701	0
.937701	1.00782	0
1.00782	1.07793	0
1.07793	1.14804	0
1.14804	1.21816	0
1.21816	1.28827	0
1.28827	1.35839	0
1.35839	1.4285	0
1.4285	> 1.4285	0

PCF] = 0

TIME: 50 SECS.

LISTNH 5000

5000 DATA 129.903, .0208, .0104, 10
 5010 DATA .728, .0093, .00465, 10
 5020 DATA 2.75E7, 54725, 27362.5, 10
 5030 DATA .005, .000968, .000484, 10
 5040 DATA .00288, .000334, .000167, 10
 5050 DATA .0036, .000685, 3.425E-4, 10

REL FMY 17:55 SB THU 04/11/68

FOWD HEAD CIRF WELD MERIOD STRESS FM-4, SPHER SECT MOTOR
1/10 OF TIME
STANDARD RUN
1.

FROM	TO	PROB

<-16252.9	-16252.9	0
-16252.9	110.936	1.46022 E-25
110.936	16474.8	2.56260 E-18
16474.8	32838.6	8.58624 E-13
32838.6	49202.4	3.63771 E-9
49202.4	65566.2	9.97860 E-7
65566.2	81930.	6.15112 E-5
81930.	98293.8	1.47640 E-3
98293.8	114658.	1.57795 E-2
114658.	131021.	8.60684 E-2
131021.	147385.	.243795
147385.	163749.	.343434
163749.	180113.	.225681
180113.	196477.	7.11609 E-2
196477.	212841.	1.16288 E-2
212841.	229204.	8.79079 E-4
229204.	245568.	3.29577 E-5
245568.	261932.	4.76476 E-7
261932.	278296.	3.62146 E-10
278296.	294660.	9.69555 E-15
294660.	311023.	8.39386 E-22
311023.	> 311023.	0

P[F]= 1.45032 E-25

RAN 497/6 SEC
LISTNH5000

5010 DATA 199300,8600,4300,10
5020 DATA .95845,.00693,.003465,10
5040 DATA 3.4E6,6120,3060,10
5050 DATA 6.2477E-3,1.9E-5,9.5E-6,10
5060 DATA .606,.00818,.00409,10
5070 DATA 6355,20.9,10.45,10
5080 DATA 1.18,.00897,.004485,10
5090 DATA 85,.17,.085,10
5100 DATA 130.428,.0456,.0228,10
5110 DATA .428,.0108,.0054,10
5120 DATA .0016,6.676E-5,3.38E-5,10

RUN .

RELFM5 18:11 SB THU 04/11/68

FAILURE OF NOZ BOLTS JNT IN TENSION DUE TO COMBD LOADS:
PRETORQUE,PRESS EJECT , AND IVC MOMENT FM 5.
STANDARD RUN

1.

FROM	TO	PROB

< 17575.8	17575.8	0
17575.8	26907.	1.44950 E-8
26907.	36238.3	3.00193 E-6
36238.3	45569.6	3.47479 E-5
45569.6	54900.8	3.23236 E-4
54900.8	64232.1	2.25055 E-3
64232.1	73563.4	1.10885 E-2
73563.4	82894.6	3.78618 E-2
82894.6	92225.9	.090463
92225.9	101557.	.156003
101557.	110888.	.201972
110888.	120220.	.201972
120220.	129551.	.156003
129551.	138882.	.090463
138882.	148213.	3.78618 E-2
148213.	157545.	1.10885 E-2
157545.	166876.	2.25055 E-3
166876.	176207.	3.23236 E-4
176207.	185539.	3.47479 E-5
185539.	194870.	3.00193 E-6
194870.	204201.	1.44950 E-8
204201.	> 204201.	0

P[F]= 0

RAN 455/6 SEC
LISTNH5000

5040 DATA 3.4E6,6120,3060,10
5050 DATA 6.2477E-3,1.9E-5,9.5E-6,10
5060 DATA .606,.00818,.00409,10
5070 DATA 6355,20.9,10.45,10
5080 DATA 1.18,.00897,.004485,10
5090 DATA 85,.17,.085,10
5120 DATA .0016,6.676E-5,3.38E-5,10
5130 DATA 14.696,.0735,.03675,10
5140 DATA .6,.077,.0385,10
5150 DATA 245307,1987,993.5,10

RELFM5 18:30 SB THU 04/11/68

FAILURE OF NOZ BOLTS JNT IN TENSION DUE TO COMBD LOADS:
PRETORQUE, PRESS. EJECT, AND TVC MOMENT
MAX CASE RUN

1.

FROM	TO	PROB

< 12927.2	12927.2	0
12927.2	22632.4	1.77511 E-10
22632.4	32337.6	1.22580 E-7
32337.6	42042.8	8.59278 E-6
42042.8	51748.	1.73523 E-4
51748.	61453.2	1.87640 E-3
61453.2	71158.4	1.08657 E-2
71158.4	80863.6	3.82026 E-2
80863.6	90568.8	9.08202 E-2
90568.8	100274.	.156075
100274.	109979.	.201978
109979.	119684.	.201973
119684.	129390.	.156003
129390.	139095.	.090463
139095.	148800.	3.78622 E-2
148800.	158505.	1.10897 E-2
158505.	168210.	2.25107 E-3
168210.	177915.	3.22902 E-4
177915.	187621.	3.36304 E-5
187621.	197326.	2.32468 E-6
197326.	207031.	1.06864 E-8
207031.	> 207031.	0

P[F]= 0

RAN 473/6 SEC
LISTNH

01 PRINT"FAILURE OF NOZ BOLTS JNT IN TENSION DUE TO COMBD LOADS:"
02 PRINT"PRETORQUE I
STOP.
READY.

LISTNH5000

5040 DATA 3.4E6,24480,12240,10
5050 DATA 6.2477E-3,1.9E-5,9.5E-6,10
5060 DATA .606,.01636,.00818,10
5070 DATA 6355,83.6,41.8,10
5080 DATA 1.18,.0897,.04485,10
5090 DATA 85,.17,.085,10
5120 DATA .0016,6.676E-5,3.38E-5,10
5130 DATA 14.696,.0735,.03675,10
5140 DATA .6,.077,.0385,10
5150 DATA 245307,1987,993.5,10

NOZ SEP DUE TO EJECT LOAD EXCEEDING PRETOURQUE LOAD. FM-6
AT LINES 2070,3070, B=228.653 FOR MAX SENSITIVITY. MIN, B=0.
STANDARD RUN B=0

1.

FROM	TO	PROB

<-15846.7	-15846.7	0
-15846.7	-6303.04	1.52915 E-10
-6303.04	2240.62	2.53808 E-6
2240.62	11284.3	2.62024 E-5
11284.3	20327.9	2.63887 E-4
20327.9	29371.6	2.31861 E-3
29371.6	38415.3	1.33029 E-2
38415.3	47458.9	.043946
47458.9	56502.6	9.48111 E-2
56502.6	65546.2	.151854
65546.2	74589.9	.193464
74589.9	83633.6	.193349
83633.6	92677.2	.15065
92677.2	101721.	9.18133 E-2
101721.	110765.	.044045
110765.	119808.	1.57835 E-2
119808.	128852.	3.79693 E-3
128852.	137896.	5.21572 E-4
137896.	146939.	4.35434 E-5
146939.	155983.	2.88369 E-6
155983.	165027.	2.26786 E-9
165027.	> 165027.	0

P[F]= 1.90941 E-6

5040 DATA 3.4E6, 6120, 3060, 10
 5050 DATA 6.2477E-3, 1.9E-5, 9.5E-6, 10
 5060 DATA .606, .00818, .00409, 10
 5070 DATA 6355, 20.9, 10.45, 10
 5080 DATA 1.18, .00897, .004485, 10
 5090 DATA 85, .17, .085, 10
 5120 DATA .0016, 6.676E-5, 3.38E-5, 10
 5130 DATA 14.696, .0735, .03675, 10
 5140 DATA .6, .077, .0385, 10

RUN

RELFM6 19:00 SB TUE 06/11/68

NOZ SEP DUE TO EJECT LOAD EXCEEDING PRETOURQUE LOAD. FM-6
AT LINES 2070,3070, =228.653 FOR MAX SENSITIVITY.MIN, B=0.
B= 228.653

1.

FROM	TO	PROB
<-15750.5	-15750.5	0
-15750.5	-6715.09	1.71905 E-10
-6715.09	2320.37	2.54173 E-6
2320.37	11355.8	2.65306 E-5
11355.8	20391.3	2.74594 E-4
20391.3	29426.7	2.45044 E-3
29426.7	38462.2	1.36361 E-2
38462.2	47497.7	4.41442 E-2
47497.7	56533.1	9.41164 E-2
56533.1	65568.6	.151874
65568.6	74604.	.193468
74604.	83639.5	.193351
83639.5	92675.	.150662
92675.	101710.	.091881
101710.	110746.	4.40582 E-2
110746.	119781.	1.58269 E-2
119781.	128817.	3.68919 E-3
128817.	137852.	4.94189 E-4
137852.	146888.	4.08014 E-5
146888.	155923.	2.89023 E-6
155923.	164959.	2.34895 E-9
164959.	> 164959.	0

P[F]= 1.88917 E-6

RAN 415/6 SEC
LISTNH5000

5040 DATA 3.4E6, 6120, 3060, 10
5050 DATA 6.2477E-3, .000019, .0000085, 10
5060 DATA .606, .00818, .00409, 10
5070 DATA 6355, 20.9, 10.45, 10
5080 DATA 1.18, .00897, .004485, 10
5090 DATA 85, .17, .085, 10
5120 DATA .0016, 6.676E-5, 3.38E-5, 10
5130 DATA 14.696, .0735, .03675, 10
5140 DATA .6, .077, .0385, 10

RUN

RELFM6 17:58 SB TUE 06/11/68

NOZ SEP DUE TO EJECT LOAD EXCEEDING PRETOURQUE LOAD. FM-6
AT LINES 2070,3070, B=228.653 FOR MAX SENSITIVITY.MIN, B=0.
B=0
1.

FROM	TO	PROB

<-97742.4	-97742.4	0
-97742.4	-80486.3	1.60919 E-6
-80486.3	-63230.2	2.20507 E-5
-63230.2	-45974.1	1.76269 E-4
-45974.1	-28718.	1.01635 E-3
-28718.	-11461.9	4.54755 E-3
-11461.9	5794.17	.01587
5794.17	23050.3	4.31387 E-2
23050.3	40306.4	9.13246 E-2
40306.4	57562.5	.150569
57562.5	74818.6	.193334
74818.6	92074.6	.193334
92074.6	109331.	.150569
109331.	126587.	9.13246 E-2
126587.	143843.	4.31387 E-2
143843.	161099.	1.58698 E-2
161099.	178355.	4.54684 E-3
178355.	195611.	1.01464 E-3
195611.	212867.	1.76445 E-4
212867.	230123.	2.37744 E-5
230123.	247380.	2.27938 E-6
247380.	> 247380.	0

PLF]= 1.63051 E-2

RAN 432/6 SEC
LISTNH5000

5040 DATA 3.4E6, 6120, 3060, 10
5050 DATA 6.2477E-3, 1.9E-5, 9.5E-6, 10
5060 DATA .606, .00818, .00409, 10
5070 DATA 6355, 20.9, 10.45, 10
5080 DATA 1.18, .00897, .004485, 10
5090 DATA 85, .17, .085, 10
5120 DATA .0016, 6.676E-5, 3.38E-5, 10
5130 DATA .14.696, .0735, .03675, 10
5140 DATA .6, .154, .077, 10

RUN

REL FM6 19:09 SB TUE 06/11/68

NOZ SEP DUE TO EJECT LOAD EXCEEDING PRETOURQUE LOAD. FM-6
AT LINES 2070,3070, B=228.653 FOR MAX SENSITIVITY-MIN, R=0.
B=228.653

1.

FROM	TO	PROB

<-32175.4	-32175.4	0
-32175.4	-21497.5	2.86101 E-9
-21497.5	-10819.5	2.87709 E-6
-10819.5	-141.581	4.10444 E-5
-141.581	10536.4	5.01678 E-4
10536.4	21214.3	3.71607 E-3
21214.3	31892.3	1.58131 E-2
31892.3	42570.2	4.40146 E-2
42570.2	53248.1	9.19224 E-2
53248.1	63926.1	.150649
63926.1	74604.	.193339
74604.	85282.	.193334
85282.	95959.9	.150575
95959.9	106638.	9.13674 E-2
106638.	117316.	4.33325 E-2
117316.	127994.	1.60796 E-2
127994.	138672.	4.43709 E-3
138672.	149350.	7.89641 E-4
149350.	160028.	7.97663 E-5
160028.	170706.	4.81893 E-6
170706.	181383.	3.98219 E-8
181383.	> 181383.	0

P[F]= 5.05762 E-5

RAN 410/6 SEC
LISTNH5000

5040 DATA 3.4E6, 6120, 3060, 10
5050 DATA 6.2477E-3, .000019, .0000085, 10
5060 DATA .606, .00818, .00409, 10
5070 DATA 6355, 20.9, 10.45, 10
5080 DATA 1.18, .00897, .004485, 10
5090 DATA 85, .17, .085, 10
5120 DATA .0016, 6.676E-5, 3.38E-5, 10
5130 DATA 14.696, .0735, .03675, 10
5140 DATA .6, .0924, .0462, 10

RUN

RELFM6 18:47 SB TUE 06/11/68

NOZ SEP DUE TO EJECT LOAD EXCEEDING PRETOURQUE LOAD. FM-6
AT LINES 2070,3070, =228.653 FOR MAX SENSITIVITY.MIN, =0.

B=0

1.

FROM	TO	PROB

<-18502.2	-18502.2	0
-18502.2	-9222.17	2.33536 E-13
-9222.17	57.845	2.50965 E-6
57.845	9337.86	2.39383 E-5
9337.86	18617.9	1.84368 E-4
18617.9	27897.9	1.22233 E-3
27897.9	37177.9	7.86086 E-3
37177.9	46457.9	3.61686 E-2
46457.9	55737.9	9.85807 E-2
55737.9	65017.9	.159057
65017.9	74298.	.196492
74298.	83578.	.193796
83578.	92858.	.151247
92858.	102138.	9.26404 E-2
102138.	111418.	4.46199 E-2
111418.	120698.	1.48513 E-2
120698.	129978.	2.91586 E-3
129978.	139258.	3.06028 E-4
139258.	148538.	2.79834 E-5
148538.	157818.	2.56517 E-6
157818.	167098.	1.25330 E-10
167098.	> 167098.	0

PLF]= 2.49401 E-6

RAN 430/6 SEC
LISTNH5000

5040 DATA 3.4E6, 6120, 3060, 10
5050 DATA 6.2477E-3, .000076, .000038, 10
5060 DATA .606, .00818, .00409, 10
5070 DATA 6355, 20.9, 10.45, 10
5080 DATA 1.18, .00897, .004485, 10
5090 DATA 85, .17, .085, 10
5120 DATA .0016, 6.676E-5, 3.38E-5, 10
5130 DATA 14.696, .0735, .03675, 10
5140 DATA .6, .077, .0385, 10

RUN

REL FM6 18:28 SB TUE 06/11/68

NOZ SEP DUE TO EJECT LOAD EXCEEDING PRETOURQUE LOAD. FM-6
AT LINES 2070,3070, B=228.653 FOR MAX SENSITIVITY.MIN, S=0.
B=0

1.

FROM	TO	PROB

<-22108.2	-22108.2	0
-22108.2	-12546.9	7.08590 E-17
-12546.9	-2985.64	1.09311 E-6
-2985.64	6575.62	2.03307 E-5
6575.62	16136.9	1.77198 E-4
16136.9	25698.1	1.02517 E-3
25698.1	35259.4	4.81516 E-3
35259.4	44820.7	2.10748 E-2
44820.7	54381.9	7.73554 E-2
54381.9	63943.2	.170955
63943.2	73504.5	.220067
73504.5	83065.7	.197828
83065.7	92627.	.152161
92627.	102188.	9.52269 E-2
102188.	111750.	.044557
111750.	121311.	.012575
121311.	130872.	1.93422 E-3
130872.	140433.	1.99803 E-4
140433.	149995.	2.41170 E-5
149995.	159556.	2.47208 E-6
159556.	169117.	6.93164 E-1
169117.	> 169117.	0

PLF]= 7.44166 E-6

RAN 422/6 SEC
LISTNH5000

5040 DATA 3.4E6, 6120, 3060, 10
5050 DATA 6.2477E-3, .000076, .000038, 10
5060 DATA .606, .00818, .00409, 10
5070 DATA 6355, 41.8, 20.9, 10
5080 DATA 1.18, .01794, .00897, 10
5090 DATA 85, .17, .085, 10
5120 DATA .0016, 6.676E-5, 3.38E-5, 10
5130 DATA 14.696, .0735, .03675, 10
5140 DATA .6, .077, .0385, 10

RUN

RELFM6 18:36 SB TUE 06/11/68

NOZ SEP DUE TO EJECT LOAD EXCEEDING PRETOURQUE LOAD. FM-6
AT LINES 2070,3070, B=228.653 FOR MAX SENSITIVITY-MIN, B=0.
B=228.653

1.

FROM	TO	PROB

<-21879.5	-21879.5	0
-21879.5	-12318.3	7.08590 E-17
-12318.3	-2756.99	1.09311 E-6
-2756.99	6804.27	2.03307 E-5
6804.27	16365.5	1.77198 E-4
16365.5	25926.8	1.02517 E-3
25926.8	35488.1	4.81516 E-3
35488.1	45049.3	2.10748 E-2
45049.3	54610.6	7.73554 E-2
54610.6	64171.9	.170955
64171.9	73733.1	.220067
73733.1	83294.4	.197828
83294.4	92855.6	.152161
92855.6	102417.	9.52269 E-2
102417.	111978.	.044557
111978.	121539.	.012575
121539.	131101.	1.93422 E-3
131101.	140662.	1.99803 E-4
140662.	150223.	2.41170 E-5
150223.	159785.	2.47208 E-6
159785.	169346.	6.93164 E-13
169346.	> 169346.	0

P[F]= 6.95546 E-6

RAN 413/6 SEC
LISTNH5000

5040 DATA 3.4E6,6120,3060,10
5050 DATA 6.2477E-3,.000076,.000038,10
5060 DATA .606,.00818,.00409,10
5070 DATA 6355,41.8,20.9,10
5080 DATA 1.18,.01794,.00897,10
5090 DATA 85,.17,.085,10
5120 DATA .0016,6.676E-5,3.38E-5,10
5130 DATA 14.696,.0735,.03675,10
5140 DATA .6,.077,.0385,10

RUN

RELFM6 18:14 SB TUE 06/11/68

NOZ SEP DUE TO EJECT LOAD EXCEEDING PRETOURQUE LOAD. FM-6
AT LINES 2070,3070, B=228.653 FOR MAX SENSITIVITY.MIN, B=0
B=0

FROM	TO	PROB
<-70769.2	-70769.2	0
-70769.2	-57451.4	2.03471 E-21
-57451.4	-44133.5	6.10704 E-15
-44133.5	-30815.6	3.72071 E-10
-30815.6	-17497.8	1.62339 E-7
-17497.8	-4179.92	6.60487 E-6
-4179.92	9137.95	1.33906 E-4
9137.95	22455.8	1.63698 E-3
22455.8	35773.7	1.21776 E-2
35773.7	49091.5	5.75501 E-2
49091.5	62409.4	.161236
62409.4	75727.3	.267306
75727.3	89045.1	.279736
89045.1	102363.	.15964
102363.	115681.	4.94763 E-2
115681.	128999.	9.94846 E-3
128999.	142317.	1.09352 E-3
142317.	155634.	5.63756 E-5
155634.	168952.	1.68257 E-6
168952.	182270.	9.18616 E-9
182270.	195588.	6.63242 E-11
195588.	> 195588.	0

P[F]= 4.87950 E-5

RAN 428/6 SEC
LISTNH5000

5040 DATA 3.4E6, 12240, 6120, 10
5050 DATA 6.2477E-3, .000076, .000038, 10
5060 DATA .606, .0818, .0409, 10
5070 DATA 6355, 41.8, 20.9, 10
5080 DATA 1.18, .01794, .00897, 10
5090 DATA 85, 1.7, .85, 10
5120 DATA .0016, 6.676E-5, 3.38E-5, 10
5130 DATA 14.696, .0735, .03675, 10
5140 DATA .6, .077, .0385, 10

APPENDIX IV

APPROACH CONCEPTS
AND
COMPUTATION TECHNIQUE

Introduction

The R||C analysis concept has been described in the previous phase III-A report (66TMP-90) and in Section 3 of the body of this report but it is desirable for purposes of this study to review briefly the mechanics of the process using a simple hypothetical example.

Let us consider a system having only one failure mode which is assumed to be time independent*. Let us assume that the requirement, R, is a function of the parameters X and Y, and that the capability, C, is a function of the parameters U and V. Specifically, let us assume that $R = X/Y$, and $C = U \cdot V$. The problem, then, is to determine the probabilistic descriptions of R and C given the probabilistic descriptions of X, Y, U, and V. The probability that C is greater than R (i. e., in this case, the probability of success, or reliability) can be computed by using the formula

$$\text{prob. } \{C > R\} = \text{prob. } \{(C - R) > 0\} = \text{prob. } \{(U \cdot V - X/Y) > 0\}$$

To evaluate this probability the density function for $(U \cdot V - X/Y)$ will be generated and the area under the function in the positive region will then be the probability value of interest.

Think of this computation as an illustration of the general approach which is a straightforward technique of using discrete approximations of continuous functions, considering all possible combinations of values, computing the probability of each combination of values, operating on the set of values appropriately to generate the output value, grouping similar output values and then computing the probability of each group. The area under each input density function was allocated to a selected set of intervals so that the combination of values referred to above are combinations of intervals of values and not combinations of discrete values—the latter is, of course, an acceptable alternate method. The density functions are combined pair-wise to reduce the total number of combinations required in the process.

As noted earlier, the capability, C, is defined by the function $(U \cdot V)$ and the requirement, R, by the function (X/Y) and the transfer function of interest by $\{(C - R) = U \cdot V - X/Y\}$. Variables U, V, X and Y each have probability density functions as shown in Figure IV.1. The figures

* The assumption of independence is not a restriction on the technique but is made, merely, to simplify the illustration.

should be interpreted as follows. Looking first at the probability density function of U —the probability that the value lies between 3 and 4 is 0.1; between 4 and 5 is 0.5; and between 5 and 6 is 0.4. The probability density functions on V , X , and Y are interpreted in the same way as those for U . The widths of the intervals are not the same for all parameters and they need not be. Any appropriate widths of intervals which adequately approximate the true density functions may be used.

Figure IV.2 illustrates the combination of the first pair of parameters, $U \cdot V$. Consider first the interval 3-4 on U and the interval 5-6 on V . All values of $U \cdot V$ resulting from these intervals will lie in a new interval having as a lower value $3 \cdot 5 = 15$, and an upper value $4 \cdot 6 = 24$. The probability associated with this new interval is $0.1 \cdot 0.1 = 0.01$, which is simply the probability that the value of U lies between 3 and 4 and the value of V lies between 5 and 6. The output of this combination of intervals is shown in Row 1 of the table. Columns 1 and 2 show the lower and upper limits of the new interval generated by combining the first interval of U with the first interval of V . Column 3 shows the probability that the new value $U \cdot V$ lies in the new interval. Columns 4, 5, and 6 show the intervals into which the outputs of the transfer of $U \cdot V$ are grouped. The probability shown in column 3 that is associated with the interval indicated by columns 1 and 2 is appropriately prorated into columns 4, 5, and 6. This process is repeated for each combination of intervals. Because U has three intervals and V has three intervals, there are nine combinations of intervals to be considered. (The numbers of intervals need not be the same.) The intervals into which the outputs of the transfer of $U \cdot V$ are to be grouped have been arbitrarily designated as 15-26, 26-37, and 37-48.

The new interval generated by the first combination of intervals is 15-24 with an associated probability of 0.01 (this is shown in the first three columns— row 1 of the table). Because this interval is wholly contained by the first interval of the output density function, the entire 0.01 is put into the 15-26 interval.

The rest of the computations for generating the output probability density function on $(C - R)$, when $(C - R)$ has been defined by $(C-R) = U \cdot V - X/Y$ (shown in Figures IV.3 and IV.4), are accomplished in basically the same manner as we have shown here. Figure IV.5 represents the total process. First operate on U and V according to the

transfer function to produce the output $U \cdot V$. Then operate on X and Y according to the transfer function to produce X/Y . Finally, operate on $(U \cdot V)$ and (X/Y) according to the transfer function to produce $\{(C - R) = U \cdot V - X/Y\}$.

It was noted earlier that discrete densities could be presented in the form of probabilities associated with discrete values of the random variables rather than the use of intervals of values. A common method is to associate the probability with the value of the variable at the interval midpoint. For example, the density of U was given with intervals as.

U	Probability
3 - 4	0.1
4 - 5	0.5
5 - 6	0.4

Using midpoints as discrete values, we could have presented it as

U	Probability
3.5	0.1
4.5	0.5
5.5	0.4

Either of these forms is acceptable for suitable accuracy can be obtained with either one by increasing the number of classes and taking smaller intervals (smaller difference between midpoints.) We have used both techniques in our $R||C$ analyses.

The use of continuous variable density functions in generating densities of combinations of random variables is naturally a preferred approach, but it is not always possible to carry out the complex integrations which are quite often encountered. Appendix VI gives a discussion of the process and it includes a number of examples for which integrations could be performed and thus closed form solutions obtained. It also includes a few cases for which integrations were too complicated to be carried out. It is instructive to observe that the discrete example presented here does provide a guideline for understanding the continuous cases because the mathematical techniques are the same in essential characteristics even though the steps do appear very different.

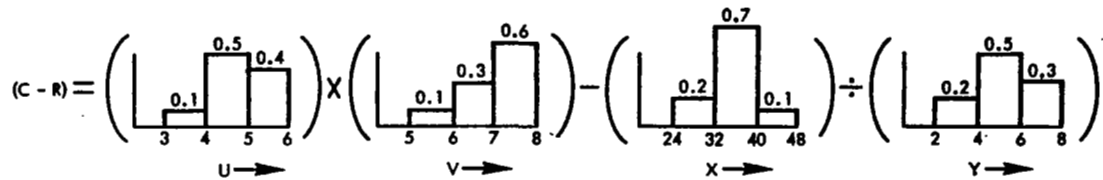
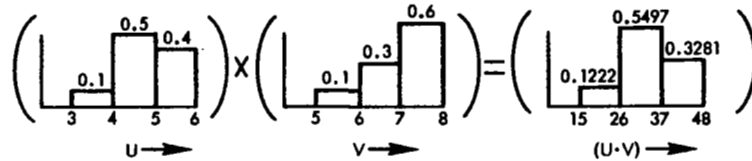
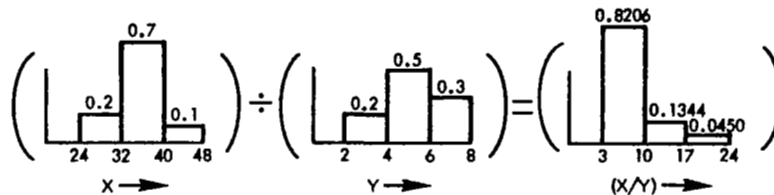


Figure IV-1. Combination of random variables.



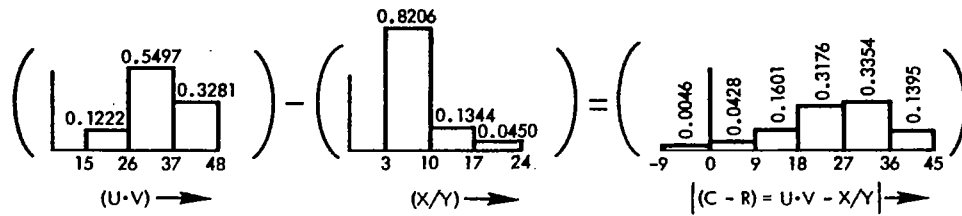
			15-26	26-37	37-48
15	24	0.01	0.0100	—	—
18	28	0.03	0.0240	0.0060	—
21	32	0.06	0.0273	0.0327	—
20	30	0.05	0.0300	0.0200	—
24	35	0.15	0.0273	0.1227	—
28	40	0.30	—	0.2250	0.0750
25	36	0.04	0.0036	0.0364	—
30	42	0.12	—	0.0700	0.0500
35	48	0.24	—	0.0369	0.2031
		1.00	0.1222	0.5497	0.3281

Figure IV-2. Combination of random variables.



			3-10	10-17	17-24
6	16	0.04	0.0160	0.0240	—
4	8	0.10	0.1000	—	—
3	5.3	0.06	0.0600	—	—
8	20	0.14	0.0233	0.0817	0.0350
5.3	10	0.35	0.3500	—	—
4	6.7	0.21	0.2100	—	—
10	24	0.02	—	0.0100	0.0100
6.7	12	0.05	0.0313	0.0187	—
5	8	0.03	0.0300	—	—
		1.00	0.8206	0.1344	0.0450

Figure IV-3. Combination of random variables.



			(-9)-0	0-9	9-18	18-27	27-36	36-45
5	23	0.1003	—	0.0223	0.0501	0.0279	—	—
(-2)	16	0.0164	0.0018	0.0082	0.0064	—	—	—
(-9)	9	0.0055	0.0028	0.0027	—	—	—	—
16	34	0.4511	—	—	0.0501	0.2256	0.1754	—
9	27	0.0739	—	—	0.0370	0.0369	—	—
2	20	0.0247	—	0.0096	0.0124	0.0027	—	—
27	45	0.2692	—	—	—	—	0.1346	0.1346
20	38	0.0441	—	—	—	0.0171	0.0221	0.0049
13	31	0.0148	—	—	0.0041	0.0074	0.0033	—
		1.0000	0.0046	0.0428	0.1601	0.3176	0.3354	0.1395

Figure IV-4. Combination of random variables.

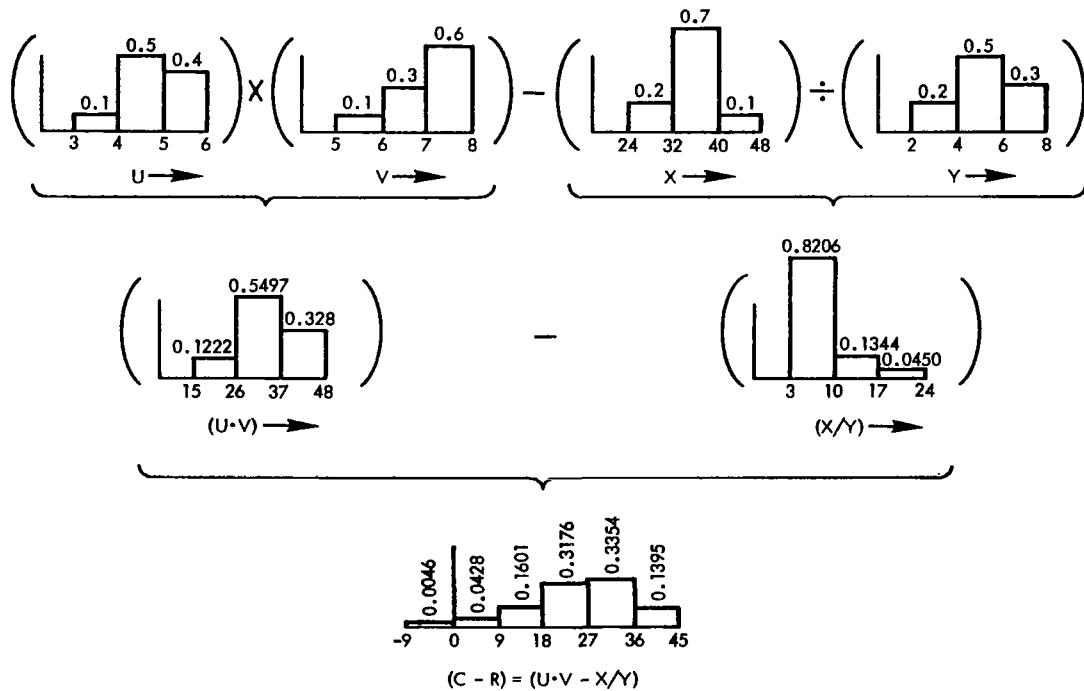


Figure IV-5. Combination of random variables.

The examples discussed thus far in this section involved independence of input parameters and transfer functions. The extension to a dependent situation is not difficult conceptually, but it does involve some computational complications. Hence, we are including a discussion of the treatment of dependency in the following section.

Computations When There is Dependence
Between Two or More Transfer Functions

Suppose we have two transfer functions,

$$U = T_1(x_1, x_2, \dots, x_m) \text{ and } v = T_2(y_1, y_2, \dots, y_n)$$

and suppose that there exists some type of correlation between the input variables, implying therefore a correlation between the outputs, U and v . Such correlation may arise from the fact that one or more x variables are identical with y variables. On the other hand, it might arise in the form of statistical correlation rather than from matching variables.

We wish to determine a computational procedure which permits us to handle any of these cases, and we will also show simplified methods for the independent and the identical variable cases. The initial step will consist of a description of the process in a functional format. This will be followed by some simple discrete examples to illustrate the mathematics involved. Expressing this in terms of only two functions is no real restriction—the extension to more is elementary.

For simplicity of presentation, we will let $m = 3$ and $n = 4$. Thus, the two transfer functions are

$$u = T_1(x_1, x_2, x_3) \text{ and } v = T_2(y_1, y_2, y_3, y_4) .$$

We will describe what must be computed, not being concerned at this point with the time sequence in which the various tasks are performed. It will be convenient to phrase the description entirely in terms of discrete variables—the extension to the continuous case is obvious.

Select a specific set of values of the input parameters. For this set, compute the associated u and v values by substituting in the transfer functions $T_1(x_1, x_2, x_3)$ and $T_2(y_1, y_2, y_3, y_4)$. From the joint density of the x 's and y 's compute the probability of the occurrence of the selected combination of x and y values. Using the standard probability notation, this probability computation is expressed by the equation

$$p(x_1, x_2, x_3, y_1, y_2, y_3, y_4) =$$

$$p(x_1)p(x_2|x_1)p(x_3|x_1, x_2)p(y_1|x_1, x_2, x_3)p(y_2|x_1, x_2, x_3, y_1) \\ p(y_3|x_1, x_2, x_3, y_1, y_2)p(y_4|x_1, x_2, x_3, y_1, y_2, y_3) .$$

Repeat these computations for every possible combination of input parameters. Find the probability of a selected u and v pair by adding together the probabilities for every combination of parameters which yield the u, v pair under consideration. Do this same thing for every possible u, v pair, thus generating the joint density of u and v .

Of course this description includes the case of independence in which the indicated conditional probabilities are in reality equal to the unconditional ones. Let us express this in basic probability language. Take as an example the probability

$$p(y_1|x_1, x_2, x_3) .$$

If y_1 is correlated with one or more of the x 's, then the density of y_1 is modified if x_1, x_2 and x_3 are fixed. This modification of the y_1 density is a reflection of the dependence. However, if y_1 is independent of x_1, x_2 , and x_3 , then its density is not modified and we would have

$$p(y_1) = p(y_1|x_1, x_2, x_3) .$$

Thus we see that the computational task is one of adjusting densities after the determination of each parameter value. It is clear that this description does indeed cover dependence whether or not it is generated by the occurrence of the same variables in the two transfer functions. The extension to more than two functions is quite clearly indicated by the above presentation.

Examples to Show the Mathematics Involved
in Treating Dependency Between Transfer
Functions with Discrete Input Parameters

Let us express these examples in terms of capability vs requirement in reliability analysis, C and R respectively. We will illustrate independence as well as the two kinds of dependence—one resulting from the occurrence of identically the same variable in C and R and the other resulting from a correlation without variable identity. This treatment should be viewed as a display of the computational task and not as a description of an optimal computation methodology.

Suppose the transfer functions are

Capability: $C = x_1 y$ and

Requirement: $R = x_2 + z$.

We have chosen to use a notation common to capability vs requirement analysis instead of the more general functional notation described earlier. This should not create any real confusion. The variables x_1 and x_2 will be treated under three different assumptions corresponding to the three cases identified above. In each of the cases, the variable densities will be as follows.

x_1	$p(x_1)$	x_2	$p(x_2)$	y	$p(y)$	z	$p(z)$
1	.3	1	.3	1	.1	1	.2
2	.5	2	.5	2	.4	2	.2
3	.2	3	.2	3	.3	3	.6
				4	.2		

The general probability symbolism is needed later in the discussion so we used it here instead of the general function notation. We chose $p(x_1)$ to be the same as $p(x_2)$ in order to fit them into the dependency case involving identical variables.

With respect to x_1 and x_2 , the basic input probabilities needed in this analysis can be expressed as the four densities

$$p(x_1), p(x_2), p(x_1, x_2) \text{ and } p(x_2|x_1)$$

shown in Table IV.6.

The basic formula for each of the three cases is

$$p(x_1, x_2) = p(x_1) p(x_2|x_1).$$

However, in the first case in which x_1 and x_2 are independent, the joint density reduces to the product of the single parameter densities since

$$p(x_2|x_1) = p(x_2),$$

giving

$$p(x_1, x_2) = p(x_1) p(x_2).$$

For example, take $x_1 = 2$ and $x_2 = 3$. Then we have

$$\begin{aligned} p(x_1 = 2, x_2 = 3) &= p(x_1 = 2)p(x_2 = 3) \\ &= (.5)(.2) \\ &= .10 \end{aligned}$$

and $p(x_2 = 3|x_1 = 2) = p(x_2 = 3) = .2$.

In the second case, we have x_1 and x_2 identically the same which means that

$$\begin{aligned} p(x_2|x_1) &= 1 \text{ if } x_2 = x_1 \\ &= 0 \text{ if } x_2 \neq x_1. \end{aligned}$$

Table IV.6. Probabilities involving x_1 and x_2 .

Case Identification	Conditional Probabilities				Joint Density					
	$p(x_2 x_1)$				$p(x_1, x_2)$					
	x_2	x_1		$p(x_2)$	x_2	x_1		$p(x_2)$		
		1	2	3		1	2	3		
Independent	1	.3	.3	.3	.3	1	.09	.15	.06	.3
	2	.5	.5	.5	.5	2	.15	.25	.10	.5
	3	.2	.2	.2	.2	3	.06	.10	.04	.2
	$p(x_1)$.3	.5	.2		$p(x_1)$.3	.5	.2	
Dependent	$p(x_2 x_1)$				$p(x_1, x_2)$					
$x_1 \equiv x_2$	x_2	x_1		$p(x_2)$	x_2	x_1		$p(x_2)$		
		1	2	3		1	2	3		
	1	1	0	0	.3	1	.3	0	0	.3
	2	0	1	0	.5	2	0	.5	0	.5
	3	0	0	1	.2	3	0	0	.2	.2
	$p(x_1)$.3	.5	.2		$p(x_1)$.3	.5	.2	
Dependent	$p(x_2 x_1)$				$p(x_1, x_2)$					
x_1 and x_2 correlated but $x_1 \neq x_2$	x_2	x_1		$p(x_2)$	x_2	x_1		$p(x_2)$		
		1	2	3		1	2	3		
	1	.5	.2	.25	.3	1	.15	.10	.05	.3
	2	.5	.5	.50	.5	2	.15	.25	.10	.5
	3	0	.3	.25	.2	3	0	.15	.05	.2
	$p(x_1)$.3	.5	.2		$p(x_1)$.3	.5	.2	

Therefore we have

$$\begin{aligned}
 p(x_1, x_2) &= p(x_1) \text{ if } x_2 = x_1 \\
 &= 0 \quad \text{if } x_2 \neq x_1 .
 \end{aligned}$$

For the third case in which x_1 and x_2 are correlated but are not identical, we merely use the general formula

$$p(x_1, x_2) = p(x_1)p(x_2|x_1) .$$

Regardless of the relationship between x_1 and x_2 , in our example it is always true that y and z are uncorrelated. Hence, we can form the joint density, $p(y, z)$, for each case. The density, $p(y, z)$, is

y \ z	1	2	3	4	p(z)
1	.02	.08	.06	.04	.2
2	.02	.08	.06	.04	.2
3	.06	.24	.18	.12	.6
p(y)	.1	.4	.3	.2	

We can express the $p(x_1, x_2, y, z)$ density in the format of the $p(y, z)$ density, three rows and four columns, in which each element is a three by three matrix formed as the product of the single $p(y, z)$ probability and the entire three by three $p(x_1, x_2)$ density. For each column, there corresponds a particular pair of x_1 and y values and for each row, there is a particular pair of x_2 and z values. Therefore, we can identify a C value for each column and an R value for each row as shown in the three $p(x_1, x_2, y, z)$ densities which follow. The row and column x_1 and x_2 values, 1, 2, and 3, increase from left to right and top to bottom respectively.

Table IV.7. Independent case. Values of $p(x_1, x_2, y, z)$, C, and R for every possible combination of variables.

$\begin{matrix} y \\ z \end{matrix}$	1			2			3			4				R
1	.0018	.0030	.0012	.0072	.0120	.0048	.0054	.0090	.0036	.0036	.0060	.0024	.0600	2
	.0030	.0050	.0020	.0120	.0200	.0080	.0090	.0150	.0060	.0060	.0100	.0040	.1000	3
	.0012	.0020	.0008	.0048	.0080	.0032	.0036	.0060	.0024	.0024	.0040	.0016	.0400	4
2	.0018	.0030	.0012	.0072	.0120	.0048	.0054	.0090	.0036	.0036	.0060	.0024	.0600	3
	.0030	.0050	.0020	.0120	.0200	.0080	.0090	.0150	.0060	.0060	.0100	.0040	.1000	4
	.0012	.0020	.0008	.0048	.0080	.0032	.0036	.0060	.0024	.0024	.0040	.0016	.0400	5
3	.0054	.0090	.0036	.0216	.0360	.0144	.0162	.0270	.0108	.0108	.0180	.0072	.1800	4
	.0090	.0150	.0060	.0360	.0600	.0240	.0270	.0450	.0180	.0180	.0300	.0120	.3000	5
	.0036	.0060	.0024	.0144	.0240	.0096	.0108	.0180	.0072	.0072	.0120	.0048	.1200	6
	.0300	.0500	.0200	.1200	.2000	.0800	.0900	.1500	.0600	.0600	.1000	.0400		
C	1	2	3	2	4	6	3	6	9	4	8	12		

Table IV. 8. Independent case. Worksheet to generate joint density of C and R.

C \ R	1	2	3	4	6	8	9	12	Sum
2	.0018	.0030	.0012	.0120	.0048	.0060	.0036	.0024	
		.0072	.0054	.0036	.0090				
Sum	.0018	.0102	.0066	.0156	.0138	.0060	.0036	.0024	.0600
C-R	-1	0	1	2	4	6	7	10	
3	.0030	.0050	.0020	.0200	.0080	.0100	.0060	.0040	
	.0018	.0030	.0012	.0120	.0048	.0060	.0036	.0024	
		.0120	.0090	.0060	.0150				
		.0072	.0054	.0036	.0090				
Sum	.0048	.0272	.0176	.0416	.0368	.0160	.0096	.0064	.1600
C-R	-2	-1	0	1	3	5	6	9	
4	.0012	.0020	.0008	.0080	.0032	.0040	.0024	.0016	
	.0030	.0050	.0020	.0200	.0080	.0100	.0060	.0040	
	.0054	.0090	.0036	.0360	.0144	.0180	.0108	.0072	
		.0048	.0036	.0024	.0060				
		.0120	.0090	.0060	.0150				
		.0216	.0172	.0108	.0270				
Sum	.0096	.0544	.0352	.0832	.0736	.0320	.0192	.0128	.3200
C-R	-3	-2	-1	0	2	4	5	8	
5	.0012	.0020	.0008	.0080	.0032	.0040	.0024	.0016	
	.0090	.0150	.0060	.0600	.0240	.0300	.0180	.0120	
		.0048	.0036	.0024	.0060				
		.0360	.0270	.0180	.0450				
Sum	.0102	.0578	.0374	.0884	.0782	.0340	.0204	.0136	.3400
C-R	-4	-3	-2	-1	1	3	4	7	
6	.0036	.0060	.0024	.0240	.0096	.0120	.0072	.0048	
		.0144	.0108	.0072	.0180				
Sum	.0036	.0204	.0132	.0312	.0276	.0120	.0072	.0048	.1200
C-R	-5	-4	-3	-2	0	2	3	6	
Sum	.0300	.1700	.1100	.2600	.2300	.1000	.0600	.0400	

Table IV.9. Independent case. Computation of C-R density.

C-R					Sum	
-5				.0036	.0036	
-4			.0102	.0204	.0306	
-3			.0096	.0578	.0132	.0806
-2		.0048	.0544	.0374	.0312	.1278
-1	.0018	.0272	.0352	.0884		.1526
0	.0102	.0176	.0832		.0276	.1386
1	.0066	.0416		.0782		.1264
2	.0156		.0736		.0120	.1012
3		.0368		.0340	.0072	.0780
4	.0138		.0320	.0204		.0662
5		.0160	.0192			.0352
6	.0060	.0096			.0048	.0204
7	.0036			.0136		.0172
8			.0128			.0128
9		.0064				.0064
10	.0024					.0024

Table IV.10. Identical variable case. Values of $p(x_1, x_2, y, z)$, C, and R for every possible combination of variables.

$y \backslash z$	1			2			3			4			Sum	R
1	.006			.024			.018			.012			.060	2
		.010			.040			.030			.020		.100	3
			.004			.016			.012			.008	.040	4
2	.006			.024			.018			.012			.060	3
		.010			.040			.030			.020		.100	4
			.004			.016			.012			.008	.040	5
3	.018			.072			.054			.036			.180	4
		.030			.120			.090			.060		.300	5
			.012			.048			.036			.024	.120	6
Sum	.030	.050	.020	.120	.200	.080	.090	.150	.060	.060	.100	.040		
C	1	2	3	2	4	6	3	6	9	4	8	12		

Table IV.11. Identical variable case. Worksheet to generate joint density of C and R.

C \ R	1	2	3	4	6	8	9	12	Sum
2	.006	.024	.018	.012					
Sum	.006	.024	.018	.012					.060
C-R	-1	0	1	2					
3	.006	.010	.018	.040	.030	.020			
		.024		.012					
Sum	.006	.034	.018	.052	.030	.020			.160
C-R	-2	-1	0	1	3	5			
4	.018	.010	.004	.040	.016	.020	.012	.008	
		.072	.054	.036	.030				
Sum	.018	.082	.058	.076	.046	.020	.012	.008	.320
C-R	-3	-2	-1	0	2	4	5	8	
5		.030	.004	.120	.016	.060	.012	.008	
					.090				
Sum		.030	.004	.120	.106	.060	.012	.008	.340
C-R		-3	-2	-1	1	3	4	7	
6			.012		.048		.036	.024	
Sum			.012		.048		.036	.024	.120
C-R			-3		0		3	6	
Sum	.030	.170	.110	.260	.230	.100	.060	.040	

Table IV.12. Identical variable case. Computation of C-R density.

C-R					Sum
-3		.018	.030	.012	.060
-2	.006	.082	.004		.092
-1	.006	.034	.058	.120	.218
0	.024	.018	.076	.048	.166
1	.018	.052	.106		.176
2	.012	.046			.058
3	.030	.060	.036		.126
4	.020	.012			.032
5	.020	.012			.032
6			.024		.024
7			.008		.008
8		.008			.008
Sum					1.000

Table IV.13. Correlated variable case, $x \neq x$. Values of $p(x_1, x_2, y, z)$, C, and R for every possible combination of variables.

$\begin{matrix} y \\ z \end{matrix}$	1			2			3			4			Sum	R
1	.003	.002	.001	.012	.008	.004	.009	.006	.003	.006	.004	.002	.060	2
	.003	.005	.002	.012	.020	.008	.009	.015	.006	.006	.010	.004	.100	3
	0	.003	.001	0	.012	.004	0	.009	.003	0	.006	.002	.040	4
2	.003	.002	.001	.012	.008	.004	.009	.006	.003	.006	.004	.002	.060	3
	.003	.005	.002	.012	.020	.008	.009	.015	.006	.006	.010	.004	.100	4
	0	.003	.001	0	.012	.004	0	.009	.003	0	.006	.002	.040	5
3	.009	.006	.003	.036	.024	.012	.027	.018	.009	.018	.012	.006	.180	4
	.009	.015	.006	.036	.060	.024	.027	.045	.018	.018	.030	.012	.300	5
	0	.009	.003	0	.036	.012	0	.027	.009	0	.018	.006	.120	6
Sum	.030	.050	.020	.120	.200	.080	.090	.150	.060	.060	.100	.040		
C	1	2	3	2	4	6	3	6	9	4	8	12		

IV-19

Table IV. 14. Correlated variable case, $x_1 \neq x_2$. Worksheet to generate joint density of C and R.

R \ C	1	2	3	4	6	8	9	12	Sum
2	.003	.002	.001	.008	.004	.004	.003	.002	
		.012	.009	.006	.006				
Sum	.003	.014	.010	.014	.010	.004	.003	.002	.060
C-R	-1	0	1	2	4	6	7	10	
3	.003	.005	.002	.020	.008	.010	.006	.004	
	.003	.002	.001	.008	.004	.004	.003	.002	
		.012	.009	.006	.015				
		.012	.009	.006	.006				
Sum	.006	.031	.021	.040	.033	.014	.009	.006	.160
C-R	-2	-1	0	1	3	5	6	9	
4	.003	.003	.001	.012	.004	.006	.003	.002	
	.009	.005	.002	.020	.008	.010	.006	.004	
		.006	.003	.024	.012	.012	.009	.006	
		.012	.009	.006	.009				
		.036	.027	.018	.015				
					.018				
Sum	.012	.062	.042	.080	.066	.028	.018	.012	.320
C-R	-3	-2	-1	0	2	4	5	8	
5	.009	.003	.001	.012	.004	.006	.003	.002	
		.015	.006	.060	.024	.030	.018	.012	
		.036	.027	.018	.009				
					.045				
Sum	.009	.054	.034	.090	.082	.036	.021	.014	.340
C-R	-4	-3	-2	-1	1	3	4	7	
6		.009	.003	.036	.012	.018	.009	.006	
					.027				
Sum		.009	.003	.036	.039	.018	.009	.006	.120
C-R	-5	-4	-3	-2	0	2	3	6	
Sum	.030	.170	.110	.260	.230	.100	.060	.040	

Table IV.15. Correlated variable case, $x_1 \neq x_2$.
 Computation of C-R density.

C-R					Sum
-4			.009	.009	.018
-3		.012	.054	.003	.069
-2	.006	.062	.034	.036	.138
-1	.003	.031	.042	.090	.166
0	.014	.021	.080	.039	.154
1	.010	.040	.082		.132
2	.014	.066	.018		.098
3	.033	.036	.009		.078
4	.010	.028	.021		.059
5	.014	.018			.032
6	.004	.009		.006	.019
7	.003		.014		.017
8		.012			.012
9	.006				.006
10	.002				.002
Sum					1.000

Simplified Computational Procedures

The preceding discussion has presented a general computational method. For the independent and the identical variable cases, we can simplify the arithmetic because of the special relationships existing for these two cases.

Independent Case

When the capability, C , and the requirement, R , are independent, we can compute their densities separately and then obtain the density of the difference, $C-R$, thus eliminating the need to derive the four variable density used in the general approach. The arithmetic is summarized as follows. First consider the computation for C and R .

Capability				Requirement			
$C = x_1 y$				$R = x_2 + z$			
x_1	1, .3	2, .5	3, .2	x_2	1, .3	2, .5	3, .2
y	1, .1	2, .4	3, .3	z	1, .2	2, .2	3, .6
	1, .03	2, .05	3, .02		2, .06	3, .10	4, .04
	2, .12	4, .20	6, .08		3, .06	4, .10	5, .04
	3, .09	6, .15	9, .06		4, .18	5, .30	6, .12
	4, .06	8, .10	12, .04				

Each tabular entry consists of a pair of numbers, the first one being the value of the input parameter or the output capability or requirement as the case may be, and the second number being the associated probability. This "pair" notation will be used throughout this section. The function densities are obtained by collecting terms.

$C = x_1 y$	Probability	$R = x_2 + z$	Probability
Value		Value	
1	.03	2	.06 = .06
2	.12 + .05 = .17	3	.10 + .06 = .16
3	.09 + .02 = .11	4	.04 + .10 + .18 = .32
4	.06 + .20 = .26	5	.04 + .30 = .34
6	.15 + .08 = .23	6	.12 = .12
8	.10 = .10		
9	.06 = .06		
12	.04 = .04		

The C-R density is computed in the following tables, again using the paired notation in which the first number is the value and the second is the probability.

We will compute the density of C-R for the identical variable case in two ways. Since $x_1 \equiv x_2$, we can drop the subscripts. The problem is to take each value of x and compute all corresponding values of xy and $x + z$ with associated probabilities, keeping proper identification. This is accomplished in the following table. The columns of blocks are identified by an x value and the rows of blocks by a y value. Within the blocks we have a sequence of values and associated probabilities corresponding to

xy ,
 $x + z$ for $z = 1$,
 $x + z$ for $z = 2$, and
 $x + z$ for $z = 3$.

R \ C	2 .06	3 .16	4 .32	5 .34	6 .12	Probability Sum
1 .03	-1 .0018	-2 .0048	-3 .0096	-4 .0102	-5 .0036	.0300
2 .17	0 .0102	-1 .0272	-2 .0544	-3 .0578	-4 .0204	.1700
3 .11	1 .0066	0 .0176	-1 .0352	-2 .0374	-3 .0132	.1100
4 .26	2 .0156	1 .0416	0 .0832	-1 .0884	-2 .0312	.2600
6 .23	4 .0138	3 .0368	2 .0736	1 .0782	0 .0276	.2300
8 .10	6 .0060	5 .0160	4 .0320	3 .0340	2 .0120	.1000
9 .06	7 .0036	6 .0096	5 .0192	4 .0204	3 .0072	.0600
12 .04	10 .0024	9 .0064	8 .0128	7 .0136	6 .0048	.0400
Probability Sum	.0600	.1600	.3200	.3400	.1200	1.0000

C-R	Probability
-5	.0036 = .0036
-4	.0102 + .0204 = .0306
-3	.0096 + .0578 + .0132 = .0806
-2	.0048 + .0544 + .0374 + .0312 = .1278
-1	.0018 + .0272 + .0352 + .0884 = .1526
0	.0102 + .0176 + .0832 + .0276 = .1386
1	.0066 + .0416 + .0782 = .1264
2	.0156 + .0736 + .0120 = .1012
3	.0368 + .0340 + .0072 = .0780
4	.0138 + .0320 + .0204 = .0622
5	.0160 + .0192 = .0352
6	.0060 + .0096 + .0048 = .0204
7	.0036 + .0136 = .0172
8	.0128 = .0128
9	.0064 = .0064
10	.0024 = .0024
Sum	1.0000

y		Value Probability		Value Probability		Value Probability	
Value	Probability	x:	1 .3	2 .5	3 .2		
1	.1	xy	1 .03	2 .05	3 .02		
		x+z	2 .006	3 .010	4 .004		
		x+z	3 .006	4 .010	5 .004		
		x+z	4 .018	5 .030	6 .012		
2	.4	xy	2 .12	4 .20	6 .08		
		x+z	2 .024	3 .040	4 .016		
		x+z	3 .024	4 .040	5 .016		
		x+z	4 .072	5 .120	6 .048		
3	.3	xy	3 .09	6 .15	9 .06		
		x+z	2 .018	3 .030	4 .012		
		x+z	3 .018	4 .030	5 .012		
		x+z	4 .054	5 .090	6 .036		
4	.2	xy	4 .06	8 .10	12 .04		
		x+z	2 .012	3 .020	4 .008		
		x+z	3 .012	4 .020	5 .008		
		x+z	4 .036	5 .060	6 .024		

Associated R and C values and their respective probabilities can now be collected together as shown below, and this leads immediately to the density of C-R which is also shown.

C = xy	R = x + z					C = xy
	2	3	4	5	6	Sum
1	.006	.006	.018			.03
2		.010	.010	.030		
Sum	.024	.024	.072			
3			.004	.004	.012	
Sum	.018	.018	.054			.17
4		.040	.040	.120		
Sum	.012	.012	.036			.11
6			.016	.016	.048	
Sum	.012	.052	.076	.120		.26
8		.020	.020	.060		
Sum		.030	.030	.090		.23
9			.012	.012	.036	
Sum			.008	.008	.024	.10
12						.06
Sum						.04

Sum: R=x+z .060 .160 .320 .340 .120

1.00

C - R = xy - (x+z)

Probability

-3	.018 + .030 + .012	=	.060
-2	.006 + .082 + .004	=	.092
-1	.006 + .034 + .058 + .120	=	.218
0	.024 + .018 + .076 + .048	=	.166
1	.018 + .052 + .106	=	.176
2	.012 + .046	=	.058
3	.030 + .060 + .036	=	.126
4	.020 + .012	=	.032
5	.020 + .012	=	.032
6	.024	=	.024
7	.008	=	.008
8	.008	=	.008

Consider now a direct computation of the density of C-R by first generating a formula for this difference, namely

$$\begin{aligned}C-R &= xy - (x+z) \\ &= x(y-1)-z .\end{aligned}$$

We can now compute all possible values of C - R together with their associated probabilities. This is shown below as a three step process in which we determine

- (1) values of $x(y-1)$ and associated probabilities,
- (2) values of $x(y-1)-z$ and associated probabilities,
- (3) density of $C-R = x(y-1)-z$ by combining values computed in (2).

			x					
			Value Probability		Value Probability		Value Probability	
y	y-1	p(y-1)	1	.3	2	.5	3	.2
1	0	.1	0	.03	0	.05	0	.02
2	1	.4	1	.12	2	.20	3	.08
3	2	.3	2	.09	4	.15	6	.06
4	3	.2	3	.06	6	.10	9	.04

		z					
		Value Probability		Value Probability		Value Probability	
x(y-1)	Probability	1	.2	2	.2	3	.6
0	.10	-1	.020	-2	.020	-3	.060
1	.12	0	.024	-1	.024	-2	.072
2	.29	1	.058	0	.058	-1	.174
3	.14	2	.028	1	.028	0	.084
4	.15	3	.030	2	.030	1	.090
6	.16	5	.032	4	.032	3	.096
9	.04	8	.008	7	.008	6	.024

x(y-1)-z	Probability
-3	.060
-2	.092
-1	.218
0	.166
1	.176
2	.058
3	.126
4	.032
5	.032
6	.024
7	.008
8	.008

APPENDIX V

COMPUTER PROCEDURES

Introduction

Even a very simple R||C analysis example can involve a rather heavy computational load so it was natural to try to develop computer procedures to handle such problems. Indeed, recognition of the burdensome arithmetic has been a strong deterrent to the use of this reliability analysis procedure even though the validity of the basic theory has been accepted for a long time. Furthermore, there has been a decided hesitation to use computers even when they were available, largely because of the apparent loss of control when the design engineer or analyst turned the work over to a programmer who then turned it over to the computer operator. This lack of control was reflected in an inability to react to problems as they arose and also to provide prompt reaction to or use of study results as they were developed by the computer.

These problems associated with computer usage have been largely solved by the introduction of time sharing computer systems. It was natural, therefore, for TEMPO to make use of the General Electric Time Sharing Computer System in achieving one of the major study objectives—showing that some system does exist for carrying out R||C analysis with the expenditure of a reasonable computational effort. Since the General Electric system turned out to be so well suited to this task and since we were not required to find more than one suitable system, no attempt was made to find others. It must be recognized, however, that even though other systems might be adaptable to this problem, the programs which we have included and the running times and costs which we have discussed in this report apply only to the General Electric system. We do not know how these items would have to be modified if one wished to adapt them to another time sharing computer system.

Some of the desirable characteristics of time sharing computer systems have been implied in the preceding discussion. It would perhaps be useful to identify them more precisely to provide an adequate background for understanding and appreciating the time sharing computer system in the R||C analysis application. Since the computer is operated from a remote access teletype console, the design engineer or analyst can operate the computer from a convenient location in his own office or work area. Not only is the operating console handy,

but it is also easy to use. It is operated much like a standard typewriter which has been tied in with a telephone. The modern compiler languages have been so simplified that programming proficiency can be achieved in a very short time. This means that the design engineer, his analyst, or any other member of the staff can learn the technique and operate the computer himself or he can participate in performing a computerized R||C analysis. Thus control of the process is not lost by going through the programmer—operator cycle required on "batch" computers. The analyst maintains complete control and he receives his answers promptly so he can debug his program with ease in a very timely fashion. The rapidity with which the answers are generated and displayed makes it easy to perform parametric studies which realistically reflect the effects of design changes. Finally, because of its high speed, flexibility of operation, and its ability to serve many operators simultaneously, the computer costs are held to extremely low levels.

Earlier discussion noted that the computer uses discrete densities, with the random variable expressed either in interval form or as separate distinct values. Data can be fed into the computer in one of these discrete density forms or in the form of a density function formula from which the computer will derive a discrete density approximation according to instructions programmed in by the operator. Of course it is possible to combine these different forms in a single R||C analysis.

The computer programs now available have the capability of combining random variables by a mix of any appropriate mathematical operations. In an R||C analysis, random variables are combined two at a time, a succession of such pair-wise combinations being used to derive the density resulting from the combination of more than two random variables.

The listings of two typical computer programs that were used in this study are included at the end of this section. The program named "F 260" is written in the Time-Sharing Fortran compiler language and it is the program that was used to illustrate a computer run as discussed in the example on the following pages. The program named "RELFMI" is written in the Time-Sharing Extended Basic compiler language and it is the program that was used to obtain the results that are shown in the discussions of the motor example in Section 5 and Appendix II. It

should be noted that this particular program listing contains the instructions for doing the computations associated with the first failure mode. The only difference in the instructions for the first failure mode and those for the other failure modes occur in line number 2000 and above.

The hypothetical example that was used in Appendix IV to illustrate the process of combining random variables was also solved on the desk side computer using the program described above. The sequence of computer operations differed slightly from that used in the hand computation of the example illustrated by Figures IV. 1 through IV. 5. Copies of the output of the computer, Figure V. 1, have been marked to show the correspondence to the results shown in Figures IV. 2, IV. 3 and IV. 4.

Recalling that the transfer function used in the example was $\{(C - R) = U \cdot V - X/Y\}$, the computer performed the following sequence of operations:

- (1) Generate density function for (X/Y) .
- (2) Save (X/Y) density function for later call-up.
- (3) Generate density function for $(U \cdot V)$.
- (4) Call back (X/Y) density function and subtract it from $(U \cdot V)$ density function thus generating the density function for $(C - R)$.

It will be observed that notations are made on the computer output sheets to point out which of the values are inputs to the computer and which ones are outputs of the computer. The print-outs that occur before the final density function print-out (i. e., for $C - R$) are optional. They have been included here in order to show the sequence of computer operations.

Figure V.1 Illustration of Computer Run

USER NUMBER --888888 ← (Each user is assigned a number)
 SYSTEM--FOR ← (Fortran compiler language)
 NEW OR OLD--OLD ← (Program is stored in computer memory)
 OLD PROBLEM NAME--F260 ← (Name of program to be brought from
 WAIT. memory)

READY ← (Computer has found program and is
 ready to act)
 RUN ← (User's command for computer to compile
 program)

F260 15:14 SB FRI 10/31/67

IN F260A } (Computer is compiling the three
 IN F260B } program sections)

PROGRAM TO COMBINE RANDOM VARIABLES

WANT TO SEE CODE, YES OR NO ← (First option of program—to print-
 ? NO out various combining operations)

NUMBER, POINTS FOR FIRST DENSITY

? 4, 24, 32, 40, 48 } (Description of first density function
 PROBABILITIES } "X")
 ? .2, .7, .1

READ OPERATION CODE (1-15) (Tells computer - operation is to
 ? 4 ← divide two random variables)

NEXT DENSITY FROM STORAGE, YES OR NO ← (At this point no den-
 ? NO sity function has been stored)

NUMBER, POINTS FOR NEXT DENSITY

? 4, 2, 4, 6, 8 } (Description of second density func-
 PROBABILITIES } tion, "Y")
 ? .2, .5, .3

NEW OUTPUT POINTS, YES OR NO

? YES } (Description of output grid for X/Y)
 NUMBER, OUTPOINT POINTS }
 ? 4, 3, 10, 17, 24

WANT TO SEE DISTRIBUTION, YES OR NO

? YES

Figure V.1 Illustration of Computer Run (continued)

*****RESULTING PROBABILITIES*****

START	STOP	PROBABILITY	
3.00	10.00	.8206	} (Density function for X/Y; see Fig. IV.3
10.00	17.00	.1344	
17.00	24.00	.045	

CHECK SUM = 1.000000
MOMENTS = 8.070917E+00 1.293864E+01 2.250325E+00 7.142340E+00

READ OPERATION CODE (1-15) ← (Tells computer to save X/Y
? 11 density function for later use)

READ OPERATION CODE (1-15) ← (Tells computer-there is a new
? 15 set of random variables on which
to operate)

NUMBER, POINTS FOR FIRST DENSITY
? 4, 3, 4, 5, 6
PROBABILITIES } (Description of first density function,
? .1, .5, .4 } "U")

READ OPERATION CODE (1-15) ← (Tells computer - operation is
? 3 to multiply two random variables)

NEXT DENSITY FROM STORAGE, YES OR NO ← (Next density function not
? NO to be taken from storage)

NUMBER, POINTS FOR NEXT DENSITY
? 4, 5, 6, 7, 8
PROBABILITIES } (Description of second density function
? .1, .3, .6 } "V")

NEW OUTPUT POINTS, YES OR NO
? YES } (Description of output grid for U·V)
NUMBER, OUTPOINT POINTS
? 4, 15, 26, 37, 48

WANT TO SEE DISTRIBUTION, YES OR NO
? YES

Figure V.1 Illustration of Computer Run (continued)

*****RESULTING PROBABILITIES*****

START	STOP	PROBABILITY	
15.00	26.00	.1222	} (Density function for U · V; see Fig. IV.2
26.00	37.00	.5497	
37.00	48.00	.3281	

CHECK SUM = 1.000000

MOMENTS = 3.376485E+01 4.935178E+01 -2.102505E-01 2.343323E+00

READ OPERATION CODE(1-15) (Tells computer - operation is to subtract
 ? 2 ← a random variable from U · V which is now
 in computer)

NEXT DENSITY FROM STORAGE, YES OR NO ← (Tells computer that the
 ? YES random variable to sub-
 tract from U · V is stored)

NEW OUTPUT POINTS, YES OR NO

? YES

NUMBER, OUTPOINT POINTS } (Description of output grid for U · V - X/Y)
 ? 7, -9, 0, 9, 18, 27, 36, 45

WANT TO SEE DISTRIBUTION, YES OR NO

? YES

*****RESULTING PROBABILITIES*****

START	STOP	PROBABILITY	
-9.00	.00	.0046	} (Density function for U · V - X/Y; see Fig. IV.4
.00	9.00	.0429	
9.00	18.00	.1601	
18.00	27.00	.3176	
27.00	36.00	.3354	
36.00	45.00	.1395	

CHECK SUM = 1.000000

MOMENTS = 2.569393E+01 9.235007E+01 -3.561212E-01 2.709346E+00

READ OPERATION CODE(1-15) (Tells computer that there are no more
 ? STOP ← calculations to make)

```

00000C*****PROG FINDS PROB OF COMB.*****
00005 $FILE F260D1/F260D2
00010      COMMON X(100),Y(200),Z(100),P(200),PP(200),RP(100),S(100)
20      COMMONZX(100),RPX(100),NX
00030 1000 FORMAT(// "PROGRAM TO COMBINE RANDOM VARIABLES")
00040 1002 FORMAT(// "OPERATION CODE")
00050 1004 FORMAT(" ADD, 1"/" SUBTRACT, 2"/" MULTIPLY, 3"/
00060      +" DIVIDE, 4"/" C*X, 5"/" X**C, 6"/" SIN(X), 7"/
00070      +" COS(X), 8"/" LOG(X), 9"/" EXP(X), 10"/
00080      +" SAVE DISTRIBUTION, 11"/
00090      +" HALVE INTERVALS BOTH/FIRST/SECOND, 12/13/14"/
00100      +" RESTART, 15 OR GREATER")
00110 1006 FORMAT(// "READ OPERATION CODE(1-15)")
00120 1010 FORMAT(/// "NUMBER, POINTS FOR FIRST DENSITY")
00130 1015 FORMAT(" PROBABILITIES")
00140 1030 FORMAT(" NUMBER, POINTS FOR NEXT DENSITY")
00150 1040 FORMAT("/ "NEXT DENSITY FROM STORAGE, YES OR NO")
00160 1060 FORMAT(// "*****RESULTING PROBABILITIES*****")
00170 1070 FORMAT("CHECK SUM =",F10.6)
00180 1080 FORMAT(//5X,"START",10X,"STOP",6X,"PROBABILITY")
00190 2000 FORMAT(" NUMBER, OUTPOINT POINTS")
00200 2020 FORMAT(" NEW OUTPUT POINTS, YES OR NO")
00210 2040 FORMAT("/ ("",14,"") AND ("",14,"") POINTS")
00220 2060 FORMAT("/ "MAX CUMULATIVE PROB DIFFERENCE =",1PE14.6)
00230 2080 FORMAT("/ "WANT TO SEE DISTRIBUTION, YES OR NO")
00240 3000 FORMAT("MOMENTS =",4(1PE14.6))
00250 3020 FORMAT("/ " WANTS TO SEE CODE, YES OR NO")
00255 3040 FORMAT(A3)
00260      IYES=/702562
00270      PRINT 1000
00280      PRINT 3020
00290      READ(1),IY
291 PRINT3040,IY
00300      IF(IY-IYES)10,5,10
00310      5 PRINT 1002
00320      PRINT 1004
330      10 PRINT 1010
00340      LSD=0
00350      READ(1),M,(Z(K),K=1,M)
00360      PRINT 1015
00370      JM1=M-1
00380      READ(1),(RP(I),I=1,JM1)
00390      15 PRINT 1006
00400      READ(1),ICODE
401 PRINT,ICODE
405 IF(ICODE-999)16,STOP,16;STOP:STOP;16:CONTINUE
00410      IF(ICODE-14)17,17,10
00420      17 IF(ICODE-11)30,30,20
00430      20 LQ=ICODE-11
00440      GO TO (22,22,25),LQ

```

F260 CONTINUED

```
00450      22 CALL HALF(N1,X)
00460          CALL PHALF(N1M1,P)
00470          GO TO (25,28,25),LQ
00480      25 CALL HALF(N2,Y)
00490          CALL PHALF(N2M1,PP)
00500      28 PRINT 2040,N1,N2
00510          LSD=ICODE
00520          ICODE=LCODE
00530          GO TO 100
00540      30 GO TO (31,31,31,31,31,31,31,31,31,31,100),ICODE
00550      31 DO 38 I=1,JM1
00560      38 P(I)=RP(I)
00570          DO 40 I=1,M
00580      40 X(I)=Z(I)
00590          LSD=0
00600          N1=JM1+1
00610          N1M1=N1-1
00620          GO TO (41,41,41,41,49,49,49,49,49,49),ICODE
00630      41 PRINT 1040
00640          READ(1),IY
641 PRINT 3040,IY
00650          IF(IY-IYES)48,42,48
00660      42 DO 43 I=1,NX
00670      43 Y(I)=ZX(I)
00680          N2M1=NX-1
00690          N2=NX
00700          DO 44 I=1,N2M1
00710      44 PP(I)=RPX(I)
00720          GO TO 49
00730      48 PRINT 1030
00740          READ(1),N2,(Y(I),I=1,N2)
00750          PRINT 1015
00760          N2M1=N2-1
00770          READ(1),(PP(I),I=1,N2M1)
00780      49 PRINT 2020
00790          READ(1),IY
791 PRINT3040,IY
00800          IF(IYES-IY)100,50,100
00810      50 PRINT 2000
00820          READ(1),M,(Z(I),I=1,M)
00830      100 CALL ADDER(N1M1,N2M1,M,ICODE)
00840          LCODE=ICODE
00850          MT=M
00860      155 MT=MT-1
00870          IF(RP(MT))156,156,157
00880      156 IF(MT-1)157,157,155
00890      157 JM1=MT
00900          T=R=CM=0.
00910          IF(LSD-12)130,120,120
00920      120 DO 125 I=1,JM1
```

F260 CONTINUED

```
00930      T=T+RP(I)
00940      R=R+S(I)
00950      S(I)=RP(I)
00960      D=ABSF(T-R)
00970      IF(D-CM)125,125,122
00980      122 CM=D
00990      125 CONTINUE
01000      PRINT 2060,CM
01010      130 PRINT 2080
01020      READ(1),IY
1021 PRINT 3040,IY
01030      IF(IYES-IY)135,137,135
01040      135 LX=2
01050      GO TO 140
01060      137 PRINT 1060
01070      PRINT 1080
01080      LX=1
01090      140 T=T1=T2=T3=T4=0.
01100      DO 200 I=1,JM1
01110      PQ=RP(I)
01120      XQ=Z(I)+(Z(I+1)-Z(I))/2.
01130      T=T+PQ
01140      S(I)=PQ
01150      T1=T1+XQ*PQ
01160      T2=T2+PQ*XQ**2
01170      T3=T3+PQ*XQ**3
01180      T4=T4+PQ*XQ**4
01190      GO TO (160,200),LX
1200      160 PRINT,Z(I),Z(I+1),RP(I)
01210      200 CONTINUE
01220      PRINT 1070,T
01230      C2=T2-T1*T1
01240      C3=T3-3.*T2*T1+2.*T1**3
01250      C4=T4-4.*T3*T1+6.*T2*T1**2-3.*T1**4
01260      C3N=C3/C2**1.5
01270      C4N=C4/C2**2
01280      PRINT 3000,T1,C2,C3N,C4N
01290      GO TO 15
01300      END
1310 $USE F260A
```

F260A

```

00000C*****PROB5 SEGMENT*****
00010      SUBROUTINE LOAD(TPR,ZL,ZH,M,Z,RP)
00020      COMMON X(100),Y(200),Z(100),P(200),PP(200),RP(100),S(100)
00030      COMMON ZX(100),RPX(100),NX
00040      SP=ZH-ZL
00050      IF(SP)20,80,20
00060      20 DO 30 JL=2,M
00070          IF(Z(JL)-ZL)30,30,25
00080      25 ZLOW=ZL
00090          JTEMP=JL
00100          GO TO 40
00110      30 CONTINUE
00120      40 CONTINUE
00130          DO 60 J=JTEMP,M
00140          IF(Z(J)-ZH)50,45,45
00150      45 JSAVE=J
00160          ZHIGH=ZH
00170          GO TO 70
00180      50 ZHIGH=Z(J)
00190          RP(J-1)=RP(J-1)+((ZHIGH-ZLOW)/SP)*TPR
00200          ZLOW=Z(J)
00210      60 CONTINUE
00220      70 RP(JSAVE-1)=RP(JSAVE-1)+((ZHIGH-ZLOW)/SP)*TPR
00230          GO TO 100
00240      80 DO 90 J=2,M
00250          IF(ZL-Z(J-1))85,82,85
00260      82 RP(J-1)=RP(J-1)+TPR
00270          JSAVE=J
00280          GO TO 100
00290      85 IF(ZL-Z(J))82,90,90
00300      90 CONTINUE
00310          RP(M-1)=RP(M-1)+TPR
00320          JSAVE=M
00330 100 CONTINUE
00340      200 RETURN
00350          END
00360      SUBROUTINE HALF(N,A)
00370          DIMENSION A(1)
00380          LX=2*N-1
00390          LY=N
00400          DO 20 I=1,N
00410              A(LX)=A(LY)
00420              LX=LX-2
00430              LY=LY-1
00440      20 CONTINUE
00450          LIM=2*N-3
00460          DO 30 I=1,LIM,2
00470      30 A(I+1)=A(I)+(A(I+2)-A(I))/2.
00480          N=2*N-1
00490          RETURN

```

F260A CONTINUED

```
00500      END
00510      SUBROUTINE PHALF(N,A)
00520      DIMENSION A(1)
00530      DO 20 I=1,N
00540      A(I)=A(I)/2.
00550      20 A(I+N)=A(I)
00560      N=2*N
00570      RETURN
00580      END
590 $USE F260B
```

```

00000C*****PROB6 SEGMENT*****
00010      SUBROUTINE ADDER(N1M1,N2M1,M,ICODE)
00020      COMMON X(100),Y(200),Z(100),P(200),PP(200),RP(100),S(100)
00030      COMMON ZX(100),RPX(100),NX
00040      GO TO (1,1,1,1,1,1,1,1,1,1,1,220),ICODE
00050      1 DO 5 I=1,M
00060      5 RP(I-1)=0.
00070      DO 48 K=1,N1M1
00080      DO 48 I=1,N2M1
00090      GO TO (8,8,8,8,800,800,800,800,800,800),ICODE
00100      8 CONTINUE
00110      GO TO (10,20,30,40),ICODE
00120      10 Q1=X(K)+Y(I)
00130      Q2=X(K+1)+Y(I+1)
00140      Q3=X(K)+Y(I+1)
00150      Q4=X(K+1)+Y(I)
00160      GO TO 45
00170      20 Q1=X(K)-Y(I)
00180      Q2=X(K+1)-Y(I+1)
00190      Q3=X(K)-Y(I+1)
00200      Q4=X(K+1)-Y(I)
00210      GO TO 45
00220      30 Q1=X(K)*Y(I)
00230      Q2=X(K+1)*Y(I+1)
00240      Q3=X(K)*Y(I+1)
00250      Q4=X(K+1)*Y(I)
00260      GO TO 45
00270      40 Q1=X(K)/Y(I)
00280      Q2=X(K+1)/Y(I+1)
00290      Q3=X(K)/Y(I+1)
00300      Q4=X(K+1)/Y(I)
00310      45 ZL=MIN1F(Q1,Q2,Q3,Q4)
00320      ZH=MAX1F(Q1,Q2,Q3,Q4)
00330      TPR=P(K)*PP(I)
00340      CALL LOAD(TPR,ZL,ZH,M,Z,RP)
00350      48 CONTINUE
00360      RETURN
00370      800 CONTINUE
00380      GO TO (49,49,49,49,500,500,49,49,49,49),ICODE
00390      500 PRINT 5000
00400      5000 FORMAT(/" READ CONSTANT")
00410      READ(1),C;PRINT,C
00420      49 DO 200 I=1,N1M1
00430      GO TO (200,200,200,200,50,60,70,80,90,100),ICODE
00440      50 Q1=C*X(I)
00450      Q2=C*X(I+1)
00460      GO TO 150
00470      60 Q1=X(I)**C
00480      Q2=X(I+1)**C
00490      GO TO 150

```


F260B CONTINUED

```
00500      70 Q1=SINF(X(I))
00510          Q2=SINF(X(I+1))
00520          GO TO 150
00530      80 Q1=COSE(X(I))
00540          Q2=COSE(X(I+1))
00550          GO TO 150
00560      90 Q1=LOGF(X(I))
00570          Q2=LOGF(X(I+1))
00590     100 Q1=EXPF(X(I))
00600          Q2=EXPF(X(I+1))
00610     150 ZL=MIN1F(Q1,Q2)
00620          ZH=MAX1F(Q1,Q2)
00630          TPR=P(I)
00640          CALL LOAD(TPR,ZL,ZH,M,Z,RP)
00650     200 CONTINUE
00660          RETURN
00670     220 DO 230 I=1,M
00680     230 ZX(I)=Z(I)
685      JM1=M-1
00690          DO 240 I=1,JM1
00700     240 RPX(I)=RP(I)
705      NX=M
00710          RETURN
00720          END
```

REL FM 1

```

01 PRINT "HØØP STRESS FAIL MØDE FWD CYL SECT, FM-1, MØTØR CASE"
02 PRINT "9/10 ØF TIME"
03 PRINT "STANDARD RUN"
04 REM THIS IS BASIC PRØG : EDI WEAVE REL AND FM1, AND IS BASIC
05 REM PRØGMS FØR REL FM1, REL FMX, REL FM4, REL FMY
10 DIM A(2,22), B(2,22), C(2,22), S(2,22)
20 H=1
30 READ M1#READ S1#READ W1#READ N1
35 P=0
40 A(1,1)=M1-N1*W1
50 FØR I=2 TØ 21
60 A(1,I)=A(1,I-1)+W1
70 A=(.3989423/S1)*W1
80 A1=(-((A(1,I)-(W1/2)-M1)+2)/(2*(S1+2)))
90 A(2,I-1)=A*EXP(A1)
95 P=P+A(2,I-1)
100 NEXT I
101 FØR I=1 TØ 20
102 A(2,I)=A(2,I)/P
103 NEXT I
110 READ M2#READ S2#READ W2#READ N2
115 P=0
120 B(1,1)=M2-N2*W2
130 FØR I=2 TØ 21
140 B(1,I)=B(1,I-1)+W2
150 B=(.3989423/S2)*W2
160 B1=(-((B(1,I)-(W2/2)-M2)+2)/(2*(S2+2)))
170 B(2,I-1)=B*EXP(B1)
175 P=P+B(2,I-1)
180 NEXT I
181 FØR I=1 TØ 20
182 B(2,I)=B(2,I)/P
183 NEXT I
190 N3=20
200 GØ SUB 3000
220 W=(U-L)/N3
230 C(1,1)=L
240 FØR I=2 TØ N3+1
250 C(1,I)=C(1,I-1)+W
255 C(2,I-1)=0
260 NEXT I
270 FØR J=2 TØ 21
280 FØR K=2 TØ 21
290 GØ SUB 2000
300 NEXT K
310 NEXT J
315 GØ SUB 2005
320 GØ TØ (330,390,500) G
330 FØR I=1 TØ N3+1
340 A(1,I)=C(1,I)

```

REL FM1 CONTINUED

```

350 A(2,I)=C(2,I)
360 NEXT I
370 IF F=0 THEN 445
375 IF F<0 THEN 4000
380 H=H+1
385 GO TO 110
390 FOR I=1 TO N3+1
400 S(1,I)=C(1,I)
410 S(2,I)=C(2,I)
420 NEXT I
430 H=H+1
440 GO TO 30
445 FOR I=1 TO N3+1
450 B(1,I)=S(1,I)
460 B(2,I)=S(2,I)
470 NEXT I
480 H=H+1
490 GO TO 190
500 P=0
510 FOR I=1 TO N3
520 P=P+C(2,I)
530 NEXT I
540 PRINT P
545 FOR I=1 TO 5
550 PRINT#PRINT#PRINT
555 NEXT I
560 S1=5#S2=20#S3=45
570 PRINT TAB(S1);"FROM";TAB(S2);"TO";TAB(S3);"PR0B"
580 FOR I=1 TO 60 STEP 3
590 PRINT TAB(I);"***";
600 NEXT I
610 PRINT " "#PRINT
620 S4=5#S5=20#S6=45
625 PRINT TAB(S4-1);"<";C(1,1);TAB(S5);C(1,1);TAB(S6);C(2,0)
630 FOR I=1 TO N3
640 PRINT TAB(S4);C(1,I);TAB(S5);C(1,I+1);TAB(S6);C(2,I)
650 NEXT I
652 PRINT TAB(S4);C(1,N3+1);TAB(S5-1);">";C(1,N3+1);TAB(S6);C(2,N3+1)
655 PRINT#PRINT#PRINT
660 P=0
670 I=1
680 IF C(1,I)<0 THEN 700
690 GO TO 760
700 IF C(1,I+1)<0 THEN 730
710 P=P+(-C(1,I)/(C(1,I+1)-C(1,I)))*C(2,I)
720 GO TO 760
730 P=P+C(2,I)
740 I=I+1
750 GO TO 680
760 PRINT "P(F)=";P

```

REL FM1 CONTINUED

```

770 END
1000 N=(N3/2)+1
1010 IF Z<C(1,N) THEN 1040
1020 N=N+5
1030 GO TO 1060
1040 N=N-5
1050 GO TO 1110
1060 FOR I=1 TO ((N3/10)-1)
1070 IF Z<C(1,N) THEN 1160
1080 N=N+5
1090 NEXT I
1100 GO TO 1160
1110 FOR I=1 TO ((N3/10)-1)
1120 IF Z>C(1,N) THEN 1180
1130 N=N-5
1140 NEXT I
1145 IF Z<C(1,N) THEN 1230
1150 GO TO 1180
1160 N=N-4
1170 GO TO 1190
1180 N=N+1
1190 FOR I=1 TO 5
1200 IF Z<C(1,N) THEN 1230
1210 N=N+1
1220 NEXT I
1230 C(2,N-1)=C(2,N-1)+A(2,J-1)*B(2,K-1)
1240 RETURN
2000 GO TO (2010,2010,2050,2010,2050,2010,2050,2010,2050,2010,2210) H
2005 GO TO (2020,2040,2020,2020,2020,2020,2020,2020,2020,2180,2200,2220) H
2010 Z=(A(1,J-1)+A(1,J))*(B(1,K-1)+B(1,K))/4
2015 GO TO 1000
2020 G=1#F=1
2025 RETURN
2040 G=2#F=1
2045 RETURN
2050 Z=(A(1,J-1)+A(1,J))/(B(1,K-1)+B(1,K))
2055 GO TO 1000
2180 G=1#F=-1
2185 RETURN
2200 G=1#F=0
2205 RETURN
2210 Z=(-A(1,J-1)-A(1,J)+B(1,K-1)+B(1,K))/2
2215 GO TO 1000
2220 G=3
2225 RETURN
3000 GO TO (3010,3010,3050,3010,3050,3010,3050,3010,3050,3010,3210) H
3010 L=A(1,1)*B(1,1)#U=A(1,21)*B(1,21)
3020 RETURN
3050 L=A(1,1)/B(1,21)#U=A(1,21)/B(1,1)
3060 RETURN

```

REL FM 1 CONTINUED

```

3210 L=-A(1,21)+B(1,1)#U=-A(1,1)+B(1,21)
3220 RETURN
4000 READ M2#READ S2#READ W2#READ N2
4010 B(1,1)=M2-N2*W2
4020 FOR I=2 TO 2*N2+1
4030 B(1,I)=B(1,I-1)+W2
4040 B=(.3989423/S2)*W2
4050 B1=(-((B(1,I)-(W2/2)-M2)+2)/(2*(S2+2)))
4060 B(2,I-1)=B*EXP(B1)
4070 NEXT I
4090 C=20
4100 FOR I=1 TO 2*N2+1
4110 B(1,I)=EXP(B(1,I)*C)
4120 NEXT I
4130 H=H+1#GO TO 190
5010 DATA 232000,2516.6,1258.3,10
5020 DATA .95845,.00693,.003465,10
5030 DATA 1.106,.0312,.0156,10
5040 DATA 3.4E6,6120,3060,10
5050 DATA 6.2477E-3,1.9E-5,9.5E-6,10
5060 DATA .606,.00818,.00409,10
5070 DATA 6355,20.9,10.45,10
5080 DATA 1.18,.00897,.004485,10
5090 DATA 85,.17,.085,10
5100 DATA 130.631,.0261,.01305,10
5110 DATA .6392,.0095,.00475,10
5120 DATA .0016,6.676E-5,3.38E-5,10

```

APPENDIX VI

THE NATURE OF THE MATHEMATICS
INVOLVED IN ANALYTICAL
MODELING USING TRANSFORMATIONS
OF STOCHASTIC VARIABLES

Introduction

The mathematical theory involved in the analytical modeling of system characteristics is essentially described by the title "transformations of stochastic variables". Of course these transformations are identical to those involved in the determination of volumes by integration, an obvious fact when it is recalled that probabilities are themselves integrals of density functions. We will first describe the process in the general language of the calculus and then translate it into the transfer function terminology of modeling analysis. Proofs will be omitted since they are available in standard mathematics books. We will write the relationships in terms of three variables—the extension to more (or less) than three is obvious.

Consider the volume differential of a function of three variables,

$$f(x, y, z) dx dy dz.$$

Let the variables u , v , and w be related to x , y , and z by the transformation functions

$$x = g_x(u, v, w),$$

$$y = g_y(u, v, w),$$

$$z = g_z(u, v, w).$$

We wish to transform the volume differential into the form

$$h(u, v, w) du dv dw .$$

The transformation is given by the expression

$$\begin{aligned} & h(u, v, w) du dv dw \\ & = f\left(g_x(u, v, w), g_y(u, v, w), g_z(u, v, w)\right) |J| du dv dw \end{aligned}$$

where

$$J = \begin{vmatrix} \frac{\partial x}{\partial u} & \frac{\partial x}{\partial v} & \frac{\partial x}{\partial w} \\ \frac{\partial y}{\partial u} & \frac{\partial y}{\partial v} & \frac{\partial y}{\partial w} \\ \frac{\partial z}{\partial u} & \frac{\partial z}{\partial v} & \frac{\partial z}{\partial w} \end{vmatrix}$$

Note that we take the absolute value of the determinant J, the Jacobian or functional determinant of the transformation of x, y, z into u, v, w. Naturally we will wish to express the determinant in terms of the new variables, u, v, and w. In some cases, we may find it simpler to compute J from the relationship

$$J^{-1} = \begin{vmatrix} \frac{\partial u}{\partial x} & \frac{\partial u}{\partial y} & \frac{\partial u}{\partial z} \\ \frac{\partial v}{\partial x} & \frac{\partial v}{\partial y} & \frac{\partial v}{\partial z} \\ \frac{\partial w}{\partial x} & \frac{\partial w}{\partial y} & \frac{\partial w}{\partial z} \end{vmatrix}$$

We shall consider only transformations for which $J \neq 0$ -we exclude the case of singular transformations for which J does vanish.

Let us now express this theory in the language of modeling analysis. We shall call the analytical representation of the model by the common engineering term "transfer function". Let the stochastic variables x, y, and z be the input parameters of the transfer function of interest, and, as before, denote the joint density of these parameters by $f(x, y, z)$. Let the transfer function itself be denoted by $T_1(x, y, z)$ and define the new variables u, v, and w by the relationships

$$\begin{aligned} u &= T_1(x, y, z) \\ v &= T_2(x, y, z) \\ w &= T_3(x, y, z) \end{aligned}$$

where T_2 and T_3 are essentially arbitrary, except for the condition that the Jacobian of the transformation be non-zero. We often set v and w equal to two of the original variables for this reduces the Jacobian to a simple partial derivative with respect to the other original variable. Solve these three equations for x , y , and z , giving the transformation in the form

$$\begin{aligned}x &= g_x(u, v, w), \\y &= g_y(u, v, w), \\z &= g_z(u, v, w).\end{aligned}$$

The joint density of u , v , and w in differential form is then given by the previously indicated relationship

$$\begin{aligned}h(u, v, w) du dv dw \\= f(g_x(u, v, w), g_y(u, v, w), g_z(u, v, w)) |J| du dv dw.\end{aligned}$$

Now we are actually interested only in the density of u , the variables v and w entering merely to permit us to define the complete transformation and we eliminate the two variables by intergration. The density of u is then obtained by carrying out this integration and by dropping du , giving

$$\int_{w_1}^{w_2} \int_{v_1}^{v_2} h(u, v, w) dv dw$$

The integration limits are chosen in the usual way as described in the calculus. This theory will be clarified by applying it to some specific examples in which we consider a number of different transfer and density function combinations.

It should be observed that there are other mathematical procedures for deriving densities of the transformations of stochastic variables. For example, a number of such transformations are accomplished through the use of Mellin transforms in a very fine report by M. D. Springer and W. E. Thompson, G. M. Defense Research Laboratories, TR 64-46, August 1964 entitled "The Distribution of Products of

Independent Random Variables". However, it was decided to restrict our discussion to cases for which we could apply the simple methods described above. Where this is not possible, we can rely on the work of Springer and Thompson as will be noted.

Some Examples of Transformations of Discrete Stochastic Variables.

Let x and y be two stochastic variables with probability density functions $p(x)$ and $p(y)$ respectively as indicated below*.

x	$p(x)$
1	.3
2	.5
3	.2

y	$p(y)$
1	.3
2	.4
3	.2
4	.1

Densities of the reciprocal and the square of each variable are obtained merely by performing the variable transformations and leaving the probabilities unchanged. This gives the following four densities.

$\frac{1}{x}$	x^2	$p(\frac{1}{x}) = p(x^2)$
1	1	.3
1/2	4	.5
1/3	9	.2

$\frac{1}{y}$	y^2	$p(\frac{1}{y}) = p(y^2)$
1	1	.3
1/2	4	.4
1/3	9	.2
1/4	16	.1

We will now derive densities of four functions of the two variables to illustrate how we combine the variables and compute the associated probabilities. The selected functions are $x + y$, $x - y$, xy , and x/y . The detailed computations are shown below and it should be noted that these four suffice to illustrate how one could handle any other function of the two variables and also how we could extend the technique to more variables. It should be mentioned that we are assuming independence of x and y . The extension to the dependent case will be commented upon later. The basic computations are summarized in Table 6.1.

* The density function notation as used here is really the usual probability symbolism. Thus, $p(x)$ is the probability associated with the event identified by the value of the variable x . We can think in terms of all possible x values or of a specific value—the meaning is always clear in context. Hence, the use of $p(x)$ and $p(y)$ in our discussion does not imply identity of the densities.

Table VI. 1.

y	p(y)	x p(x)	1 .3	2 .5	3 .2
1	.3	p(x, y)	.09	.15	.06
		x+y	2	3	4
		x-y	0	1	2
		xy	1	2	3
		x/y	1	2	3
2	.4	p(x, y)	.12	.20	.08
		x+y	3	4	5
		x-y	-1	0	1
		xy	2	4	6
		x/y	1/2	1	3/2
3	.2	p(x, y)	.06	.10	.04
		x+y	4	5	6
		x-y	-2	-1	0
		xy	3	6	9
		x/y	1/3	2/3	1
4	.1	p(x, y)	.03	.05	.02
		x+y	5	6	7
		x-y	-3	-2	-1
		xy	4	8	12
		x/y	1/4	1/2	3/4

For each possible pair of x and y values, Table VI. 1 shows the values of five different items:

- (1) The probability of the x, y pair which, by virtue of their independence, is merely the product of their respective probabilities,
- (2) $x + y$,
- (3) $x - y$,

(4) xy , and

(5) x/y .

For example, let $x = 3$ and $y = 2$. We have

$$p(x=3, y=2) = p(x=3) p(y=2)$$

$$= (.2)(.4) = .08$$

$$x + y = 3 + 2 = 5$$

$$x - y = 3 - 2 = 1$$

$$xy = (3)(2) = 6$$

$$x/y = 3/2.$$

Now to find the density functions of interest, we must add probabilities associated with all of the ways of obtaining each function value. For example,

$$p(x - y = 1) = p(x = 2, y = 1) + p(x = 3, y = 2)$$

$$= .15 + .08$$

$$= .23$$

All such additions are shown in Table VI.2, the values being read directly from Table VI.1.

It is obvious that the case of dependence between variables x and y can be handled quite easily. The computational procedure requires the calculation of the joint probability of each possible x, y pair, this probability then being associated with the corresponding value of the function of the pair—the $x + y$, $x - y$, or whatever it might be. Thus, we would use the conditional probability formula

$$p(x, y) = p(x) p(y|x)$$

which expresses the probability of the joint occurrence of x and y as the product of the probability of x and the probability of y , given the occurrence of x .

Table VI. 2.

$x + y$	Density	
2	.09	= .09
3	.15 + .12	= .27
4	.06 + .20 + .06	= .32
5	.08 + .10 + .03	= .21
6	.04 + .05	= .09
7	.02	= .02

$x - y$	Density	
-3	.03	= .03
-2	.06 + .05	= .11
-1	.12 + .10 + .02	= .24
0	.09 + .20 + .04	= .33
1	.15 + .08	= .23
2	.06	= .06

xy	Density	
1	.09	= .09
2	.15 + .12	= .27
3	.06 + .06	= .12
4	.20 + .03	= .23
6	.08 + .10	= .18
8	.05	= .05
9	.04	= .04
12	.02	= .02

x/y	Density	
1/4	.03	= .03
1/3	.06	= .06
1/2	.12 + .05	= .17
2/3	.10	= .10
3/4	.02	= .02
1	.09 + .20 + .04	= .33
3/2	.08	= .08
2	.15	= .15
3	.06	= .06

Continuous Stochastic Variable.

Transformations and Functions to be Considered

We will consider in some detail six transformations of input stochastic variables which are described by four different density function types. These transformations and functions are as follows:

Transformations

Applied to a single variable:

Reciprocal
Power

Applied to a pair of variables

Sum
Difference
Product
Quotient

Density Functions of Input Variables

Rectangular
Gaussian
Gamma
Cauchy

In discussing transformations of pairs of variables we will restrict our treatment to the case in which the same density type applies to each variable of the pair. We will further restrict ourselves to the case in which the variables of the pair are independent.

The expressions for these four density function types are as follows, the function parameters being subject to the usual restrictions.

Table VI. 3.

Name	Density Function $f(x)$	Range of Variable x
Rectangular	$1/a$ 0	$0 \leq x \leq a$ $x < 0, x > a$
Gaussian	$\frac{1}{\sqrt{2\pi}\sigma} e^{-\frac{(x-\bar{x})^2}{2\sigma^2}}$	$-\infty < x < \infty$
Gamma	$\frac{1}{\Gamma(\alpha+1)\beta^{\alpha+1}} x^\alpha e^{-x/\beta}$ 0	$x \geq 0$ $x < 0$
Cauchy	$\frac{a}{\pi(a^2 + x^2)}$	$-\infty < x < \infty$

Note: For simplicity and consistent with the usage of many authors, we have adopted the functional symbol, $f(x)$, as a general identification of the density function of an input stochastic variable. It will be seen that this is a convenient symbolism and that it will cause no problem—the meaning of $f(x)$ will be clear in context. When treating more than one density in a particular derivation, appropriate modification of the symbol will be made.

Transformations Involving Only One Stochastic Variable

Consider the stochastic variable, x , with density $f(x)$ and the transformation of the variable defined by

$$T(x) = x^n$$

We are especially interested in two values of the exponent: $n = -1$ which gives the reciprocal and $n = 2$ which gives the square.

Denote the new variable by u_n . Then

$$u_n = x^n \quad \text{or} \quad x = u_n^{1/n} .$$

The Jacobian reduces to a single derivative in the one variable case. It is

$$J = \frac{dx}{du_n} = \frac{1}{n} u_n^{\frac{1-n}{n}} .$$

Therefore the differential form of the density of u_n is

$$f(u_n^{1/n}) \left| \frac{1}{n} u_n^{\frac{1-n}{n}} \right| du_n .$$

The density function is obtained here by merely dropping the differential since there are no variables to eliminate by integration.

For the two cases of interest we will use the following notation. For the reciprocal, $n = -1$, we will replace u_{-1} by y and we will denote the density of y by $g(y)$. Then

$$\begin{aligned} g(y) &= f(y^{-1}) \left| -y^{-2} \right| \\ &= y^{-2} f(y^{-1}) . \end{aligned}$$

For the square, we will replace u_2 by z and we will represent the density of z by $h(z)$. Then

$$\begin{aligned} h(z) &= f(z^{1/2}) \left| \frac{1}{2} z^{-1/2} \right| \\ &= \frac{1}{2} z^{-1/2} f(z^{1/2}) . \end{aligned}$$

A warning is appropriate at this point. Care must be exercised in the use of these formulas to take proper account of signs and variable ranges. This is of course a repetition of our experience in the calculus when these same problems were encountered. We can expect them to occur again in the treatment of transformations involving

two variables where we will also have the problems associated with determining limits of integration. The specific derivations to be included herein will illustrate how we handle these complications.

The Density of the Reciprocal of a Stochastic Variable for the Four Functions. Using the formulas derived above, we can immediately write the density of the reciprocal of the stochastic variable for each of the four functions. They are as follows.

Rectangular:

$$g(y) = \frac{1}{ay^2} , \frac{1}{a} \leq y < \infty$$

$$= 0 \quad y < \frac{1}{a}$$

Gaussian:

$$g(y) = y^{-2} (\sqrt{2\pi} \sigma)^{-1} e^{-\frac{(y^{-1} - \bar{x})^2}{2\sigma^2}} , -\infty < y < \infty .$$

Gamma:

$$g(y) = \frac{1}{\Gamma(\alpha+1) \beta^{\alpha+1}} y^{-2-\alpha} e^{-1/\beta y} , 0 \leq y < \infty$$

Cauchy:

$$g(y) = \frac{a y^{-2}}{\pi(a^2 + y^{-2})}$$

$$= \frac{a}{\pi(a^2 y^2 + 1)} , -\infty < y < \infty .$$

Certain aspects of the variable ranges should be noted. Of course y decreases as x increases, thus generating an inversion and the negative and positive portions of the x range required separate treatment. The following range relationships apply.

x range	Corresponding y range (not reversed)
0 to a	∞ to $1/a$
$-\infty$ to 0	0 to $-\infty$
0 to ∞	∞ to 0

Note the two transforms of the limit where $x = 0$. As we go to zero through negative values of x , y approaches $-\infty$ while on the positive x side, y approaches $+\infty$. The first of the three listed intervals applies to the rectangular density, the second and third combine to give the ranges for the Gaussian and the Cauchy densities, and the third one by itself applies to the Gamma density.

The discussion of the four reciprocal densities will be delayed until later. However, we do wish to make one observation. In the Cauchy density, if we set $a = 1$, it turns out that the density of y is exactly the same as the density of x , a rather interesting relationship which has implications on the densities of products and quotients of Cauchy variables as we will see.

The Density of the Square of a Stochastic Variable For the Four Functions. The transformation formulas for the square of the stochastic variable x , with density $f(x)$, as derived above are

$$z = x^2, \quad x = z^{1/2}$$

$$h(z) = \frac{1}{2} z^{-1/2} f(z^{1/2}).$$

However, we must take heed of the warning which followed the derivation of the function $h(z)$ regarding the correct procedure for handling ranges over which x is negative. The method is, of course, to modify the above equations by using the absolute value of x . Thus, let

$$|x| = z^{1/2}$$

which merely says

$$-x = z^{1/2} \text{ for } -\infty < x \leq 0,$$

$$x = z^{1/2} \text{ for } 0 \leq x < \infty$$

In practice, it is usually convenient to apply the sign change on x over the negative range to modify the density $f(x)$ before applying the square transformation, thus eliminating all negative x values. This will be illustrated in the examples given below.

First, let us look at a very simple density not discussed previously as an illustration of the sign change method.

Let $f(x) = \frac{1}{8}(x + 1)$, $-1 \leq x \leq 3$. This is the triangular density in Figure VI.1.

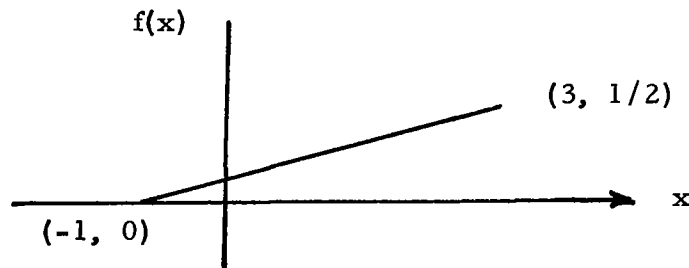


Figure VI.1

Transforming the portion for the negative values of x gives

$$f(-x) = \frac{1}{8}(-x + 1)$$

with new range $0 \leq x \leq 1$. Hence, for this range, we have

$$\frac{1}{8}(-x + 1) + \frac{1}{8}(x + 1) = \frac{1}{4}, \quad 0 \leq x \leq 1$$

and for the remaining range, we have

$$\frac{1}{8}(x+1), \quad 1 \leq x \leq 3.$$

The graph of this transformed x density is shown in Figure VI.2, the added increment being the shaded portion

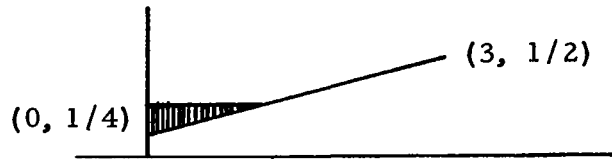


Figure VI.2

We can now write the density of $h(z)$ by applying the previously derived transformation formulas. Thus, we have

$$h(z) = \frac{1}{8} z^{-1/2}, \quad 0 \leq z \leq 1,$$

$$h(z) = \frac{1}{16} \frac{z^{1/2} + 1}{z^{1/2}} = \frac{1}{16} (1 + z^{-1/2}), \quad 1 \leq z \leq 9.$$

The range computations are quite direct. As x goes from 0 to 1, so also does z and as x goes from 1 to 3, $z = x^2$ goes from 1 to 9.

For the rectangular density, we expressed the function over a positive range on x as

$$f(x) = \frac{1}{a}, \quad 0 \leq x \leq a.$$

Hence we can write the square transformation immediately as

$$h(z) = \frac{1}{2a} z^{-1/2}, \quad 0 \leq z \leq a^2.$$

We again encounter the negative x problem in deriving the density of the square where x has a Gaussian distribution. This is handled again by the transformation of the $f(x)$ density for the negative range on x . Thus, for

$$f(x) = \frac{1}{\sqrt{2\pi}\sigma} e^{-\frac{(x - \bar{x})^2}{2\sigma^2}}$$

over the range $-\infty < x < 0$, we will replace x by $-x$, giving

$$\frac{1}{\sqrt{2\pi}\sigma} e^{-\frac{(x + \bar{x})^2}{2\sigma^2}}$$

where x now ranges from 0 to $+\infty$. We replaced $(-x - \bar{x})^2$ by its equivalent, $(x + \bar{x})^2$ to simplify the exponent. It is now possible to express the complete density by adding this transform to the original density over the positive x range, giving the function

$$f^*(x) = \frac{1}{\sqrt{2\pi}\sigma} \left[e^{-\frac{(x + \bar{x})^2}{2\sigma^2}} + e^{-\frac{(x - \bar{x})^2}{2\sigma^2}} \right], 0 \leq x < \infty.$$

We can now apply the $z = x^2$ transformation directly to this new function, giving, for the Gaussian case,

$$h(z) = \frac{1}{2\sqrt{2\pi}\sigma} z^{-1/2} \left[e^{-\frac{(z^{1/2} + \bar{x})^2}{2\sigma^2}} + e^{-\frac{(z^{1/2} - \bar{x})^2}{2\sigma^2}} \right], 0 \leq z < \infty.$$

It is interesting to note the simplification which occurs if $\bar{x} = 0$. Then we have

$$h(z) = \frac{1}{\sqrt{2\pi}\sigma} z^{-1/2} e^{-z/2\sigma^2}, 0 \leq z < \infty.$$

This case of the zero mean illustrates the situation in which $f(x)$ is symmetrical about the origin and the transform on the negative x range merely changes

$$f(x) , -\infty < x < \infty$$

into

$$2f(x) , 0 \leq x < \infty .$$

Naturally, if the original range had been finite, say $-c$ to $+c$, then the transformed x density would have been defined over the positive portion $0 \leq x \leq c$. We will encounter another symmetrical case when we treat the Cauchy distribution.

It is useful to observe that the distribution of x for the symmetrical Gaussian density is actually the well-known χ^2 density,

$$\frac{1}{2^{n/2} \Gamma(\frac{n}{2})} e^{-\chi^2/2} (\chi^2)^{\frac{n-2}{2}} d\chi^2$$

where $n = 1$. We wrote the differential form of the density to permit us to transform from the variable χ^2 to the variable z to establish the equivalence of these functions. Thus, let $n = 1$ and let

$$\chi^2 = z/\sigma^2 .$$

This gives

$$d\chi^2 = \frac{1}{\sigma^2} dz .$$

Substituting in the χ^2 density, we have

$$\begin{aligned} & \frac{1}{2^{1/2} \Gamma(\frac{1}{2})} e^{-z/2\sigma^2} \left(\frac{z}{\sigma^2}\right)^{-1/2} \frac{1}{\sigma^2} dz \\ &= \frac{1}{\sqrt{2\pi}\sigma} z^{-1/2} e^{-z/2\sigma^2} dz , \end{aligned}$$

thereby checking the relationship stated above.

The Gamma density was defined for $x \geq 0$ so the density of $z = x^2$ can be written immediately. It is

$$h(z) = \frac{1}{2 \Gamma(\alpha + 1) \beta^{\alpha + 1}} z^{\frac{\alpha - 1}{2}} e^{-z/\beta}, \quad 0 \leq z < \infty.$$

For the Cauchy distribution, we merely double the density on the positive portion of the x range to reflect the symmetrical negative portion, giving

$$f^*(x) = \frac{2a}{\pi(a^2 + x^2)}, \quad 0 \leq x < \infty.$$

The density of $z = x^2$ is then given as

$$h(z) = \frac{a}{\pi z^{1/2}(a^2 + z)}, \quad 0 \leq z < \infty.$$

Densities of Sums and Differences of Stochastic Variables

For these transformations we can restrict the discussion to only two variables since this is immediately extendible to more than two by adding variables one at a time. Furthermore, subtraction need not be discussed separately since every difference can be expressed as a sum: i. e., $x - y = x + (-y)$.

We will use the following notation. Let x and y be the two variables with densities $f_1(x)$ and $f_2(y)$ respectively. Let $w = x + y$ and let $f(w)$ denote the density* of w . The basic formula is

*Since we are using subscripts on the symbols for the densities of x and y , the symbol $f(w)$ is available for the density of the sum, $w = x + y$. Repetitive use of a symbol when properly described should be acceptable.

$$f(w) = \int_{x_1}^{x_2} f_1(x) f_2(w-x) dx$$

where the limits of integration are the bounds on x for fixed w . The determination of these limits will be illustrated in the examples included herein. This is the same as the transformation

$$w = x + y, \quad v = x$$

which has a Jacobian equal to unity. We chose here not to replace x by v , a common practice in such simple cases.

In deriving the density function of the sum of two variables each of which has a uniform or rectangular density, we encounter a good illustration of the complexities which sometimes arise from finite variable ranges. Let the two input densities be

$$f_1(x) = \frac{1}{a}, \quad 0 \leq x \leq a,$$

$$f_2(y) = \frac{1}{b}, \quad 0 \leq y \leq b.$$

Without loss of generality, we can let $a > b$. (Later we will treat the case $a = b$.) The density of $w = x + y$ is given by

$$f(w) = \int_{x_1}^{x_2} \frac{1}{ab} dx = \frac{1}{ab} (x_2 - x_1)$$

but there are complications in computing x_1 and x_2 . We can explain them by reference to Figure VI.3.

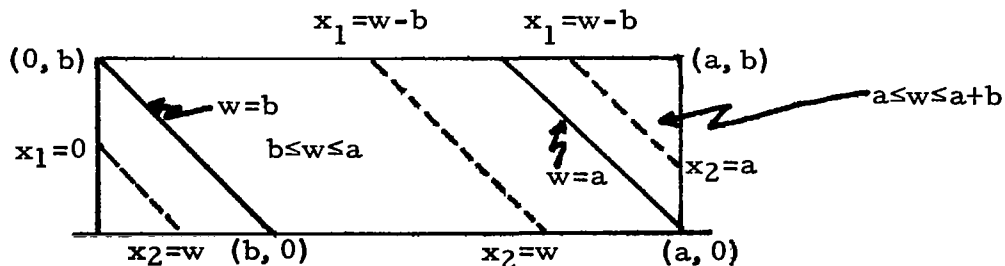


Figure VI.3

The w range is broken into three intervals

$$0 \leq w \leq b, \quad b \leq w \leq a, \quad \text{and} \quad a \leq w \leq a + b .$$

For fixed w , $x + y = w$ is a straight line of slope negative one. The solid lines $w = b$ and $w = a$ separate the three areas of interest. The dotted lines are used to determine the x_1 and x_2 values in these ranges. It is apparent from the figure just why we must treat the intervals separately. Substituting the limits in the formula

$$f(w) = \frac{1}{ab} (x_2 - x_1)$$

gives

$$f(w) = \frac{1}{ab} w, \quad 0 \leq w \leq b$$

$$= \frac{1}{ab} b = \frac{1}{a}, \quad b \leq w \leq a$$

$$= \frac{1}{ab} (a + b - w), \quad a \leq w \leq a + b .$$

The graph of $f(w)$ is quite interesting. As the functional representation shows, it consists of three segments which are plotted in Figure VI. 4 .

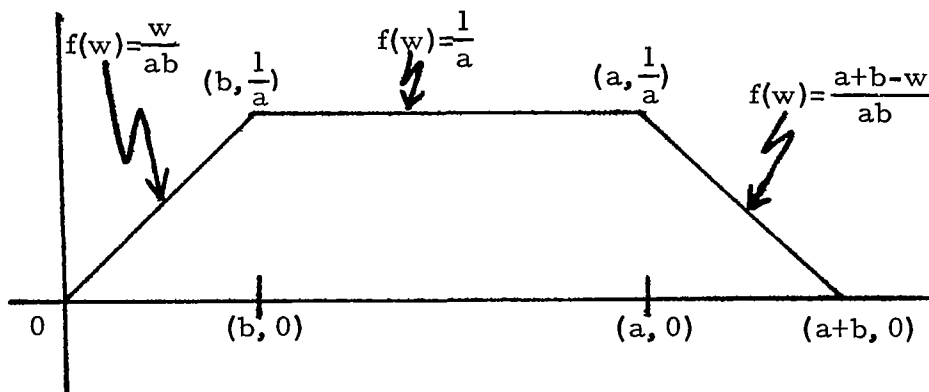


Figure VI. 4

Obviously, if $a = b$,

$$\begin{aligned} f(w) &= \frac{w}{2} & 0 \leq w \leq a \\ &= \frac{2a - w}{2} & a \leq w \leq 2a \end{aligned}$$

and the graph is triangular, the $f(w) = \frac{1}{a}$ segment vanishing.

Consider next the case of two normal distributions, denoting means by \bar{x} and \bar{y} and standard deviations by σ_x and σ_y for x and y respectively. The formula for $f(w)$ is

$$f(w) = \int_{-\infty}^{\infty} \frac{1}{2\pi\sigma_x\sigma_y} e^{-\frac{(x-\bar{x})^2}{2\sigma_x^2} - \frac{(w-x-\bar{y})^2}{2\sigma_y^2}} dx .$$

In this case, the limits are determined by observing that x can range from $-\infty$ to $+\infty$ for any fixed w . We will not bother to perform the simple integration required to obtain the well known result

$$f(w) = \frac{1}{\sqrt{2\pi(\sigma_x^2 + \sigma_y^2)}} e^{-\frac{(w - \bar{x} - \bar{y})^2}{2(\sigma_x^2 + \sigma_y^2)}} .$$

Next consider the case of two gamma densities

$$\begin{aligned} f_1(x) &= \frac{1}{\alpha! \beta^{\alpha+1}} x^{\alpha} e^{-x/\beta}, & 0 \leq x < \infty \\ f_2(y) &= \frac{1}{a! \beta^{a+1}} y^a e^{-y/\beta}, & 0 \leq y < \infty . \end{aligned}$$

In this derivation we have chosen to use the factorial notation, $\alpha!$ and $a!$ in place of $\Gamma(\alpha+1)$ and $\Gamma(a+1)$ to simplify typing. Note also that the parameter β is common to the two densities, an assumption needed

to get a simple answer. We can express $f(w)$ as

$$f(w) = \int_0^w \frac{e^{-\frac{w}{\beta}}}{\alpha! a! \beta^{\alpha+a+2}} x^\alpha (w-x)^a dx .$$

To evaluate this integral, we will transform it into a beta function form by letting $x = wt$. Then $dx = w dt$ and the integral becomes

$$f(w) = \int_0^1 \frac{e^{-\frac{w}{\beta}}}{\alpha! a! \beta^{\alpha+a+2}} w^{\alpha+a+1} t^\alpha (1-t)^a dt .$$

The beta density is commonly written as

$$\beta(x) = \frac{(\alpha+\beta+1)!}{\alpha! \beta!} x^\alpha (1-x)^\beta , \quad 0 \leq x \leq 1 .$$

Hence,

$$\int_0^1 t^\alpha (1-t)^a dt = \frac{\alpha! a!}{(\alpha+a+1)!} .$$

Then we have

$$\begin{aligned} f(w) &= \frac{1}{\alpha! a! \beta^{\alpha+a+2}} e^{-\frac{w}{\beta}} w^{\alpha+a+1} \frac{\alpha! a!}{(\alpha+a+1)!} \\ &= \frac{1}{(\alpha+a+1)! \beta^{\alpha+a+2}} w^{\alpha+a+1} e^{-\frac{w}{\beta}} \end{aligned}$$

also a gamma density.

The Density of the Sum of Two Stochastic Variables Having Identical Cauchy Densities. Let us now derive the density function of the sum of two stochastic variables having identical Cauchy densities. Thus, let

$$f_1(x) = \frac{a}{\pi(a^2 + x^2)}, \quad f_2(y) = \frac{a}{\pi(a^2 + y^2)} \quad -\infty < x, y < \infty.$$

Letting $w = x + y$, we have

$$f(w) = \int_{-\infty}^{\infty} \frac{a^2}{\pi^2(a^2 + x^2)[a^2 + (w - x)^2]} dx$$

In order to perform this integration, we will express the integrand in the form

$$\frac{a^2}{\pi^2} \left[\frac{A + Bx}{a^2 + x^2} + \frac{C + Dx}{a^2 + (w - x)^2} \right]$$

where A , B , C , and D are functions of w which is considered to be constant for this integration. It is not difficult to verify that they are

$$A = \frac{1}{4a^2 + w^2}, \quad B = \frac{2}{w(4a^2 + w^2)}, \quad C = \frac{3}{4a^2 + w^2}, \quad D = \frac{-2}{w(4a^2 + w^2)}$$

Therefore the integral can be written as

$$\frac{a^2}{\pi^2(4a^2 + w^2)} \int_{-\infty}^{\infty} \left[\frac{1 + 2w^{-1}x}{a^2 + x^2} + \frac{3 - 2w^{-1}x}{a^2 + (w - x)^2} \right] dx$$

We now modify the expression to be

$$\begin{aligned}
 & \frac{a^2}{\pi^2(4a^2+w^2)} \int_{-\infty}^{\infty} \left[\frac{1}{a^2+w^2} + \frac{2w^{-1}x}{a^2+x^2} + \frac{1}{a^2+(w-x)^2} - \frac{w^{-1}(-2w+2x)}{a^2+(w-x)^2} \right] dx \\
 &= \frac{a^2}{\pi^2(4a^2+w^2)} \left[\frac{1}{a} \arctan \frac{x}{a} + w^{-1} \ln(a^2+x^2) - \frac{1}{a} \arctan \frac{(w-x)}{a} - w^{-1} \ln\{a^2+(w-x)^2\} \right]_{-\infty}^{\infty} \\
 &= \frac{a}{\pi^2(4a^2+w^2)} (2\pi) \\
 &= \frac{2a}{\pi(4a^2+w^2)} .
 \end{aligned}$$

It is interesting to modify this density by the variable transformation

$$2z = w, \quad 2dz = dw .$$

Then we have for the density of z ,

$$\frac{a}{\pi(a^2+z^2)},$$

exactly the same density as for x and y .

The Density of the Product of Two Stochastic Variables

Let the two variables be x and y with densities

$$f_1(x) \text{ and } f_2(y) .$$

Let

$$u = x y \text{ and } v = x .$$

Solve for x and y , giving

$$x = v \text{ and } y = u v^{-1}$$

The Jacobian of the transformation is

$$J = v^{-1}$$

and the transformed density in differential form is

$$f_1(v) f_2(u v^{-1}) v^{-1} dv du .$$

As noted in the derivation of the sums of stochastic variables, it is common to omit the substitution $x = v$, which in this case gives

$$f_1(x) f_2(u x^{-1}) x^{-1} dx du .$$

Then the density of u , $P(u)$, is derived by integration as

$$P(u) = \int_{x_1}^{x_2} f_1(x) f_2(u x^{-1}) x^{-1} dx ,$$

the limits being determined in the usual way.

The Density of the Product of Two Stochastic Variables, Each having a Rectangular Density. Let

$$f_1(x) = \frac{1}{a} , \quad 0 \leq x \leq a \text{ and}$$

$$f_2(y) = \frac{1}{b} , \quad 0 \leq y \leq b .$$

Then the density of the product, $u = xy$, is

$$\begin{aligned}
 P(u) &= \int_{\frac{u}{b}}^a \frac{1}{ab} x^{-1} dx \\
 &= \frac{1}{ab} \ln x \Big|_{u/b}^a \\
 &= \frac{1}{ab} \left[\ln a - \ln \frac{u}{b} \right]
 \end{aligned}$$

or

$$P(u) = \frac{1}{ab} \ln \frac{ab}{u}, \quad 0 \leq u \leq ab$$

The Density of the Product of Two Stochastic Variables, Each Having A Gaussian or a Gamma Density. For these two cases, the simple methodology which we have adopted leads to integrals which are too complicated to handle. For derivations using more sophisticated methods, refer to the paper by Springer and Thompson which was mentioned earlier. This paper includes a table of ordinates for the Gaussian case and these were used to plot the curve to be presented later. For the gamma product, we used numerical techniques and a GE time sharing computer to derive the table of ordinates.

The Density of the Product of Two Stochastic Variables Each Having a Cauchy Density. Let us consider two stochastic variables with Cauchy densities.

$$f_1(x) = \frac{a}{\pi(x^2 + a^2)}, \quad -\infty < x < \infty \text{ and}$$

$$f_2(y) = \frac{b}{\pi(y^2 + b^2)}, \quad -\infty < y < \infty .$$

The density of the product $u = xy$, $P(u)$, is obtained as follows. The joint density of x and y in differential form is

$$\frac{ab}{\pi^2(x^2 + a^2)(y^2 + b^2)} dx dy .$$

Transform this into the differential form of the joint density of x and u by the expressions used before,

$$y = ux^{-1} , \quad dy = x^{-1} du ,$$

giving

$$\frac{ab}{\pi^2(x^2 + a^2)(u^2x^{-2} + b^2)} x^{-1} dx du .$$

The density of u can be obtained by integrating on x . To do this, make the substitution $z = x^2$ and the accompanying differential change, $dz = 2x dx$. Multiply by 2 to overlap the negative and positive ranges, giving

$$P(u) = \int_0^{\infty} \frac{ab}{\pi^2(z + a^2)(u^2 + b^2z)} dz ,$$

the limits on z corresponding to $-\infty$ to ∞ for x . By using partial fractions, we can express this as

$$\begin{aligned} P(u) &= \frac{ab}{\pi^2(u^2 - a^2b^2)} \int_0^{\infty} \left(\frac{1}{z + a^2} - \frac{b^2}{u^2 + b^2z} \right) dz \\ &= \left[\frac{ab}{\pi^2(u^2 - a^2b^2)} \ln \frac{z + a^2}{u^2 + b^2z} \right]_0^{\infty} \\ &= \frac{ab}{\pi^2(u^2 - a^2b^2)} \left[\ln \frac{1}{b^2} - \ln \frac{a^2}{u^2} \right] \\ &= \frac{ab}{\pi^2(u^2 - a^2b^2)} \ln \frac{u^2}{a^2b^2} , \quad -\infty < u < \infty . \end{aligned}$$

Consider the case in which the densities of x and y are identical, obtained by letting $a = b$. Then we have

$$P(u) = \frac{a^2}{\pi^2 (u^2 - a^2)} \ln \frac{u^2}{a^2}, \quad -\infty < u < \infty.$$

If we further simplify this by a unit change in which we set $a = 1$, we find that

$$P(u) = \frac{1}{\pi^2 (u^2 - 1)} \ln u^2, \quad -\infty < u < \infty.$$

The Density of the Quotient of Two Stochastic Variables

The notation which will be used in this case is similar to that used for the product. The variables are x and y with densities

$$f_1(x) \text{ and } f_2(y).$$

Let

$$v = x/y \text{ and } u = y$$

Solve for x and y , giving

$$x = uv \text{ and } y = v.$$

The Jacobian is v and the joint density in differential form changes from

$$f_1(x) f_2(y) dx dy$$

into

$$f_1(uv) f_2(v) |v| du dv.$$

It is common not to replace y by v . Thus, we have the joint density differential in the form

$$f_1(yv) f_2(y) |y| dy dv.$$

The density of v , $Q(v)$, is obtained by evaluating the integral

$$Q(v) = \int_{y_1}^{y_2} f_1(yv) f_2(y) |y| dy,$$

the limits y_1 and y_2 being determined in the usual way.

Density of the Quotient of Two Stochastic Variables with Rectangular Densities. Let

$$f_1(x) = \frac{1}{a}, \quad 0 \leq x \leq a \quad \text{and}$$

$$f_2(y) = \frac{1}{b}, \quad 0 \leq y \leq b.$$

Using the transformation formulas derived above, the density of the quotient, $v = x/y$, is

$$\begin{aligned} Q(v) &= \int_0^{y_1} \frac{1}{ab} y dy \\ &= \frac{1}{2ab} y_1^2 \end{aligned}$$

where the values of y_1 can be determined as follows. For fixed v , the graph of $yv = x$ is a straight line through the origin. Reference to Figure VI.5 shows how y_1 is determined in two ranges.

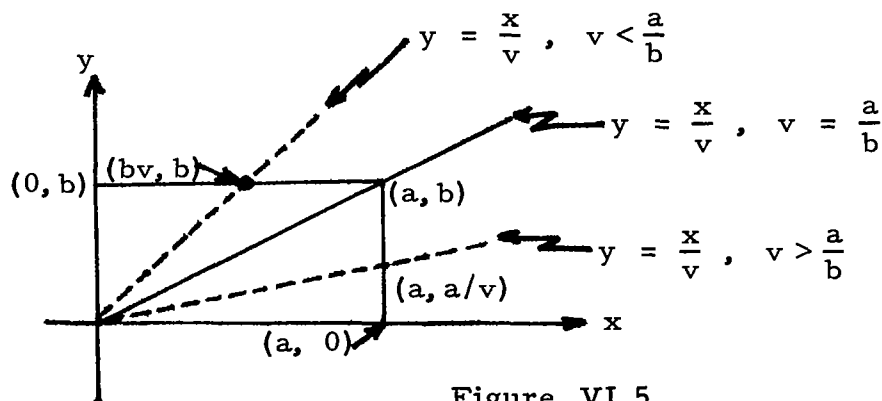


Figure VI.5

We can see that

$$y_1 = b \text{ for } v < \frac{a}{b}, \text{ and}$$

$$y_1 = a/v \text{ for } v > \frac{a}{b}$$

Therefore

$$Q(v) = \frac{b}{2a} \text{ for } v < \frac{a}{b} \text{ or } 0 \leq v \leq \frac{a}{b}$$

$$= \frac{a}{2bv^2} \text{ for } v > \frac{a}{b} \text{ or } \frac{a}{b} \leq v < \infty .$$

Density of the Quotient of Two Stochastic Variables Having Identical Gaussian Distribution with Zero Means. Because of mathematical complexities in the more general case, we will restrict ourselves to the derivation of the density of the quotient of two stochastic variables having identical Gaussian densities with zero means. Thus, let

$$f_1(x) = \frac{1}{\sqrt{2\pi}\sigma} e^{-\frac{x^2}{2\sigma^2}} \text{ and } f_2(y) = \frac{1}{\sqrt{2\pi}\sigma} e^{-\frac{y^2}{2\sigma^2}}, \text{ } -\infty < x, y < \infty .$$

The joint density of x and y in differential form is

$$\frac{1}{2\pi\sigma^2} e^{-\frac{x^2 + y^2}{2\sigma^2}} dx dy$$

As before, use the substitution $x = yv$, $dx = |y| dv$ to obtain the joint density of y and v in differential form as

$$\frac{1}{2\pi\sigma^2} e^{-\frac{y^2 v^2 + y^2}{2\sigma^2}} |y| dy dv$$

The density of v , $Q(v)$, is obtained by the following integration.

$$\begin{aligned}
 Q(v) &= \int_{-\infty}^{\infty} \frac{1}{2\pi\sigma^2} e^{-\frac{(v^2+1)}{2\sigma^2} y^2} |y| dy \\
 &= \frac{1}{\pi\sigma^2} \int_0^{\infty} e^{-\frac{(v^2+1)}{2\sigma^2} y^2} y dy \\
 &= \frac{1}{\pi\sigma^2} \left[\frac{-\sigma^2}{v^2+1} e^{-\frac{(v^2+1)}{2\sigma^2} y^2} y^2 \right]_0^{\infty} \\
 &= \frac{1}{\pi(v^2+1)} .
 \end{aligned}$$

Thus, the ratio of two variables with identical Gaussian densities and having zero means turns out to be the Cauchy distribution.

Density of the Quotient of Two Stochastic Variables Having Gamma Densities. In this case, we will denote the densities of the stochastic variables, x and y , by the two gamma functions

$$\begin{aligned}
 f_1(x) &= \frac{1}{\Gamma(\alpha+1)\beta^{\alpha+1}} x^\alpha e^{-\frac{x}{\beta}} \quad \text{and } 0 \leq x < \infty \\
 f_2(y) &= \frac{1}{\Gamma(a+1)b^{a+1}} y^a e^{-\frac{y}{b}} \quad 0 \leq y < \infty .
 \end{aligned}$$

To obtain the joint density, we again form the product which will be transformed by the substitution $x = vy$, $dx = v dy$, giving in differential the joint density of y and v ,

$$\frac{1}{\Gamma(\alpha + 1) \Gamma(a + 1) \beta^{\alpha + 1} b^{a + 1}} (vy)^{\alpha} y^a e^{-\frac{vy}{\beta} - \frac{y}{b}} v dy dv .$$

The density of v is obtained by integrating on y . Omitting factors not containing y , we have the integral

$$\int_0^{\infty} y^{\alpha + a + 1} e^{-\left(\frac{v}{\beta} + \frac{1}{b}\right)y} dy$$

By reference to the gamma function in integral form, we can see that the value of this integral is

$$\Gamma(\alpha + a + 2) \left(\frac{v}{\beta} + \frac{1}{b}\right)^{-(\alpha + a + 2)}$$

Therefore the density of v is

$$Q(v) = \frac{\Gamma(\alpha + a + 2)}{\Gamma(\alpha + 1) \Gamma(a + 1) \beta^{\alpha + 1} b^{a + 1}} v^{\alpha} \left(\frac{v}{\beta} + \frac{1}{b}\right)^{-(\alpha + a + 2)}$$

If x and y have identical densities, that is, if $a = \alpha$ and $b = \beta$, then

$$\begin{aligned} Q(v) &= \frac{\Gamma(2\alpha + 2)}{[\Gamma(\alpha + 1)]^2 \beta^{2\alpha + 2}} v^{\alpha} \left(\frac{v}{\beta} + \frac{1}{\beta}\right)^{-(2\alpha + 2)} \\ &= \frac{\Gamma(2\alpha + 2)}{[\Gamma(\alpha + 1)]^2} v^{\alpha} (v + 1)^{-(2\alpha + 2)} \end{aligned}$$

The Density of the Quotient of Two Stochastic Variables Each Having a Cauchy Density. Again we will consider two stochastic variables with Cauchy densities

$$f_1(x) = \frac{a}{\pi(x^2 + a^2)}, \quad -\infty < x < \infty \text{ and}$$

$$f_2(y) = \frac{b}{\pi(y^2 + b^2)}, \quad -\infty < y < \infty .$$

Using the previously discussed transformation,

$$x = vy, \quad dx = |y| dv,$$

in the product of the two densities, we have the joint density of y and v in differential form as

$$\frac{ab}{\pi^2(v^2 y^2 + a^2)(y^2 + b^2)} |y| dy dv .$$

Transforming to a positive range for y , thereby multiplying by 2, we have the density of v , $Q(v)$, as

$$Q(v) = \int_0^{\infty} \frac{2ab}{\pi^2(v^2 y^2 + a^2)(y^2 + b^2)} y dy .$$

We can easily verify that

$$\frac{1}{(v^2 y^2 + a^2)(y^2 + b^2)} = \frac{1}{b^2 v^2 - a^2} \left(\frac{v^2}{v^2 y^2 + a^2} - \frac{1}{y^2 + b^2} \right)$$

which, when substituted in the integral, gives

$$Q(v) = \frac{ab}{\pi^2 (b^2 v^2 - a^2)} \int_0^\infty \left[\frac{v^2}{v^2 y^2 + a^2} - \frac{1}{y^2 + b^2} \right]^2 y \, dy .$$

Integrating, we have

$$\begin{aligned} Q(v) &= \frac{ab}{\pi^2 (b^2 v^2 - a^2)} \left[\ln \frac{v^2 y^2 + a^2}{y^2 + b^2} \right]_0^\infty \\ &= \frac{ab}{\pi^2 (b^2 v^2 - a^2)} \left[\ln v^2 - \ln \frac{a^2}{b^2} \right] \\ &= \frac{ab}{\pi^2 (b^2 v^2 - a^2)} \ln \frac{b^2 v^2}{a^2} , \quad -\infty < v < \infty . \end{aligned}$$

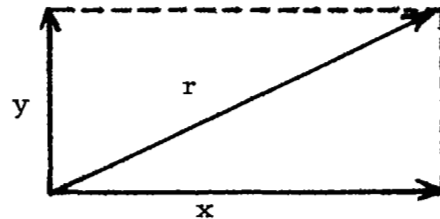
It is interesting to write the density of the quotient of stochastic variables with identical Cauchy densities. Thus let $a = b$, giving

$$Q(v) = \frac{1}{\pi^2 (v^2 - 1)} \ln v^2 , \quad -\infty < v < \infty .$$

Note that "a" does not enter in the expression for $Q(v)$, a natural consequence of the fact that the ratio of x to y is dimensionless in this case. Note further that the quotient is density is the same as the product for $a = 1$, an obvious result in view of the fact that the reciprocal of a Cauchy variables has the same Cauchy density as the variable if $a = 1$.

A Special Example - The Generation
of the Rayleigh Density as a Transformation
of a Pair of Gaussian Densities

An interesting example of the transformation of a pair of Gaussian densities is provided by the following problem. Suppose we have a pair of independent forces, x and y , acting at right angles and having identical Gaussian densities with a mean of zero and a standard deviation of σ . The problem is to derive the density of the resultant force, r . The relationships of the force vectors is diagramed in the traditional way with x and y shown as the sides of a rectangle and r as the diagonal.



The zero mean merely implies that the forces are equally likely to act in either direction, positive or negative.

The densities of x and y are

$$\frac{1}{\sqrt{2\pi}\sigma} e^{-\frac{x^2}{2\sigma^2}} \quad \text{and} \quad \frac{1}{\sqrt{2\pi}\sigma} e^{-\frac{y^2}{2\sigma^2}}$$

and the joint density in differential form is

$$\frac{1}{2\pi\sigma^2} e^{-\frac{1}{2\sigma^2}(x^2 + y^2)} dx dy .$$

Since $r = \sqrt{x^2 + y^2}$, we can solve this problem by transforming to polar coordinates, r and θ , and integrating on θ . The differential product is replaced by

$$r \, d\theta \, dr.$$

The integration is

$$\int_0^{2\pi} \frac{1}{2\pi\sigma^2} e^{-\frac{r^2}{2\sigma^2}} r \, d\theta \, dr$$

$$= \frac{1}{\sigma^2} e^{-\frac{r^2}{2\sigma^2}} r \, dr, \quad r \leq 0$$

which is the Rayleigh density. It is perhaps more common to modify the constant by the substitution

$$r_0 = 2\sigma^2$$

giving the function in the form

$$\frac{2r}{r_0} e^{-\frac{r^2}{r_0}} \, dr, \quad r \geq 0.$$

Here again we have illustrated with a rather typical engineering example that a transformation of Gaussian densities can indeed lead to non-Gaussian outputs.

Implications of the Discussion of Transformations of Stochastic Variables

In drawing conclusions from this discussion of transformations of stochastic variables, we will restrict our coverage to include only a few transformation properties. We will concentrate on those properties which seem to be at odds with intuition or, in other words, properties which at times seem to be misunderstood, thereby resulting in certain erroneous analyses. It is perhaps worth noting here that these problems arise because of a frequently observed characteristic of probability. It is unsafe to trust intuition by guessing or anticipating answers to problems in probability for it is so easy to guess wrong—probability problem solutions often provide interesting surprises.

Perhaps the most significant observation is that transformations of stochastic variables tend to change the density types. Stated in another way, even if all the input variables in a transfer function have the same kind of density, we cannot expect the output to be the same. For example, the ratio of two Gaussian (normal) variables is definitely not normal—in the case which was used herein, a Cauchy distribution was obtained. Of course, the density form is sometimes preserved—the sum of Gaussian variables is still Gaussian.

Although we did not bother to cover this point in the derivations, it is nevertheless true that moments of transformed variables are not in general equal to the corresponding transformation of the moments of the input stochastic variables. As a simple illustration and one which is really obvious, for any density with zero mean, the reciprocal of the variable can have a density with a finite mean. Indeed, if the density of the variable is symmetrical about zero, then the density of the reciprocal is also and hence it will have a zero mean. Thus, it is necessary to derive the proper relationships on moments and it will not be wise to guess at such relationships.

The discussion did point out the difference between the density of the square of a variable and the density of the product of two independent variables having identical densities. The square of a variable represents the case of complete dependence or perfect correlation if you will. The product is the opposite extreme—complete independence with absolutely no correlation.

It is interesting to look also at the case of a variable divided by itself as contrasted with the ratio of two independent variables having identical distributions. The variable divided by itself is the trivial case in which the quotient must be unity and the associated probability is also unity. The quotient of two independent variables is of course non-trivial—the density may exhibit quite unusual characteristics as compared with the common density of the input variables. For example, one can verify that for the uniform density example used herein, the quotient has an infinite mean value—a somewhat striking characteristic.

In deriving the closed form solutions presented herein, it was observed that finite limits on the input variables tend to be more difficult to handle than infinite limits. In actual engineering applications, it is likely that many variables will have finite bounds, perhaps arising by truncation of a Gaussian or Gamma or some other density form. This will have no impact on a computer analysis based on discrete approximations, but it would be significant if one chooses to derive closed form solutions.

Summary of Closed Form Solutions

The discussion of closed form solutions is summarized by the formulas and graphs in Figure VI. 6. This figure shows graphs of the densities of the variable, its reciprocal and its square and densities of the sum, product and quotient of two variables for the uniform, Gaussian, Gamma, and Cauchy distributions. Formulas for the closed form solutions were derived and are shown for all but two cases—the products of two Gaussian and two Gamma variables. These cases involve derivations which are much more complicated than the others in the figure. As noted earlier, an excellent treatment of some of this theory is included in the publication "The Distribution of Products of Independent Random Variables" by M. D. Springer and W. E. Thompson, G. M. Defense Research Laboratories, TR 64-46, August 1964 as noted in the discussion. In this paper, Springer and Thompson used Mellin transforms to derive many closed form relationships and some in infinite series form. Springer and Thompson provided us with a table of ordinates for the density of the product of two Gaussian variables to permit plotting this curve in the figure. We developed the ordinates for the case of the product of two gamma's by using the GE time sharing computer. Curves for the uniform density and sum were plotted from their simple equations but all other curves were plotted from coordinates generated on the G. E. time sharing computer. The tabular values generated by these computer runs are included after Figure VI. 6. It is of interest to note that the computer output was formatted on 8-1/2 by 11 inch sheets immediately ready for reproduction without retyping. It is also interesting to know that all of these computations required less than one minute of computer time—each page took only a few seconds.

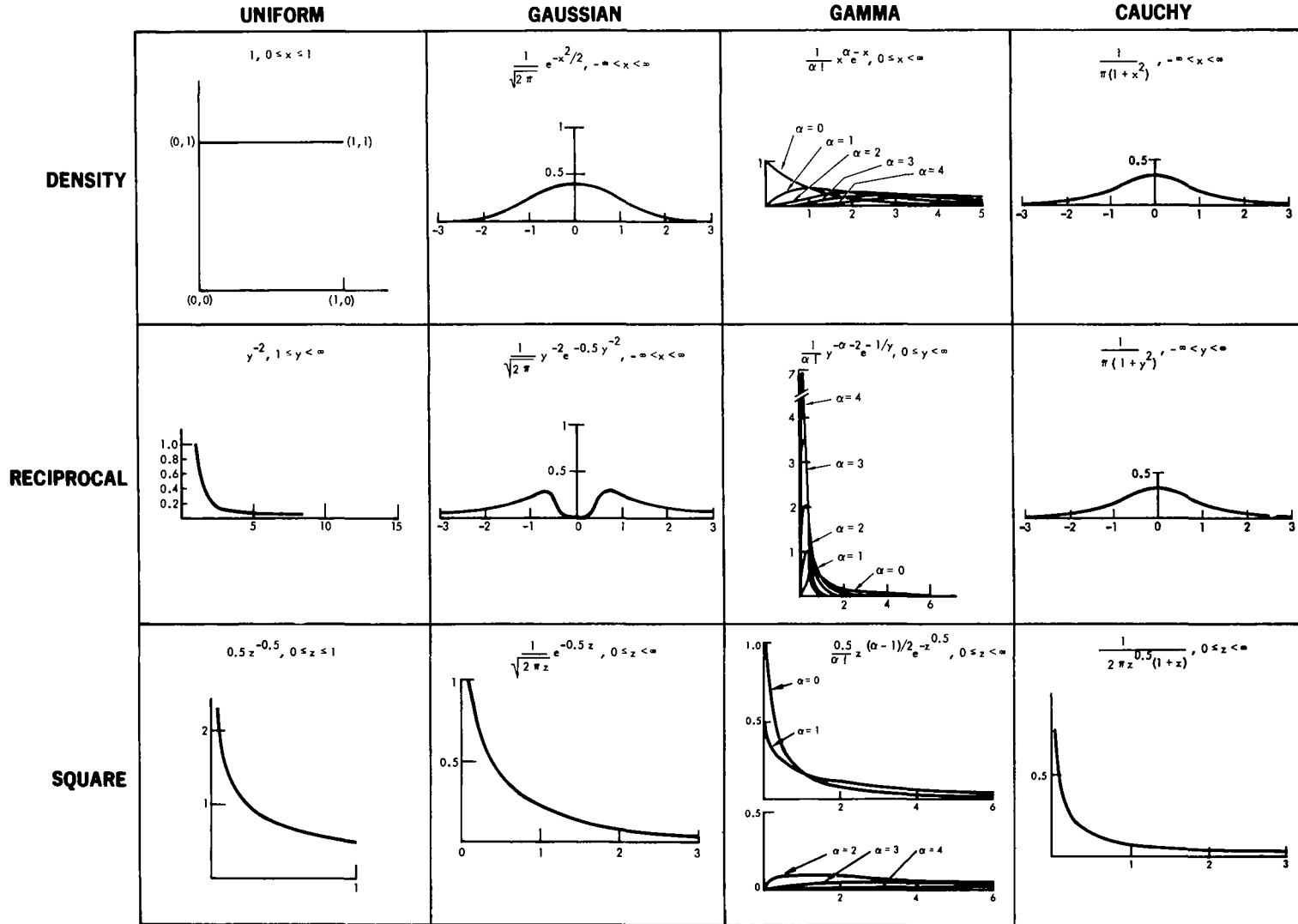


Figure VI.6

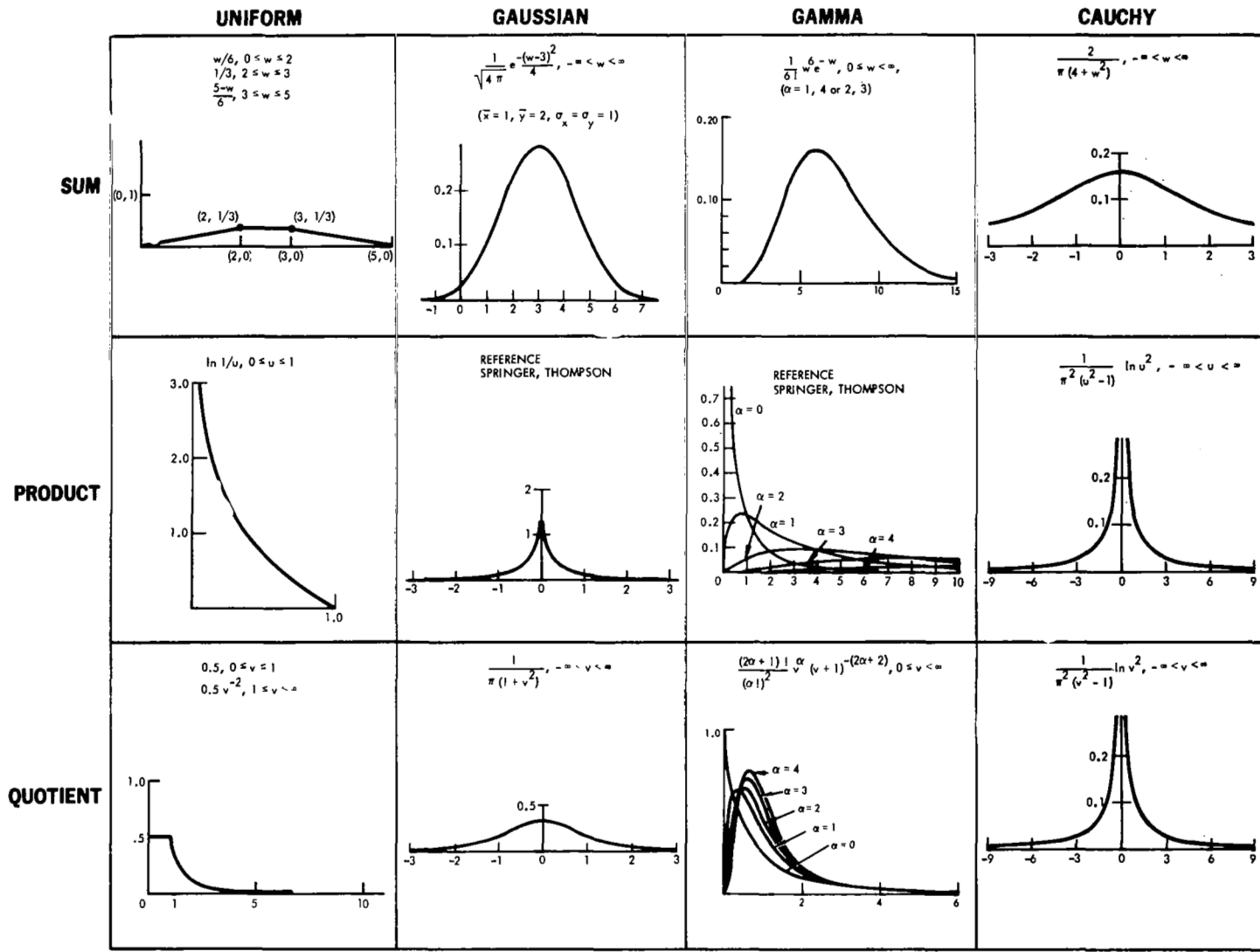


Figure VI.6 (continued)

UNIFORM DISTRIBUTION

VARIABLE	RECIPROCAL	QUOTIENT	VARIABLE	SQUARE	PRODUCT
.5	4	2	.05	2.23607	2.99573
1	1	.5	.1	1.58114	2.30259
1.5	.444444	.222222	.15	1.29099	1.89712
2	.25	.125	.2	1.11803	1.60944
2.5	.16	.03	.25	1	1.33629
3	.111111	.055556	.3	.912371	1.20397
3.5	.061633	.040816	.35	.845154	1.04952
4	.0625	.03125	.4	.790569	.916291
4.5	.049383	.024691	.45	.745356	.798508
5	.04	.02	.5	.707107	.693147
5.5	.033058	.016529	.55	.6742	.597837
6	.027778	.013889	.6	.645497	.510826
6.5	.023669	.011834	.65	.620174	.430783
7	.020408	.010204	.7	.597614	.356615
7.5	.017178	.008889	.75	.57735	.281682
8	.015625	.007813	.8	.559017	.223144
8.5	.013341	.00692	.85	.542326	.162517
9	.012346	.006173	.9	.527046	.105361
9.5	.01108	.00554	.95	.512739	.051293
10	.01	.005	1	.5	0

GAUSSIAN DISTRIBUTION

VARIABLE	DENSITY	RECIPROCAL	SQUARE	VARIABLE	SUM
.1	.396952	0	1.20004	3.2	.279288
.2	.391042	.000037	.807171	3.4	.271034
.3	.381388	.017136	.62691	3.6	.257815
.4	.36827	.107552	.516441	3.8	.240386
.5	.352065	.215964	.439391	4	.219696
.6	.333224	.276325	.381545	4.2	.196811
.7	.312254	.293465	.336014	4.4	.172319
.8	.289691	.235389	.298983	4.6	.145747
.9	.266035	.26567	.268137	4.8	.125492
1	.241971	.241971	.241971	5	.103777
1.1	.217652	.218104	.219456	5.2	.08412
1.2	.194186	.195772	.199866	5.4	.066636
1.3	.171365	.175604	.182661	5.6	.052052
1.4	.149727	.157712	.167432	5.8	.039735
1.5	.129518	.141977	.153866	6	.029733
1.6	.110921	.128188	.141714	6.2	.021807
1.7	.094049	.116111	.130778	6.4	.015678
1.8	.07895	.105522	.120895	6.6	.011043
1.9	.065616	.096217	.111932	6.8	.007631
2	.053991	.088016	.103777	7	.005167
2.1	.043954	.080767	.096337	7.2	.003429
2.2	.035475	.074336	.089531	7.4	.002231
2.3	.028327	.068613	.083293	7.6	.001422
2.4	.022395	.063502	.077562	7.8	.000889
2.5	.017523	.058923	.072289	8	.000545
2.6	.013583	.054808	.067428	8.2	.000327
2.7	.010421	.051097	.062941	8.4	.000192
2.8	.007915	.047742	.058792	8.6	.000111
2.9	.005953	.044677	.054952	8.8	.000063
3	.004432	.041931	.051393	9	.000035

GAMMA DISTRIBUTION-DENSITY

VARIABLE	ALPHA				
	0	1	2	3	4
.2	.818731	.163746	.016375	.001092	.000055
.4	.67032	.268128	.053626	.00715	.000715
.6	.548812	.329237	.093786	.019757	.002964
.8	.449329	.359463	.143785	.038343	.007669
1	.367879	.367879	.18394	.061313	.015328
1.2	.301194	.361433	.21686	.086744	.026093
1.4	.246597	.345236	.241665	.112777	.039472
1.6	.201897	.323034	.258428	.137828	.055131
1.8	.165299	.297538	.267784	.160671	.072302
2	.135335	.270671	.270671	.180447	.090224
2.2	.110803	.243767	.266144	.196639	.108151
2.4	.090718	.217729	.261263	.209014	.125408
2.6	.074274	.193111	.251045	.217572	.141422
2.8	.06081	.170268	.238375	.222434	.155739
3	.049787	.149361	.224042	.224042	.168031
3.2	.040762	.130439	.208702	.222616	.178093
3.4	.033373	.113469	.192898	.218617	.185825
3.6	.027324	.098365	.177058	.212469	.191222
3.8	.022371	.085009	.161517	.204588	.194359
4	.018316	.073263	.146525	.195367	.195367
4.2	.014976	.062981	.132261	.185165	.194424
4.4	.012277	.05402	.118845	.174305	.191736
4.6	.010052	.046238	.106348	.163068	.187528
4.8	.00823	.039503	.094807	.151691	.182029
5	.006738	.03369	.084224	.140374	.175467
5.2	.005517	.028636	.074584	.129279	.168063
5.4	.004517	.02439	.065852	.118533	.16002
5.6	.003698	.020708	.057983	.108234	.151528
5.8	.003023	.01756	.050923	.098452	.142755
6	.002479	.014873	.044618	.089235	.133855

GAMMA DISTRIBUTION-RECIPROCAL

VARIABLE	ALPHA				
	0	1	2	3	4
.2	.168449	.842243	2.10561	3.50935	4.38668
.4	.513031	1.28258	1.60322	1.33602	.835012
.6	.524654	.874424	.728667	.404826	.168677
.8	.447664	.55958	.349737	.145724	.045539
1	.367879	.367879	.18394	.061313	.015328
1.2	.301804	.251504	.104793	.029109	.006064
1.4	.249766	.178404	.063716	.01517	.002709
1.6	.209086	.130679	.040837	.008503	.001329
1.8	.177084	.09838	.027328	.005061	.000703
2	.151633	.075816	.018954	.003159	.000395
2.2	.131144	.059611	.013548	.002053	.000233
2.4	.114451	.047688	.009935	.00138	.000144
2.6	.100697	.03873	.007448	.000955	.000092
2.8	.089244	.031873	.005692	.000678	.00006
3	.079615	.026538	.004423	.000491	.000041
3.2	.071447	.022327	.003489	.000363	.000028
3.4	.064463	.01896	.002788	.000273	.00002
3.6	.058446	.016235	.002255	.000209	.000014
3.8	.053229	.014008	.001843	.000162	.000011
4	.048675	.012169	.001521	.000127	.000008
4.2	.044678	.010638	.001266	.000101	.000006
4.4	.041152	.009353	.001063	.000081	.000005
4.6	.038025	.008266	.000899	.000065	.000004
4.8	.03524	.007342	.000765	.000053	.000003
5	.032749	.00655	.000655	.000044	.000002
5.2	.030512	.005868	.000564	.000036	.000002
5.4	.028496	.005277	.000489	.00003	.000001
5.6	.026673	.004763	.000425	.000025	.000001
5.8	.025019	.004314	.000372	.000021	.000001
6	.023513	.003919	.000327	.000018	.000001

GAMMA DISTRIBUTION-SQUARE

VARIABLE	*****				
	0	1	2	3	4
.2	.714879	.319704	.071488	.010657	.001191
.4	.420016	.265643	.084004	.01771	.0028
.6	.297503	.230445	.069251	.023044	.004463
.8	.228549	.204421	.09142	.027256	.006095
1	.18394	.18394	.09197	.030657	.007664
1.2	.152626	.167195	.091577	.033439	.009158
1.4	.129432	.153146	.090602	.035734	.01057
1.6	.111575	.141132	.08926	.037635	.011901
1.8	.097424	.130708	.087682	.039212	.013152
2	.085955	.121558	.085955	.040519	.014326
2.2	.076488	.113451	.084137	.041599	.015425
2.4	.068553	.10621	.08227	.042484	.016454
2.6	.061831	.099699	.08038	.043203	.017416
2.8	.056063	.093412	.078488	.043779	.018314
3	.051073	.088461	.076609	.04423	.019152
3.2	.04672	.083576	.074752	.044574	.019934
3.4	.042897	.079099	.072926	.044823	.020662
3.6	.039519	.074982	.071134	.044989	.02134
3.8	.036516	.071183	.06938	.045032	.02197
4	.033834	.067668	.067668	.045112	.022556
4.2	.031427	.064407	.065997	.045085	.023099
4.4	.029259	.061374	.06437	.045008	.023602
4.6	.027298	.058543	.062786	.044887	.024068
4.8	.025517	.055909	.061245	.044727	.024493
5	.023899	.053439	.059747	.044532	.024894
5.2	.022419	.051124	.058291	.044308	.025259
5.4	.021065	.048951	.056876	.044056	.025594
5.6	.019822	.046907	.055502	.04378	.025901
5.8	.018678	.044983	.054167	.043484	.026181
6	.017624	.043169	.052871	.043169	.026435

GAMMA DISTRIBUTION-LM

VARIABLE	*****				
	0	1	2	3	4
.3	0	0	.000001	0	0
.6	0	0	.000036	0	0
.9	0	0	.0003	0	0
1.2	0	0	.001249	0	0
1.5	0	0	.00353	0	0
1.8	0	0	.007809	0	0
2.1	0	0	.014587	0	0
2.4	0	0	.024078	0	0
2.7	0	0	.036162	0	0
3	0	0	.050409	0	0
3.3	0	0	.066158	0	0
3.6	0	0	.082608	0	0
3.9	0	0	.098925	0	0
4.2	0	0	.114321	0	0
4.5	0	0	.12812	0	0
4.8	0	0	.139798	0	0
5.1	0	0	.149	0	0
5.4	0	0	.155539	0	0
5.7	0	0	.159382	0	0
6	0	0	.160623	0	0
6.3	0	0	.159461	0	0
6.6	0	0	.156166	0	0
6.9	0	0	.151053	0	0
7.2	0	0	.144458	0	0
7.5	0	0	.136718	0	0
7.8	0	0	.128156	0	0
8.1	0	0	.119067	0	0
8.4	0	0	.109716	0	0
8.7	0	0	.100328	0	0
9	0	0	.09109	0	0

Gamma Products

$\alpha = 0, 1, 2, 3, 4.$

(From runs of F260 Program)

Ordinate at midpoint between "START" and "STOP" is five times the probability. Curves were drawn by plotting the probability and changing the vertical scale.

Gamma Product

$\alpha = 0$

START	STOP	PROBABILITY
.00	.20	.3384
.20	.40	.1557
.40	.60	.099
.60	.80	.0703
.80	1.00	.0527
1.00	1.20	.0414
1.20	1.40	.033
1.40	1.60	.027
1.60	1.80	.0222
1.80	2.00	.0188
2.00	2.20	.016
2.20	2.40	.0136
2.40	2.60	.0117
2.60	2.80	.0102
2.80	3.00	.0088
3.00	3.20	.0079
3.20	3.40	.0068
3.40	3.60	.0061
3.60	3.80	.0053
3.80	4.00	.0048
4.00	4.20	.0043
4.20	4.40	.0039
4.40	4.60	.0034
4.60	4.80	.0032
4.80	5.00	.0028
5.00	5.20	.0026
5.20	5.40	.0023
5.40	5.60	.0021
5.60	5.80	.0019
5.80	6.00	.0017
6.00	6.20	.0016
6.20	6.40	.0015
6.40	6.60	.0013
6.60	6.80	.0012
6.80	7.00	.0011
7.00	7.20	.0011
7.20	7.40	9.43681E-04
7.40	7.60	8.94820E-04
7.60	7.80	8.23562E-04
7.80	8.00	7.55059E-04
8.00	8.20	7.01411E-04
8.20	8.40	6.62229E-04
8.40	8.60	5.93497E-04
8.60	8.80	5.68472E-04
8.80	9.00	5.22160E-04
9.00	9.20	4.82370E-04
9.20	9.40	4.52413E-04
9.40	9.60	4.29304E-04
9.60	9.80	3.83981E-04
9.80	10.00	3.70714E-04
10.00	20.00	.0055

Gamma Product
 $\alpha = 1$

Gamma Product
 $\alpha = 2$

START	STOP	PROBABILITY	START	STOP	PROBABILITY
.00	.20	.0321	.00	.20	.0012
.20	.40	.0423	.20	.40	.0033
.40	.60	.0467	.40	.60	.0059
.60	.80	.0473	.60	.80	.0084
.80	1.00	.0461	.80	1.00	.0105
1.00	1.20	.0442	1.00	1.20	.0122
1.20	1.40	.0419	1.20	1.40	.0137
1.40	1.60	.0395	1.40	1.60	.0148
1.60	1.80	.0371	1.60	1.80	.0158
1.80	2.00	.0349	1.80	2.00	.0166
2.00	2.20	.0328	2.00	2.20	.0172
2.20	2.40	.0306	2.20	2.40	.0176
2.40	2.60	.0287	2.40	2.60	.018
2.60	2.80	.027	2.60	2.80	.0182
2.80	3.00	.0251	2.80	3.00	.0183
3.00	3.20	.0238	3.00	3.20	.0184
3.20	3.40	.0221	3.20	3.40	.0183
3.40	3.60	.021	3.40	3.60	.0183
3.60	3.80	.0194	3.60	3.80	.0181
3.80	4.00	.0185	3.80	4.00	.018
4.00	4.20	.0173	4.00	4.20	.0177
4.20	4.40	.0163	4.20	4.40	.0175
4.40	4.60	.0152	4.40	4.60	.0172
4.60	4.80	.0146	4.60	4.80	.017
4.80	5.00	.0134	4.80	5.00	.0166
5.00	5.20	.0129	5.00	5.20	.0164
5.20	5.40	.0121	5.20	5.40	.016
5.40	5.60	.0114	5.40	5.60	.0157
5.60	5.80	.0108	5.60	5.80	.0154
5.80	6.00	.0101	5.80	6.00	.015
6.00	6.20	.0097	6.00	6.20	.0147
6.20	6.40	.0091	6.20	6.40	.0143
6.40	6.60	.0086	6.40	6.60	.014
6.60	6.80	.0082	6.60	6.80	.0137
6.80	7.00	.0077	6.80	7.00	.0133
7.00	7.20	.0074	7.00	7.20	.0131
7.20	7.40	.0068	7.20	7.40	.0126
7.40	7.60	.0066	7.40	7.60	.0124
7.60	7.80	.0063	7.60	7.80	.012
7.80	8.00	.0059	7.80	8.00	.0117
8.00	8.20	.0056	8.00	8.20	.0114
8.20	8.40	.0054	8.20	8.40	.0112
8.40	8.60	.005	8.40	8.60	.0107
8.60	8.80	.0049	8.60	8.80	.0106
8.80	9.00	.0046	8.80	9.00	.0102
9.00	9.20	.0043	9.00	9.20	.0099
9.20	9.40	.0042	9.20	9.40	.0097
9.40	9.60	.004	9.40	9.60	.0095
9.60	9.80	.0037	9.60	9.80	.0091
9.80	10.00	.0036	9.80	10.00	.0089
10.00	20.00	.0704	10.00	20.00	.2352

Gamma Product
 $\alpha = 3$

START	STOP	PROBABILITY
.00	.20	2.85197E-05
.20	.40	1.26807E-04
.40	.60	3.55770E-04
.60	.80	6.82424E-04
.80	1.00	.0011
1.00	1.20	.0015
1.20	1.40	.002
1.40	1.60	.0025
1.60	1.80	.003
1.80	2.00	.0035
2.00	2.20	.004
2.20	2.40	.0045
2.40	2.60	.005
2.60	2.80	.0055
2.80	3.00	.006
3.00	3.20	.0063
3.20	3.40	.0068
3.40	3.60	.0071
3.60	3.80	.0075
3.80	4.00	.0078
4.00	4.20	.0081
4.20	4.40	.0084
4.40	4.60	.0087
4.60	4.80	.0088
4.80	5.00	.0091
5.00	5.20	.0093
5.20	5.40	.0095
5.40	5.60	.0096
5.60	5.80	.0097
5.80	6.00	.0099
6.00	6.20	.01
6.20	6.40	.0101
6.40	6.60	.0101
6.60	6.80	.0102
6.80	7.00	.0102
7.00	7.20	.0103
7.20	7.40	.0103
7.40	7.60	.0103
7.60	7.80	.0103
7.80	8.00	.0103
8.00	8.20	.0103
8.20	8.40	.0103
8.40	8.60	.0102
8.60	8.80	.0102
8.80	9.00	.0101
9.00	9.20	.0101
9.20	9.40	.01
9.40	9.60	.01
9.60	9.80	.0099
9.80	10.00	.0098
10.00	20.00	.3629

Gamma Product
 $\alpha = 4$

START	STOP	PROBABILITY
.00	.20	4.93797E-07
.20	.40	3.01330E-06
.40	.60	1.26716E-05
.60	.80	3.26122E-05
.80	1.00	6.57359E-05
1.00	1.20	1.09647E-04
1.20	1.40	1.70719E-04
1.40	1.60	2.43246E-04
1.60	1.80	3.33558E-04
1.80	2.00	4.32614E-04
2.00	2.20	5.41872E-04
2.20	2.40	6.67298E-04
2.40	2.60	8.05899E-04
2.60	2.80	9.42595E-04
2.80	3.00	.0011
3.00	3.20	.0012
3.20	3.40	.0014
3.40	3.60	.0016
3.60	3.80	.0018
3.80	4.00	.0019
4.00	4.20	.0021
4.20	4.40	.0023
4.40	4.60	.0025
4.60	4.80	.0026
4.80	5.00	.0028
5.00	5.20	.003
5.20	5.40	.0032
5.40	5.60	.0033
5.60	5.80	.0035
5.80	6.00	.0037
6.00	6.20	.0038
6.20	6.40	.004
6.40	6.60	.0042
6.60	6.80	.0043
6.80	7.00	.0045
7.00	7.20	.0046
7.20	7.40	.0048
7.40	7.60	.0049
7.60	7.80	.005
7.80	8.00	.0051
8.00	8.20	.0053
8.20	8.40	.0054
8.40	8.60	.0055
8.60	8.80	.0056
8.80	9.00	.0057
9.00	9.20	.0058
9.20	9.40	.0059
9.40	9.60	.006
9.60	9.80	.0061
9.80	10.00	.0061
10.00	20.00	.33

CAMA DISTRIBUTION-DENSITY

VARIABLE	*****				ALPHA	*****			
	0	1	2	3	4				
.2	.694444	.578704	.401878	.260476	.162798				
.4	.510204	.62474	.637489	.607133	.557571				
.6	.390625	.549316	.64373	.70408	.742584				
.8	.308642	.457247	.564503	.650456	.722729				
1	.25	.375	.46375	.546875	.615234				
1.2	.206612	.307356	.38102	.440849	.491857				
1.4	.173611	.253183	.307688	.348997	.381716				
1.6	.147929	.210077	.248611	.2746	.292474				
1.8	.127551	.175708	.201706	.216113	.22328				
2	.111111	.148148	.164609	.170706	.170706				
2.2	.097656	.125835	.135223	.13558	.131079				
2.4	.086505	.107757	.111859	.108375	.10125				
2.6	.07716	.092878	.093165	.087222	.087842				
2.8	.069252	.08057	.078115	.070686	.061679				
3	.0625	.070313	.065918	.057678	.048666				
3.2	.056689	.061703	.055966	.047379	.038677				
3.4	.051653	.054428	.047793	.039169	.030955				
3.6	.047259	.048242	.041037	.032582	.024944				
3.8	.043403	.042951	.035419	.027261	.020233				
4	.04	.0384	.03072	.022933	.016515				
4.2	.036982	.034466	.026767	.019402	.013561				
4.4	.034294	.031048	.023424	.016494	.0112				
4.6	.031838	.028064	.020583	.01409	.0093				
4.8	.029727	.02545	.018157	.01209	.007763				
5	.027778	.023148	.016075	.010419	.006512				
5.2	.026015	.021115	.014282	.009016	.005488				
5.4	.024414	.019312	.01273	.007832	.004646				
5.6	.022957	.017708	.011382	.006829	.003951				
5.8	.021626	.016276	.010208	.005975	.003573				
6	.020408	.014994	.00918	.005246	.00289				

CAUCHY DISTRIBUTION

VARIABLE	DENSITY	SQUARE	SUM	VARIABLE	PRODUCT
.1	.315158	.457536	.158758	.3	.288106
.2	.306067	.296568	.157579	.6	.161742
.3	.292028	.22352	.155653	.9	.112371
.4	.274405	.179747	.153034	1.2	.083768
.5	.254648	.150053	.149793	1.5	.065732
.6	.234051	.123418	.146014	1.8	.053174
.7	.213631	.111898	.141746	2.1	.04407
.8	.194091	.098856	.137203	2.4	.03727
.9	.175862	.088297	.132353	2.7	.031999
1	.159155	.079578	.127324	3	.027828
1.1	.144032	.072261	.122192	3.3	.024463
1.2	.130455	.06604	.117026	3.6	.021703
1.3	.118331	.060691	.111884	3.9	.019408
1.4	.107537	.056046	.106815	4.2	.017477
1.5	.097942	.05198	.101859	4.5	.015833
1.6	.089413	.048393	.097046	4.8	.014422
1.7	.081828	.04521	.092398	5.1	.013201
1.8	.075073	.042367	.087931	5.4	.012136
1.9	.069048	.039815	.083656	5.7	.0112
2	.063662	.037513	.079578	6	.010374
2.1	.058837	.035428	.075693	6.3	.00964
2.2	.054505	.033532	.072016	6.6	.008965
2.3	.050666	.031801	.068527	6.9	.008398
2.4	.047037	.030216	.065297	7.2	.007868
2.5	.043905	.02876	.062109	7.5	.00739
2.6	.041019	.027418	.059165	7.8	.006956
2.7	.038397	.026178	.056388	8.1	.006561
2.8	.036008	.02503	.053769	8.4	.0062
2.9	.033827	.023964	.051299	8.7	.005869
3	.031831	.022972	.048971	9	.005566

DISCAL

```

10 PRINT "*****"
20 FOR K=1 TO 8
30 PRINT\PRINT\PRINT\PRINT\PRINT\PRINT\PRINT\PRINT\PRINT\PRINT
40 IF K>5.5 THEN 110
50 GO TO (500,600,700,800,900,1000,1100,1200) K
60 PRINT
70 PRINT TAB(13);"***** ALPHA *****"
80 PRINT TAB(2);"VARIABLE";TAB(17);"0";TAB(29);"1";TAB(41);"2";
90 PRINT TAB(53);"3";TAB(65);"4"
100 GO TO 120
110 GO TO (500,600,700,800,900,1000,1100,1200) K
120 PRINT
130 I=0
140 IF K>7.5 THEN 170
150 N=3
160 GO TO 180
170 N=2
180 FOR X=.1 TO N STEP .1
190 I=I+1
200 GO TO (530,630,730,830,930,1030,1130,1230) K
210 GO SUB 400
220 PRINT TAB(I(0));V(0);TAB(12+I(1));V(1);TAB(24+I(2));V(2);
230 PRINT TAB(36+I(3));V(3);TAB(48+I(4));V(4);TAB(60+I(5));V(5)
250 IF I<2.5 THEN 280
260 PRINT
270 I=0
280 NEXT X
290 IF K>7.5 THEN 320
300 PRINT\PRINT\PRINT\PRINT\PRINT\PRINT\PRINT\PRINT\PRINT\PRINT
310 GO TO 330
320 PRINT\PRINT\PRINT\PRINT\PRINT\PRINT\PRINT\PRINT\PRINT\PRINT
321 PRINT\PRINT\PRINT\PRINT\PRINT\PRINT\PRINT\PRINT\PRINT\PRINT
322 PRINT\PRINT\PRINT
330 PRINT "*****"
340 NEXT K
350 END
400 FOR J=0 TO 5
410 V(J)=INI(V(J)*1E6+.5001)/1E6
420 I=0
430 FOR Z=2 TO 0 STEP -1
440 IF ABS(V(J)+.0001)>=10*Z THEN 470
450 I=I+1
460 NEXT Z
465 IF V(J)<>0 THEN 470
466 I=2
470 I(J)=I
480 NEXT J
490 RETURN
500 PRINT TAB(23);"GAMMA DISTRIBUTION-DENSITY"
510 GO TO 60

```

DISCAL CONTINUED

```

1040 V(1)=C*EXP(-.5*(X+2))
1045 V(2)=(C/(X+2))*EXP(-.5/(X+2))
1050 V(3)=(C/SQR(X))*EXP(-.5*X)
1055 V(4)=3+(2*V(0))
1060 V(5)=.282095*EXP(-((V(4)-3)+2)/4)
1065 GO TO 210
1100 PRINT TAB(27);"CAUCHY DISTRIBUTION"
1105 PRINT\PRINT
1110 PRINT TAB(2);"VARIABLE";TAB(16);"DENSITY";TAB(28);"SQUARE";
1115 PRINT TAB(40);"SUM";TAB(50);"VARIABLE";TAB(64);"PRODUCT"
1120 GO TO 120
1130 D=.31831
1135 V(0)=X
1140 V(1)=D/(1+(X+2))
1145 V(2)=D/(2*SQR(X)*(1+X))
1150 V(3)=2*D/(4+(X+2))
1155 V(4)=3*V(0)
1160 V(5)=(D+2)*(1/((V(4)+2)-1))*LOG(V(4)+2)
1165 GO TO 210
1200 PRINT TAB(26);"UNIFORM DISTRIBUTION"
1205 PRINT\PRINT
1210 PRINT TAB(2);"VARIABLE";TAB(15);"RECIPROCAL";TAB(27);"QUOTIENT";
1215 PRINT TAB(38);"VARIABLE";TAB(51);"SQUARE";TAB(63);"PRODUCT"
1220 GO TO 120
1230 V(0)=5*X
1235 V(1)=1/(V(0)+2)
1240 V(2)=V(1)/2
1245 V(3)=X/2
1250 V(4)=1/(2*SQR(V(3)))
1255 V(5)=LOG(1/V(3))
1260 GO TO 210

```


DISCAL CONTINUED

```

530 V(0)=2*X
540 V(1)=EXP(-V(0))
550 V(2)=V(1)*V(0)
560 V(3)=V(2)*V(0)/2
570 V(4)=V(3)*V(0)/3
580 V(5)=V(4)*V(0)/4
590 GO TO 210
600 PRINT TAB(22);"GAMMA DISTRIBUTION-RECIPROCAL"
610 GO TO 60
630 V(0)=2*X
640 V(1)=EXP(-1/V(0))/(V(0)+2)
650 V(2)=V(1)/V(0)
660 V(3)=V(2)/(2*V(0))
670 V(4)=V(3)/(3*V(0))
680 V(5)=V(4)/(4*V(0))
690 GO TO 210
700 PRINT TAB(24);"GAMMA DISTRIBUTION-SQUARE"
710 GO TO 60
730 V(0)=2*X
740 V(1)=EXP(-SQR(V(0)))/(2*SQR(V(0)))
750 V(2)=V(1)*SQR(V(0))
760 V(3)=V(2)*SQR(V(0))/2
770 V(4)=V(3)*SQR(V(0))/3
780 V(5)=V(4)*SQR(V(0))/4
790 GO TO 210
800 PRINT TAB(25);"GAMMA DISTRIBUTION-SUM"
810 GO TO 60
830 V(0)=3*X
840 V(1)=0
850 V(2)=0
860 V(3)=EXP(-V(0))*(V(0)+6)/720
870 V(4)=0
880 V(5)=0
890 GO TO 210
900 PRINT TAB(23);"GAMMA DISTRIBUTION-QUOTIENT"
910 GO TO 60
930 V(0)=2*X
940 V(1)=1/((V(0)+1)+2)
950 V(2)=(V(1)+2)*6*V(0)
960 V(3)=V(2)*V(1)*5*V(0)
970 V(4)=V(3)*V(1)*(14/3)*V(0)
980 V(5)=V(4)*V(1)*(9/2)*V(0)
990 GO TO 210
1000 PRINT TAB(26);"GAUSSIAN DISTRIBUTION"
1005 PRINT\PRINT
1010 PRINT TAB(2);"VARIABLE";TAB(16);"DENSITY";TAB(27);"RECIPROCAL";
1015 PRINT TAB(39);"SQUARE";TAB(50);"VARIABLE";TAB(64);"SUM"
1020 GO TO 120
1030 C=.398942
1035 V(0)=X

```

REFERENCES

1. General Electric, TEMPO, Reports

Engineering Evaluation Planning Study for Large Solid Propellant Stages: Phase I, RM62TMP-64, by C. R. Herrmann, Dec. 1962 (Confidential)

Engineering Evaluation Planning Study for Large Solid Propellant Stages: Phase II, RM64TMP-31, 3 volumes, Volume III (Secret), by C. R. Herrmann, P. M. Carrick, R. G. Herrmann, April 65.

The Analytical Approach and Physics-of-Failure Technique for Large Solid Rocket Reliability. TEMPO Report 66TMP-90, 1 March 1967. C. R. Herrmann and G. E. Ingram.

An Application of the "Requirement vs Capability" Approach to Estimating the Reliability of Large Solid Rocket Motors: Interim Report, 67TMP-116, by C. R. Herrmann, G. E. Ingram, E. L. Welker. 2 Jan 1968.

2. Phase I Progress Report, 260 Inch Motor Reliability Study, Aerojet General Corporation. 17 April through 15 Oct 1967. Report NAS 7-572 PR-6.

3. AGC Data Packets supplied between June 2, 1967 and Oct. 20, 1967 are in general contained in the above report (Reference 2). These packets include:

Some preliminary data on LSBR and insulation erosion rates for 260 SL-1, 260SL-2, Polaris and Minuteman;

LSBR distribution data for 260SL-1, SL-2, and propellant modules distribution data for 260SL-3;

260 inch diameter motor, Saturn 1 B Improvement Insulation Design, DLNA;

260/SIV-B Data for Burn Through Failure Mode Design Parameters;

Polaris Motor Insulation Erosion Data;

Requirement/Capability Data for Inner Bore Hoop Strain and Interface Shear Stress (Firing and Flight Conditions);

Propellant Grain Requirement and Capability Data for Storage Conditions; and

Propellant Grain Requirement and Capability Data for 260/SIV-B Booster Motor.

4. AGC Data Packages II-1 through II-6, supplied between Jan 26, 1968 and April 3, 1968 which include the following:
 - (II-1) Failure of Longitudinal Weld in Hoop Stress;
 - (II-2) Failure of Forward Head Circumferential Weld in Meridional Stress;
 - (II-3) Failure of Forward Skirt Forging in Combined Compression, Shear, and Bending;
 - (II-4) Failure of Nozzle Joint Bolts in Tension Due to Combined Pretorque Load, Pressure Ejection Load, and TVC Moment;
 - (II-5) Separation of Nozzle and Chamber Flange Due to Ejection Load per Bolt Exceeding Pretorque Load per bolt;
 - (II-6) Failure of Insulation/Case Bond in Shear Stress.
5. Phase II Report, 260-inch Motor Reliability Study, Aerojet General Corporation. 16 October 1967 through 17 May 1968. Report NAS 7-572 PR-12.